19951206 52

N95-27072

704.219

6

CLASSICAL NOVAE AND RECURRENT NOVAE - GENERAL PROPERTIES

M. Hack, P.L. Selvelli, and H. Duerbeck

I. INTRODUCTION.

In this chapter, we will describe the observable characteristics of classical novae and recurrent novae obtained by different techniques (photometry, spectroscopy, and imaging) in all the available spectral ranges. We will consider the three stages in the life of a nova: quiescence (pre- and post-outburst), outburst, final decline and nebular phase.

Since the majority of these objects has been observed only—or much more extensively—in the optical range, we will start discussing these observations. In section 6.II.A we will describe the photometric properties during the quiescent phase. Quiescent novae, as a rule, present light variability; in several cases, this variability can be interpreted as characteristic of an eclipsing binary, with period shorter than 1 day (only known exception—GK Per with a period of about 2 days). These curves are, however, variable from one period to the other; in several cases rapid (minutes), irregular, small amplitude (few tenths of magnitude) variations are observed. We will describe some characteristic examples since each object is a special case. Many of them—in quiescence—are indistinguishable from dwarf novae and nova-like stars and, in fact, are classified as such and have been extensively discussed in Chapters 2 and 3. In 6.II.B we describe the photometric properties during outburst, the classification according the rate of decline (magnitudes per day), which permits us to define very fast, fast, intermediate, slow, and very slow novae and the correlation between luminosity and speed class.

In 6.III.A, we report the scanty data on the spectra of the few known prenovae and those on the spectra of old novae and those of dwarf novae and nova-like, which, however, are almost undistinguishable (see also Chapters 2 and 3).

In 6.III.B, 6.III.C, and 6.III.D, we describe the typical spectra appearing from the beginning of the outburst—just before maximum—up to the nebular phase and the correlation between spectral type at maximum, expansional velocity, and speed class of the nova.

In 6.IV.A, we report the existing infrared observations, which permit us to explain some of the characteristics of the outburst light curve, and give evidence of the formation of a dust shell in slow and intermediate novae (with the important exception of the very slow nova HR Del 1967) and its absence or quasi-absence in fast novae. In 6.V and 6.VI, the ultraviolet and X-ray observations are described. The far ultraviolet spectra of several old novae have been provided by the International Ultraviolet Explorer (IUE). Some of them can be fitted by the Rayleigh-Jeans tail of hot black bodies, indicating the presence of a hot companion. In other cases, the spectrum is flat, as due to free-free transitions of ionized gas, or can be fitted by a power law. In 6.VI, the X-ray observations of novae—mainly from the two satellites EINSTEIN and EXOSAT—are reported. Several novae are soft X-ray sources, indicating the presence of regions in the nova system having temperatures as high as 10^6 K or more. Correlations between X-ray flux and speed class seem to exist.

PRECEDING PAGE BLANK NOT FILMED

In 6.VII, observations of the final decline and of the envelopes appearing several months after outburst are reported. Spectra, images and radioastronomical observations are the tools for studying the envelopes.

II. PHOTOMETRIC PROPERTIES

About 170 novae have been observed up to now, and 55 of them have been observed at minimum light. The known recurrent novae are five only. A catalogue of all known novae has been published by Duerbeck (1987c) giving designations, positions and finding charts, magnitude at minimum and maximum, light-curve type according the classification scheme by Duerbeck (1981) and references.

II.A. NORMAL (OR QUIESCENT) PHASE

A study of all the existent observations has been made by Robinson (1975). He observes that the ejected material gives little insight into the nature of the underlying star. It is important to compare pre-eruption and post-eruption stages, in order to see if differences exist between the two stages, and therefore what has been the effect of the explosion on the stellar structure or on the stellar atmosphere, or on the system as a whole, in case of binary systems.

Old novae (that we consider as the "normal state," or non-eruptive state of novae) are variable, and several of them present non-periodical short time-scale variability (Mumford, 1966a, 1966b). Flickering with an amplitude of 0.1 - 0.2 mag over a time scale of minutes is a common feature among old novae, as well as among dwarf novae and nova-like stars. Walker (1957) noted it first in DQ Her. However DQ Her is peculiar in having also periodic variations, with P = 71 sec, amplitude of 0.04 mag (Walker, 1956), which are rarely observed in other novae (Robinson and Nather, 1977). Another nova, V 533 Her, has presented the same phenomenon (Patterson, 1979a) with a period of 63 sec. These oscillations disappeared in 1982 (Robinson and Nather, 1983). The properties of the oscillations were very similar in both stars, although the outburst properties were very different. In 1981, Warner has observed another nova, RR Pic, presenting very short-lived, rapid oscillations with periods of 20 - 40 seconds. Rapid coherent oscillations (where for coherent oscillations we mean that they stay in phase for time long compared to the period, that is for several hours, Robinson, 1976) with periods of few seconds are also observed sometimes in dwarf novae and nova-like. They are not common and seem to appear with about the same frequency in all classes of cataclysmic variables (old novae, dwarf novae, and nova-like).

Most prenovae, as well as pastnovae, are low-amplitude (few tenths of magnitude) variables. Robinson (1975) found that the preeruption and posteruption magnitudes are the same for all the 18 stars for which both magnitudes are known. The only exception was BT Mon, for which m (prenova) was recorded as fainter than 16.8 because it was not observable on about 150 Harvard patrol plates taken between 1898 and 1939 (with limiting magnitude of about 17), while m (post-nova) is equal to 15.8. However, a recent photometric study of BT Mon (Robinson et al., 1982) shows that there is no compelling reason to believe that the preeruption magnitude was different from its posteruption magnitude. In fact, BT Mon is an eclipsing binary with period 8h.01 or 1.0014d/3. Now the eclipse lasts about 1.6 h and is 2.7 mag deep. The Harvard plates were exposed at about the same hour every night, so BT Mon was always in eclipse at the epoch of these observations.

Also the light curves for pre and posteruption, when known, are the same, with one exception, V446 Her. In the latter case, the pre-eruption light curve has an amplitude of almost 4 mag, while the post-eruption light curve presents variation of no more than 0.4 mag. Hence in general, a nova eruption has very little effect either on the erupting star or on the binary system as a whole.

Of over 12 stars for which pre-eruption light curves were well known, 6 present probable or

conclusive changes in the light curves as early as 1 to 15 years before the eruption.

Several old novae have been extensively observed and their photometric characteristics present many similarities with dwarf novae and nova-like stars. In the following sections, we will give some examples of the photometric behavior of some old novae.

The binary character of the old nova V603 Aql (1918) was discovered by Kraft (1964), who derived an orbital period of 3h19m.5 from Palomar coudé spectrograms. There is evidence of 3 minima observed with IUE(*) by Rahe et al. (1980) and by Slovak (1980) at the McDonald Observatory during more than two complete cycles. These measurements, as well as those made by Slovak, show a period compatible with that derived by the RV curve determined by Kraft. The shape of the light curve varies from cycle to cycle. The observed minimum was interpreted by the authors as a partial eclipse of the accretion disk around the compact companion by the late component or as an occultation of a hot spot by the disk itself. The absence of any secondary minimum may probably be due to the fact that the major fraction of light is emitted by the disk, in case an eclipse really occurs. However, the low value of v sin i obtained by Kraft (38 km/sec) and a detailed study of the nova ejecta made by Weaver (1974) suggest a rather low inclination and hence make improbable the occurence of an eclipse.

Actually, Cook (1981) brings arguments against the possibility of eclipse, because the values of the orbital period and RV amplitude of the primary (sdBe according to Kraft) suggest $i<20°$. In this case, the light variations could be explained by orientation effects, due to asymmetric distribution of light in the disk. Such alternative explanation of the light variation was already suggested by Rahe et al. They suggest that the surface of the secondary facing the primary is heated by a strong, optically unseen (UV and/or X) flux, hence, the light variations are explained by varying orientation of the secondary. Ultraviolet observations of V603 Aql made with OAO 2 (Gallagher and Holm, 1974) and by Lambert et al. with IUE (1980) confirm the presence of a large ultraviolet flux.

Because the IUE FES observations give a rather coarse temporal resolution, Slovak (1981) has made a series of high-speed photometric observations of V 603 Aql. He does not find any evidence for eclipse or other periodic features, therefore making it difficult to accept the alternative explanation of the varying aspect of the surface of the secondary facing the primary and heated by its UV flux. It is suggested that transient phenomena lasting for a few cycles can occur in the accretion disk and produce the irregular minima. Random flickering of large amplitude (0.20 - 0.30 mag) has been observed by all the quoted authors. Search for coherent oscillations was made by Slovak with negative result.

Extensive photometric and polarimetric observations were made by Haefner and Metz (1985). Contrarily to what Slovak found, they observe a light curve characterized by the appearance of a hump structure repeating with a period of 3h 18m.9. Moreover, linear and circular polarization are modulated with a period of 2h48m.0. We will come back in chapter 7 on the model proposed to explain these observations (see also Chapter 4.III.F.2). Let us say here that they are able to explain the observations by assuming an intermediate polar (i.e., a magnetic degenerate component whose rotation is not synchronized to the orbit) combined with a temporarily existing eccentric disk.

A field of 10^6 gauss in indicated by the measured circular polarization.

The very fast nova V 1500 Cyg presented a periodic 3.3-hour variation within one week of the outburst, a characteristic never observed before for any other nova from broad-band photometry, (Tempesti, 1975) and from the H

(*)The Fine Error Sensor (FES) aboard the satellite gives a measure of the stellar flux related to the stellar visual magnitude (Holm and Crabb, 1979, NASA-IUE Letter 7).

Alpha profile (Campbell, 1975, 1976). The period was changing, decreasing by about 2% in 10 months in 1976 (Patterson 1978 and references therein). In 1977, the period increased again by 1%. Figure 6.1 by Kleine and Kohoutek (1979) gives the period length vs. time. Photometry through October 1978 establishes that the period has stabilized at 0.139617 +/- 0.000002 days in early 1977 (Patterson, 1979b). The amplitude of the light variation is changing from cycle to cycle, being around 0.64 - 0.72 mag. Later observations extending to 1981 confirm the stabilization of the period (Kruszewski et al., 1983). These authors suggest that the change $\Delta P/P = -3.5 \times 10^{-5}$ occurred between 1977 and 1978 can be caused by the slow outflow of matter through the outer Lagrangian point of the binary system (little more than 10^{-6} solar masses should be sufficient to explain the period change).

A series of observations made by Pavlenko (1983) covering 19 cycles of 3.3 h between July 25 and October 5, 1981 indicate night to night changes in the form of the light curve, its amplitude (from a minimum of 0.4 to a maximum of 1 mag), and the mean brightness. It seems therefore very probable that the 3.3 h period represents the orbital period of the system. In addition, as in the majority of cataclysmic variables, small amplitude rapid flickering (time scale 1 to 10 minutes) is present in the light curve of this old nova.

It is interesting to compare the light curves of the two old novae V1500 Cyg 1975 and CP Pup 1942. They share the common property of having been very fast novae with exceptionally large outburst amplitude—larger than 19 mag and more than 17 mag respectively—more typical of a supernova rather than a nova; however, the radial velocities observed during the eruption indicate in both cases that they are classical novae (V exp.<2200 km/s for V 1500 Cyg, and < 1400 km/s for CP Pup, while SNs have radial velocities larger than 10,000 km/s). High speed photometric observations of CP Pup were made by Warner (1985b) (Figure 6.2). The photometric period is 0.06614 d (or 1.58736 hours) and differs from the spectroscopic one, as shown in Figure 6.2. The light curve is variable in shape, amplitude and mean brightness and low amplitude flickering with time scale of 1 - 10 min in superposed. CP Pup is the classical nova with the shortest known period and the only one below the gap in the periods shown by the CVs between 2.1 and 2.82 hours.

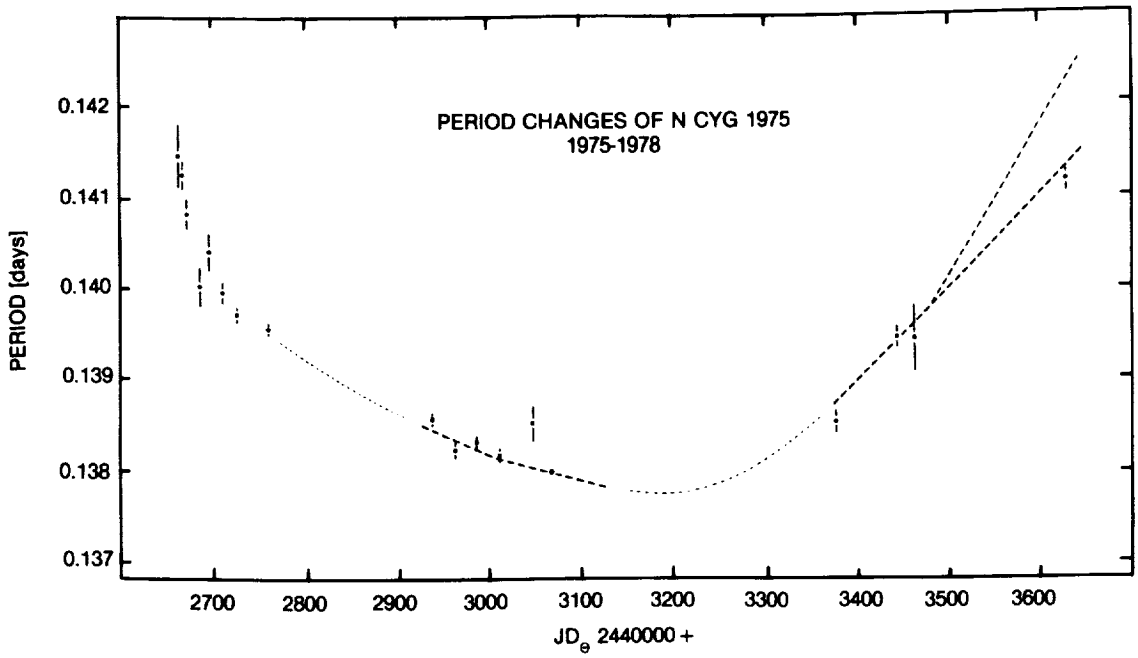

Figure 6-1. Photometric period variations for V 1500 Cyg (1975). (from Kleine and Kohoutek, 1979)

V1668 Cyg 1978 has been observed near its maximum light in the attempt to detect short-period variations like those observed in old novae (Giuricin et al., 1979). The time resolution was 0.01 sec. Rapid flickering (down to 0.2 sec was observed. No stable periodic brightness variations were detected, although there is strong evidence of the existence of short-lived oscillations during the nights of September 14 and 15, 1978. Precisely during the first night (J.D.2443766.5), oscillations with periodicity of about 0.067 sec and 0.01 sec, lasting 100 - 200 sec were seen. During the second night (J.D.2443767.4), a different phenomenon was observed: the presence of oscillations with a period of 5.26 sec monotonically decreasing in amplitude and lasting 500 sec (Figure 6.3a, 3b).

Photoelectric observations with a lower time resolution (10 sec) were made by Campolonghi et al. (1980) during several nights in September and October 1978. Superposed on the decline following the outburst, they found a periodic variation of brightness with a period of 10.54 hours and amplitude of 0.15 mag. This behavior is very similar to that shown by V

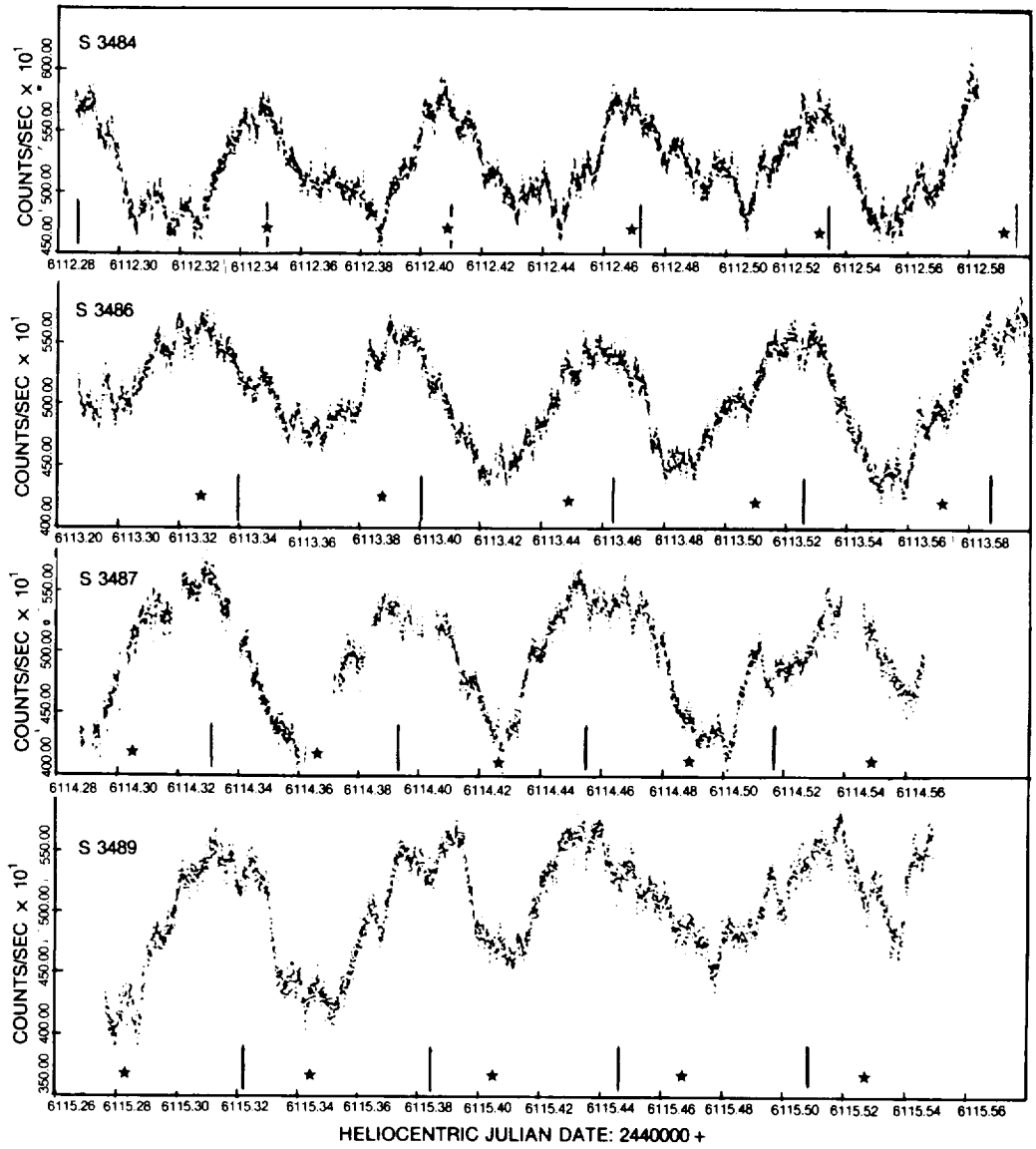

Figure 6-2. Light curves of CP Pup: Vertical arrows indicate predicted times of maxima according to the photometric ephemeris. Stars indicate times of maxima according to the spectroscopic period. (from Warner, 1985b)

1500 Cyg 1975. The authors suggest that this behavior is probably common to all novae and is not due to any eclipse in the system but rather to pulsation of the envelope produced by periodic perturbation of it caused by the binary system orbiting inside it. The light curve of the almost pole-on old nova system of V603 Aql 1918 could be explained by this mechanism.

The slow nova HR Del 1967 was also found to present a short period light variability with P = 0.1775 d and amplitude 0.16 mag in 1977 and 0.10 mag in 1979 (Kohoutek and Pauls, 1980). The photometric period seemed to be identical with the spectroscopic one according to Hutchings (1979a). However the scatter of the photometric data is large and the spectroscopic radial velocities were obtained from different cycles with a gap of almost one year. More recent data by Bruch (1982) give a spectroscopic period (which represents the orbital motion of the binary) P = 0.2141674. Kohoutek and Pauls also observed that the U, B, V, colors suggest a tendency for the system to be redder at maximum light, although the presence of the nebular emission lines can severely affect the colors. From these data, it seems more probable that the light curve features are due to the presence of an accretion disk of nonuniform brightness rather than to eclipse (see also Chapter 8).

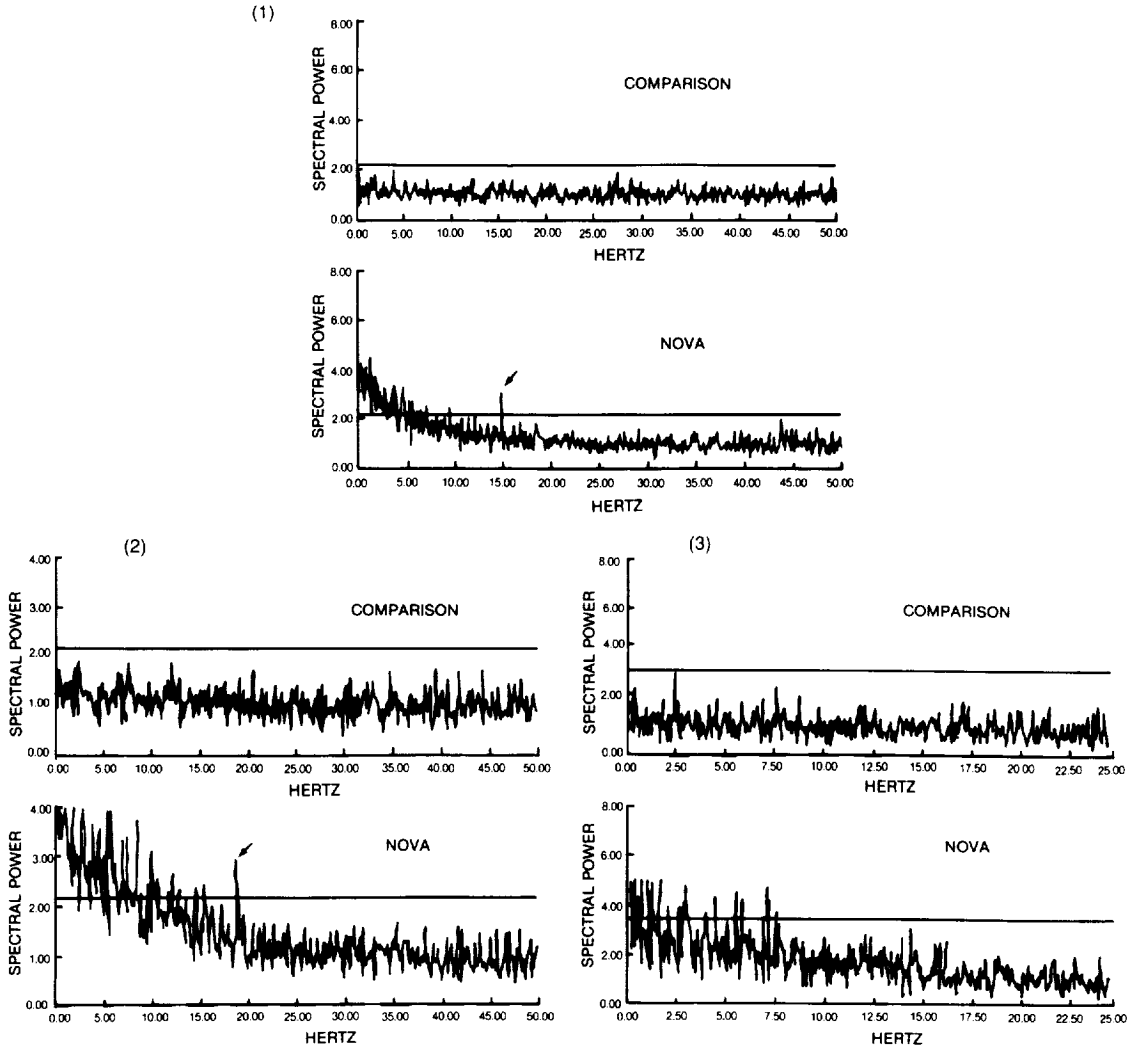

Figure 6-3a. Rapid photometry of V 1668 Cyg (1978). Observations of Sep. 14, 1978: Simultaneous power spectra of the nova and the comparison star. The peak at 15 Hz is evident in the upper graph (1) started at U.T. = JD 2443766.45555; time interval 154 s. The same peak is disappeared in the power spectra obtained with 50 Hz (graph 2) and 25 Hz (graph 3) upper frequency limits, started 2648 seconds later for the same time interval of 154 s.

DQ Her 1934 has been extensively observed since the epoch of the outburst. We will discuss it in larger detail in the chapter devoted to single objects. However, it is interesting to briefly discuss it here for comparison with the photometric behavior of the other old novae. DQ Her shows a light curve indicating clearly the presence of eclipse of a hot companion. The phase interval $0 < \phi < 0.06$ is repeating with slight variation from cycle to cycle, while the phase interval $0.06 < \phi < 0.3$ shows strong deviation from one cycle to the other. Less strong but still remarkable variations from cycle to cycle are observed at phases included between 0.3 and 0.9. The light curve is very similar to those of typical dwarf novae (see Chapters 2.II.B.1 and 3.IV.B.1). Dmitrienko and Cherepashchuk (1980) discuss this curve. They con-

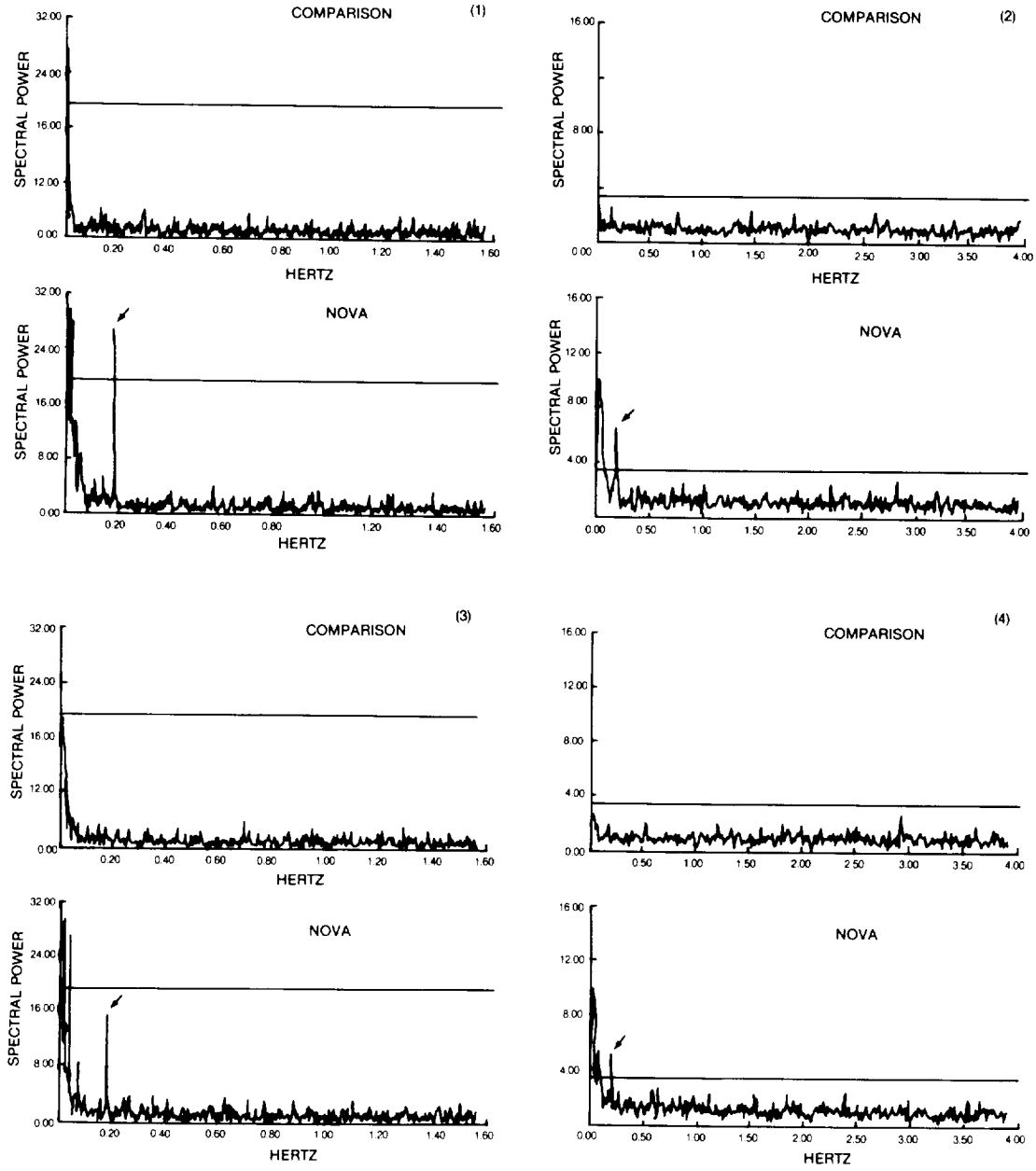

Figure 6-3b. Observations of Sep. 15, 1978. Same as a) The sequence of power spectra shows evidence of a transient peak at 0.19 Hz whose amplitude decreases with time: starting times: 1) JD 2443767.37265, time interval 655 s; 2) 2443767.37325, time interval 655 s; 3) 2443767.38794, time interval 655 s; 4) 2443767.38888, time interval 573s. (from Giuricin et al. 1979)

clude that the hot companion is a white dwarf of abnormally high luminosity (20-200 $L_\odot$) and temperature of about 1.0-1.7 x 10^5 K, practically unchanged for some 20 years. Such prolongated persistence of this anomalous brightness and temperature may imply continuous accretion of material from the accretion disk. Unlike other old novae, DQ Her presents the coherent oscillations with a period of 71.066 sec and a mean amplitude of 0.04 mag. One explanation that has been discussed in Chapter 4.III.F.2 is that the white dwarf in DQ Her is magnetized and that the gas accreting into the white dwarf funnels down the magnetic field lines, creating bright regions at the poles. The 71-sec periodicity is thought to be produced by rotation of the white dwarf with a period of 71 sec or possibly of 142 sec. (see Patterson, 1980). The other nova showing a similar behavior, according to observations made in 1978 and 1980, was V533 Her 1963, which had a periodicity of 63.6 sec, (Patterson, 1979a, and Middleditch and Nelson, 1980) very similar to that presented by DQ Her and was therefore explained by the same mechanism. However, observations by Robinson and Nather made in 1982 (1983) indicate that the 63-sec periodicity has disappeared. Hence, it cannot be related to rotation of a magnetic white dwarf. A similar behavior was shown by WZ Sge—an object whose belonging to the class of recurrent novae or of dwarf novae is a matter of discussion. Although the mechanism explaining the periodicities in WZ Sge is not known with certainty, the most probable explanation is pulsation of the white dwarf (Robinson et al., 1978 and Middleditch and Nelson, 1979). Hence, it seems probable that V533 Her and WZ Sge obey to the same mechanism, different from that active in DQ Her. We will discuss other evidences in favor or against the presence of a magnetic field in Chapter 7.

The old nova GK Per 1901 is exceptional among old novae for several reasons:

a) The orbital period derived by radial velocity measurements (Kraft, 1964; Bianchini et al., 1981) is about 1.9 days, much longer than those of the other old novae. These authors derived an eccentricity of 0.4, which was also exceptional. However, a more recent analysis by Crampton et al. (1983) reveals a period of 1.99679 d with a circular orbit.

b) Almost all old novae have an optical spectrum dominated by the light of the hot primary (white dwarf or accretion disk); GK Per, on the contrary, shows the presence of a K2IV component (Kraft, 1964; Gallagher and Oinas, 1974).

c) GK Per shows strong fluctuations in luminosity together with spectral variations.

d) GK Per is a transient hard X-ray source (King et al., 1979).

e) GK Per is a nonthermal radiosource (Reynolds and Chevalier, 1984).

All these characteristics will be discussed extensively in Chapter 8. Sabbadin and Bianchini (1983) have collected all the existing photometric observations of this old nova since the 1901 outburst (February 22, V=0.2 mag.). The light curve from February 1901 to 1904 is the typical light curve of a fast nova. During the period March through June 1901, a series of semiperiodic oscillations are superposed over the secular decrease of brightness. The historical preoutburst minimum of 15 mag was reached again in 1916. The observations at minimum show a gradual passage from continuous, irregular fluctuations (from 1916 to 1947) to the present epoch, when the old nova is generally quiescent, and at intervals of several hundreds of days, endures outbursts of 2-2.5 mag that we will call minor outbursts, for distinguishing them from the 1901 typical nova outburst. The minor outbursts became evident in July 1948 for the first time.

Details of the behavior of GK Per during these quasi-periodical outbursts are given by Bianchini and Sabbadin (1982), Bianchini et al. (1982, 1986) and by Szkody et al. (1985). The outburst that occurred in February through April 1981 was particularly large, with an

amplitude of 3 mag (Bianchini et al., 1982). Spectra obtained at different moments of the outburst vary and will be discussed in the relative Section 6.III.

High-speed optical photometry of GK Per made during the minor outburst occurred in 1983 (Mazeh et al., 1985b) shows the presence of a small amplitude (4%) periodic modulation of 360 +/- 7 sec on September 12, while on August 11 and 18, a 400-sec modulation was observed, together with a long-term (0.8 hours) variation. Similar periodic modulations were observed also in the X-ray range (E >2 keV) with EXOSAT with a periodicity of 351 sec during the same outburst (Watson et al., 1984).

Another well-studied old nova is RR Pic 1925. The prenova was observed on several occasions since 1889, and it always was at constant brightness of 12.75 visual magnitude. Its present magnitude, 60 years after outburst, is 12.3 and is still becoming fainter.

Van Houten (1966), Mumford (1971) and Vogt (1975) have made photometric observations and found a light curve with a broad irregular maximum repeating with a period of 0.1450255 d, and interpreted this behavior as due to orbital motion. The binary nature of RR Pic was confirmed by spectroscopic observations of Wyckoff and Wehinger (1977). Further photometric observations were made by Marino and Walker (1982), Haefner and Metz (1982), and Kubiak (1984). High-speed photometry on 23 nights from December 1972 to December 1984 has been made by Warner (1986a). These data show that in the 1970s there was a strong orbital modulation of brightness, which has been replaced in the 1980s by an irregular, shallow eclipse superimposed on a flickering background. The disappearance of the orbital modulation coincided with decline in mean brightness of the system. The figure 6.4, taken from Warner, indicates that the curves in the 1970s have a double-humped shape with one large broad maximum and a second lower one, a principal minimum (No. 1) at the end of the principal maximum, at phase near 0.43 P, and a second minimum (No. 2) at phase near 0.74 P. In the 1980s, the first minimum has become very little, whereas the second minimum is now the dominant recurrent feature. The flickering on time scales of 5-10 min is stronger in the 1980s than in the 1970s.

Classical novae are often observed to be brighter than their prenova magnitude for several tens of years after outburst, sometimes for more than 100 years. Hence, to know the true state of "old nova," it should be desirable to observe novae that erupted centuries ago. Unfortunately, very few accurate positions of old novae erupted before Nova Oph 1848 exist. However, two very old novae have been firmly identified recently: they are WY Sge 1783 and CK Vul 1670. Nova CK Vul was discovered by Père Dom Anthelme, monk in Dijon, on June 20, 1670, and a month later, by Hevelius on July 25 in Poland. By collecting all the existing records, Shara et al. (1985) have reconstructed the light curve of this object, which reached two maxima of visual magnitude 3 in June 1670 and of magnitude 2.6 in April 1671.

To present two maxima is an unusual behavior, which has been observed in some very slow novae, as , for instance, in HR Del. Now at the position of CK Vul they have found a central star of magnitude R=20.7 surrounded by a nebulosity with a morphology suggestive of equatorial ejection and several bright subcondensations very similar to those observed in more recent and well-studied old novae. We will come back to CK Vul in section 6.III, devoted to the spectra of old novae, and in Section 6.VII, on nova shells. No photometric measurements of this star have yet been made.

WY Sge 1783 was discovered by the French astronomer D'Agelet when it was of magnitude 5.4 +/- 0.4. On the basis of the position, the brightness, rapidly and irregularly fluctuating between 18.6 and 19.5 photographic magnitude, the blue color, and the absence of any measurable proper motion (which, if measurable would indicate that the star is nearby and the observed fifth magnitude at maximum would not be consistent with the brightness expected from a nova explosion), Weaver

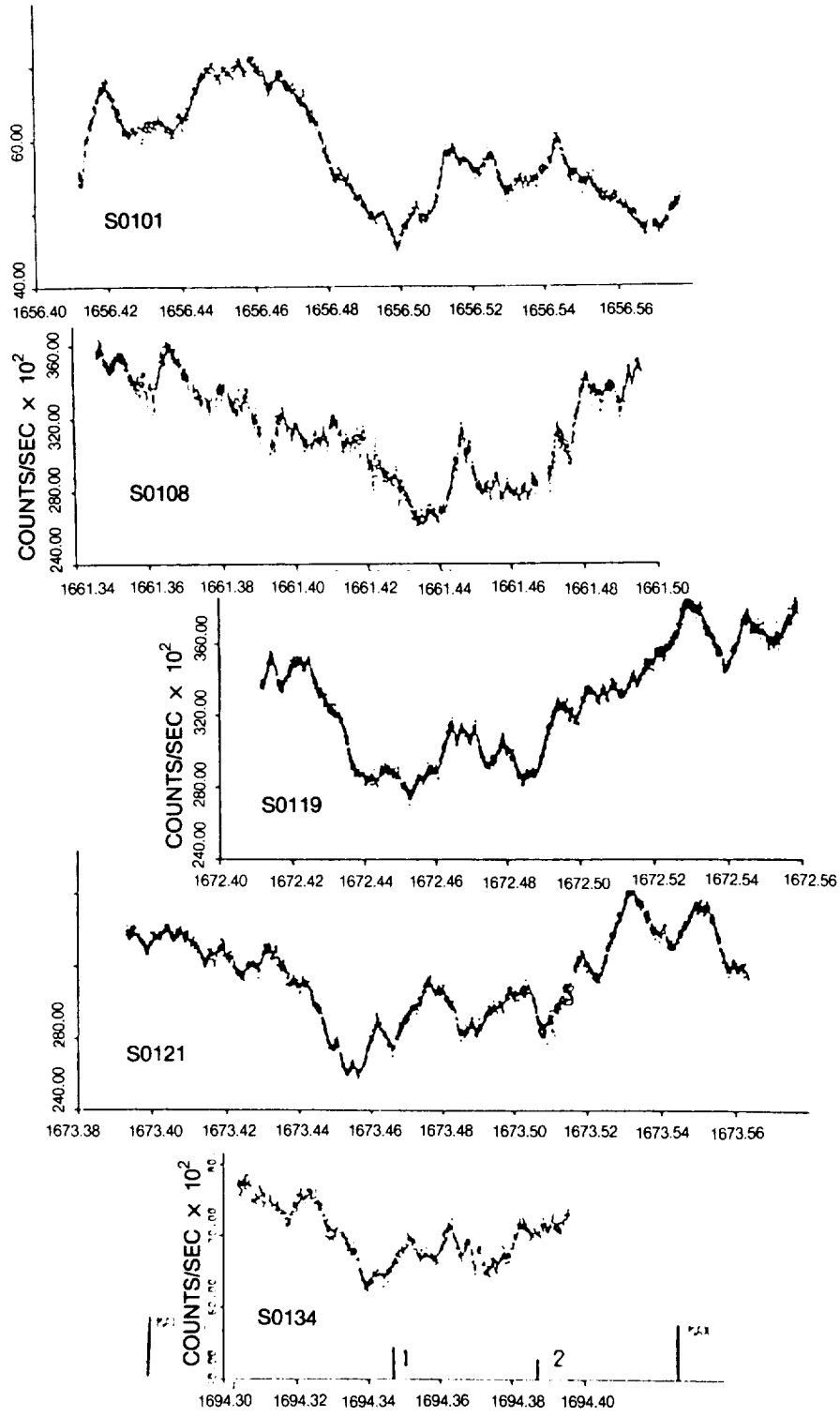

Figure 6-4. Light curves of RR Pic: a) Dec. 1972-Jan. 1973 aligned in orbital phase (Abscissa JD+2444000). Positions of the broad maximum and two minima calculated from Vogt's (1975) ephemeris are indicated.b) same as a), period Dec. 1973-Nov. 1975.c) same as a), period Feb. 1980-Dec. 1981.d) same as a), period Dec. 1981-Dec. 1984. e) Decline portion of the outburst light curve. (from Warner, 1986a)

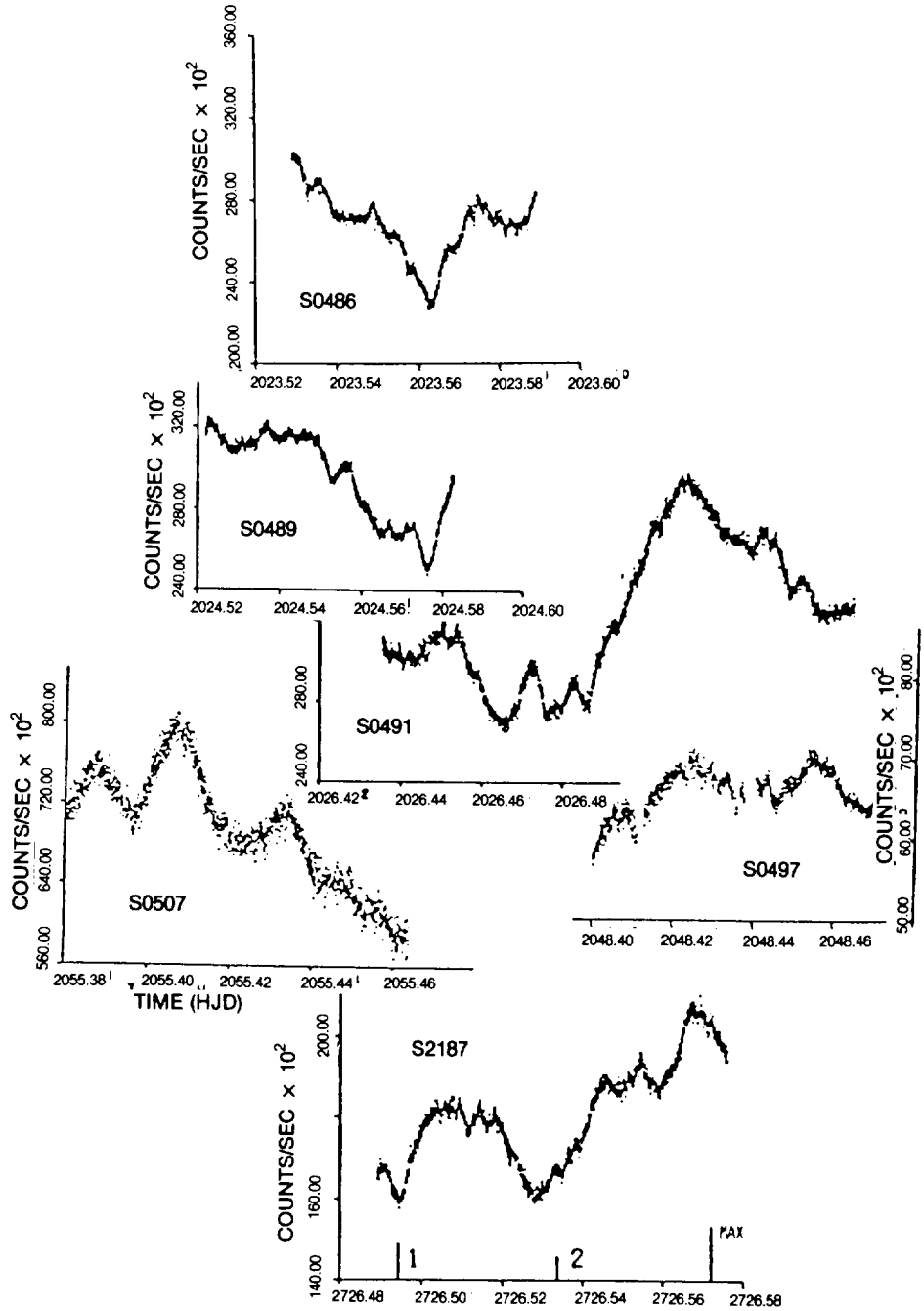
COUNTS/SEC x 10²
S0486
2023.52
2023.54
2023.56
2023.58
2023.60
S0489
2024.52
2024.54
2024.56
2024.58
2024.60
S0491
2026.42
2026.44
2026.46
2026.48
S0497
2048.40
2048.42
2048.44
2048.46
S0507
2055.38
2055.40
2055.42
2055.44
2055.46
TIME (HJD)
S2187
MAX
1
2
2726.48
2726.50
2726.52
2726.54
2726.56
2726.58

Figure 6.4b

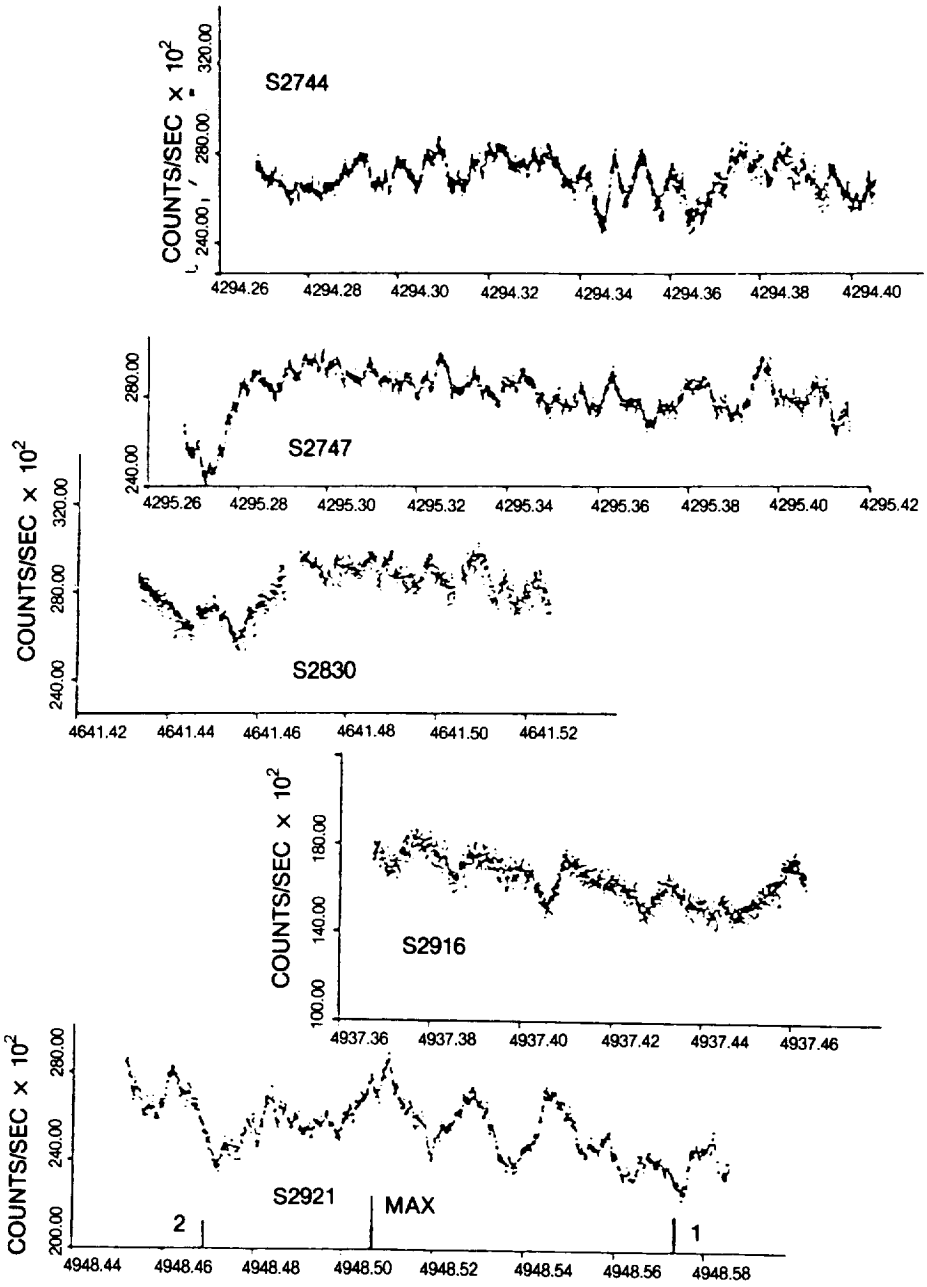
COUNTS/SEC x 10²
320.00
280.00
240.00
S2744
4294.26
4294.28
4294.30
4294.32
4294.34
4294.36
4294.38
4294.40
S2747
4295.26
4295.28
4295.30
4295.32
4295.34
4295.36
4295.38
4295.40
4295.42
S2830
4641.42
4641.44
4641.46
4641.48
4641.50
4641.52
180.00
140.00
100.00
S2916
4937.36
4937.38
4937.40
4937.42
4937.44
4937.46
200.00
S2921
MAX
2
1
4948.44
4948.46
4948.48
4948.50
4948.52
4948.54
4948.56
4948.58

Figure 6.4c

(1951) identified the old nova with a faint blue star less than 6 arc sec from the position given by D'Agelet. Warner (1971) has observed this star photometrically with time resolution of 5 sec. It presents rapid flickering with time scales of 5-15 min and amplitude of 0.1-0.2 mag. This kind of rapid variation, which is ubiquitous in nova remnants, is a strong indication that the Weaver identification with the Nova Sge 1783 is correct. Shara and Moffat (1983) and Shara et al. (1984) have observed it again both photometrically and spectroscopically. The spectrum shows the characteristics expected for old novae. We will come back to this in Section 6.III.A.

Photoelectric photometry has permitted to derive a light curve with a deep minimum (1.5-2 mag) lasting about 30 min, rapid egresses (5 min) and slightly slower ingresses and a period of 3h41m14s. On one night (June 17, 1982), it was 1.6 mag brighter than normal, and the

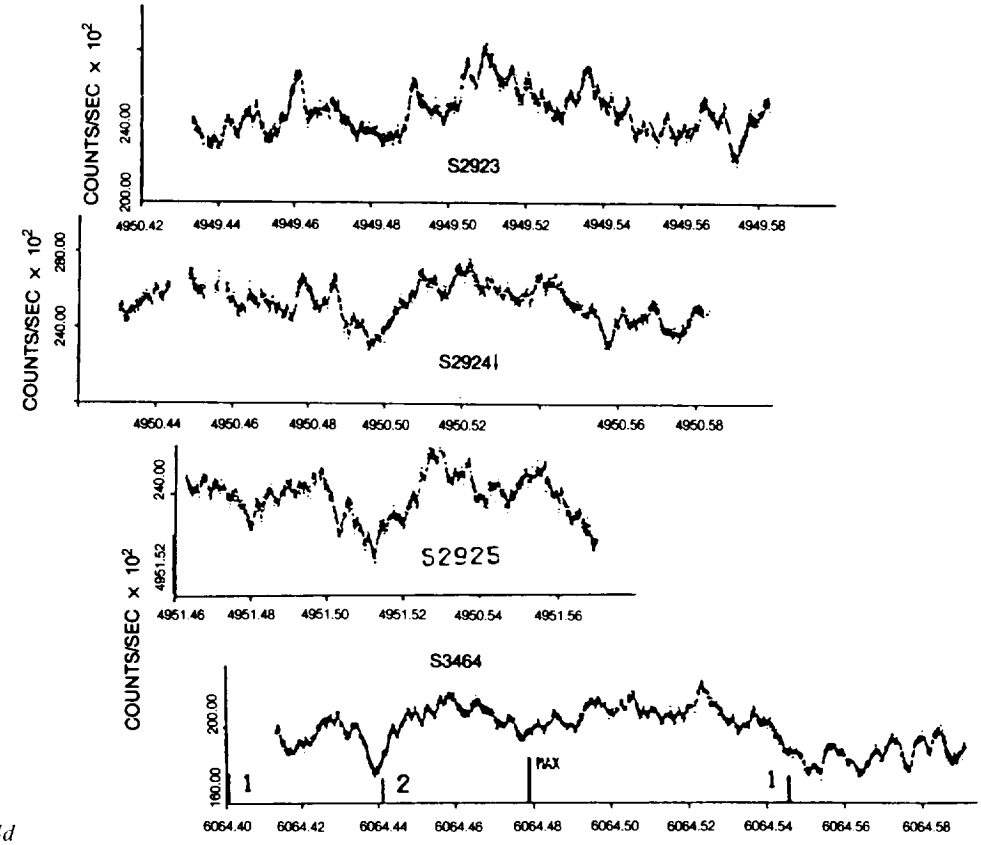

Figure 6.4d

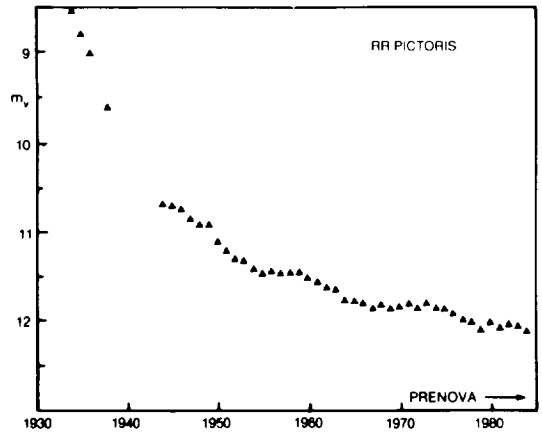

Figure 6.4e

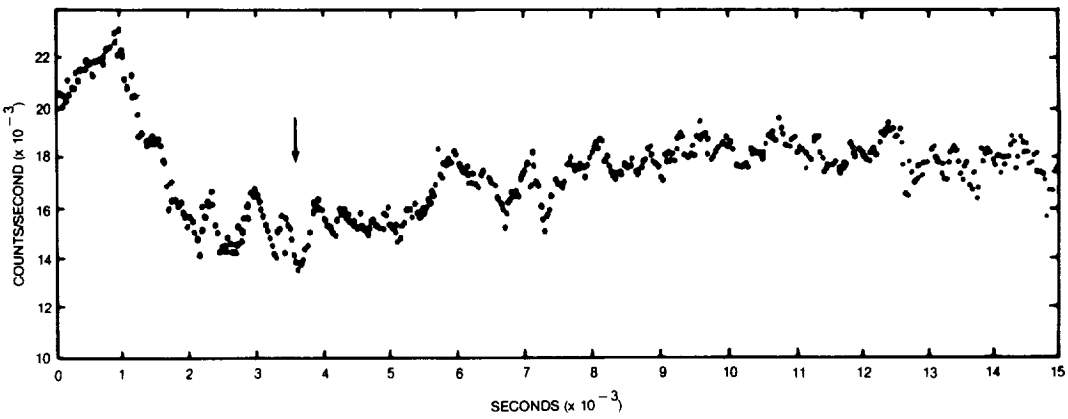

Figure 6-5. High speed photometry of the old nova WY Sge observed on June 16-17, 1982. An expected eclipse centered at the position indicated by the arrow is not seen. The flickering is about half its usual amplitude, while the nova is about four times brighter than usual.
(from Shara et al., 1984)

Table 6.1a (*)
Optical oscillations in cataclysmic variables

Object	Type	Orbital period(hr)	Coherent periods(s)	Quasi periods (s)	Additional references
SS Cyg	DN	6.60	7.5-9.7	32, 36	
RU Peg	DN	8.99	11.6-11.8	51	
TT Ari	NL	3.2		12, 32, 40, 50-1100	Jensen *et al.* (1983) Mardirossian et al.(1980) Sztajno (1979)
EM Cyg	DN	6.98	14.6-21.2		Steiman et al. (1982)
Z Cam	DN(Z)	6.96	16.0-18.8		
V436 Cen	DN(SU)	1.50	19.5-20.1		
VW Hyi	DN(SU)	1.78	20-32	23,88,253,413	Robinson and Warner (1984) Warner (unpublished)
HT Cas	DN	1.77	20.2-20.4	100	
RR Pic	N	3.48		20-40	Schoembs and Stolz (1981)
KT Per	DN		22.0-29.2	82-147	
SY Cnc	DN		23.3-33.0		
AH Her	DN	5.93	24.0-38.8	100	
CN Ori	DN	3.91	24.3-25.0		Schoembs (1982)
CDP -48° 1577	NL	4.5:	24.6-29.1		Warner et al. (1984)
PS74	DN(SU)	2.0:	27-29	248	Warner (unpublished)
Z Cha	DN(SU)	1.79	24.8, 27.7		Warner (unpublished)
WZ Sge	DN	1.36	27.87, 28.97		
UX UMa	NL	4.72	28.5-30.0		
V3885 Sgr	NL	4.94	29.32		Warner (unpublished)
AE Aqr	NL	9.88	33.08	36	
RX And	DN	5.08		36	
V2051 Oph	DN(SU)	1.50	40		O'Donoghue and Warner (unpublished)
V533 Her	N	-	63,63		Robinson and Nather (1979)
DQ Her	N	4.65	71.07		
U Gem	DN	4.25		73-146	
YZ Cnc	DN (su)	2.21		75-95	
X Leo	DN	-	160		
GK Per	N, DN	1.99d		360-390	Watson *et al.* (1984)
RW Sex	NL	5.93		620,1280	
V442 Cen	DN	11:		925	Marino and Walker (1984)

(*) from Warner (1986b)

ORIGINAL PAGE IS
OF POOR QUALITY

Table 6.1b

X-ray oscillations in cataclysmic variables

Object	Type	Orbital period(hrs)	Coherent period (s)	Quasi periods (s)	References
SS Cyg	DN	6.60		9-12	Cordova *et al.* (1984)
TT Ari	NL	3.2		9,12,32	Jensen *et al.* (1983)
VW Hyi	DN (SU)	1.78	14.06		Heise *et al.* (1984)
U Gem	DN	4.25		20-30	Cordove *et al.* (1984)
AE Aqr	NL	9.88	33		Patterson (1980)
YZ Cnc	DN (SU)	2.21		227	Cordova and Mason (1984)
GK Per	N, DN	1.99 d	351		Watson *et al.* (1984)

expected eclipse minimum was not seen (Figure 6.5). One and three nights later, it was back at its quiescent brightness. This behavior is very similar to that observed in dwarf novae. Warner (1986b) gives a list of the cataclysmic variables for which rapid coherent or quasi-periodic oscillation have been observed (Table 6.1). He defines quasi-periodic oscillations as those in which the coherence length may be as short as a few cycles, while coherent oscillations last at least for hundreds of cycles. Of the over 30 cataclysmic variables exhibiting, or which have exhibited, one or both of these kinds of oscillations, only four are classical novae: DQ Her and V533 Her (coherent oscillations) and RR Pic and GK Per (quasi-periodic oscillations). The latter has presented a coherent oscillation with period of 351 sec in the X-ray range.

II.B. ACTIVE PHASE

Many cataclysmic variables exhibit unpredicted and abrupt changes in their luminosity. We have two aspects of such changes: their rise and their fall. On completely unpredictable objects like classical novae, we cannot anticipate the epoch of outburst, and therefore we have very scanty data on the characteristics of their rise to maximum, and these are always due to chance. Thus we can classify the light curves of novae only on the basis of their fall. Dwarf novae, on the other hand, are classified on grounds of repetitive features in the outburst light curves.

Both classical and recurrent novae are therefore classified according to the rapidity of their decline from maximum in Na: fast novae, t(3) < 100 days, rate of decline > 0.2 mag/d; Nb: slow novae, t(3) > 150 days, rate of decline < 0.02 mag/d; Nc: very slow novae: they stay at maximum for several years; t(3) is the time employed for a brightness decrease of 3 magnitudes.

A more detailed classification is given by Duerbeck (1981) and reported in his catalogue of novae (1987c).

The number of novae in class Na is much larger than that on Nb in our Galaxy, while in M 31 there is evidence of the reverse (Arp, 1956). Arp excludes the possibility of any observational bias. This result suggests that this property of novae is related to an overall characteristic of the galaxy, like, for instance, the chemical composition. Unfortunately, the large majority of the observational data for extragalactic novae consist of light curves; no spectra are available to check this hypothesis.

Maximum brightness and rate of decline are correlated, in the sense that the larger is the absolute brightness of a nova at maximum, the faster is its decline (Arp, 1956, from observations of novae in M 31; McLaughlin, 1945, from observations of novae in our Galaxy). The empirical relation found by these authors has been recalibrated by Pfau (1976), and more recently by Shara (1981) who used 47 well-observed novae: 11 in our Galaxy, 26 in M 31, 7 in the LMC, and 3 in the SMC. The importance to know such relation is evident, since it permits us to derive the luminosity at maximum from relatively easily observable characteristics like the light curve, and because the determination of the energy emitted and mass ejected depend on our knowledge of the distances.

The recent calibrations give the following relations:

- M phot = -10.5 + 1.82 log t(2) (Schmidt-Kaler, 1965, based on galactic novae only)
- M(B) = -11.5 + 1.8 log t(2) (Pfau, 1976)
- M phot = -11.3 + 2.4 log t(3) (de Vaucouleur, 1978)
- M(B) = -11.3 + 2.4 log t(3) (Shara, 1981)

A still more recent relation has been found by Cohen (1985) who used a large number of observations of nova shells and used the expansion parallax method(*):

Mv(max) = -10.70 (+/- 0.30) + 2.41 (+/- 0.25) log t(2).

Payne-Gaposchkin (1957), by an examination of the light curves observed at that time (about 40 cases), is able to describe a certain number of typical light curves, which are correlated with the decline rate. Fast and very fast novae generally present a smooth early decline, and a generally smooth transition, while slow novae present oscillations during the early decline (and often more than one maximum) and they oscillate and dip during the transition phase (Figure 6.6). The oscillations in magnitude have periodicities of the order of few days and amplitudes < 1 mag. Insight into the nature of the dip has been given by infrared observations, which show that a maximum IR luminosity is reached just when the visual dip occurs. This can be explained by the formation

(*) The observed expansion velocity and the time elapsed from the outburst permit us to derive the true dimension, in kms of the nebula. By comparing it with the observed angular size, the distance is derived.

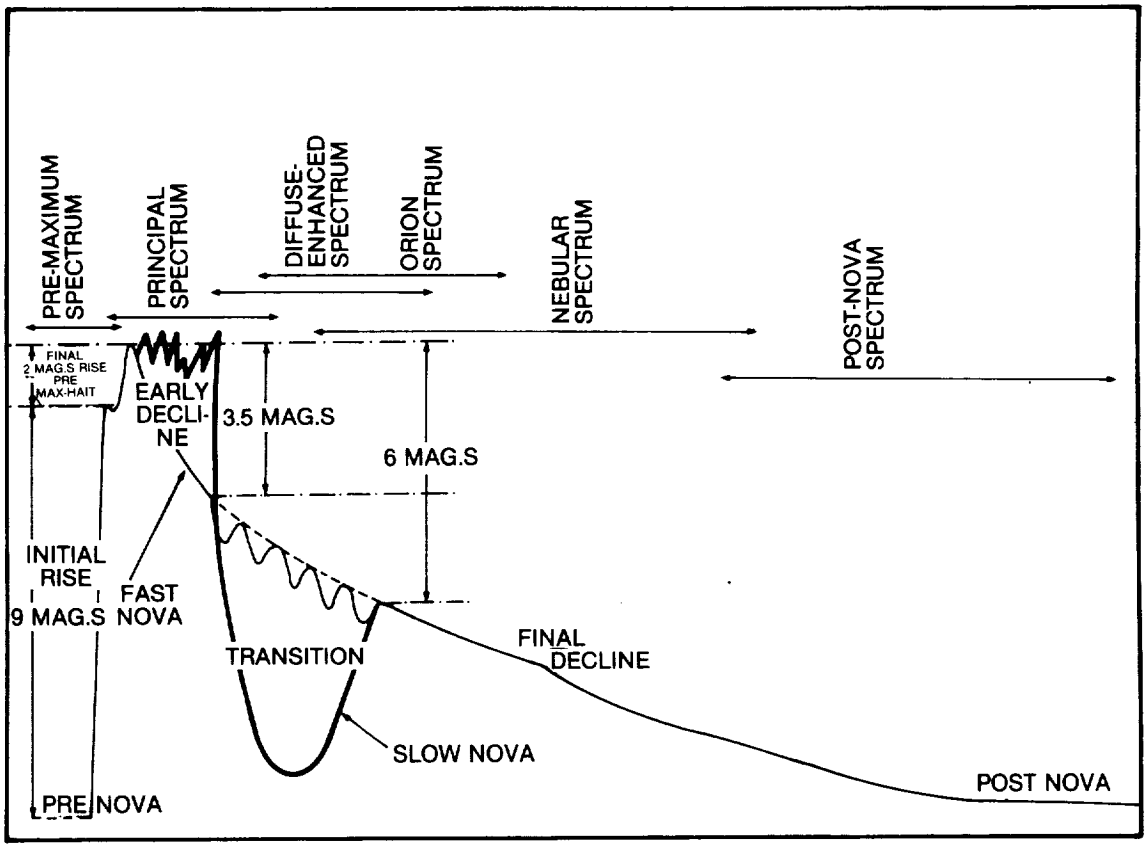

Figure 6-6. Schematic light curve for fast and slow novae. Three typical behaviors are observed during the transition stage: oscillations can be present or absent both in fast and slow novae. The deep minimum is typically found in slow novae. The position on the light curve when the various spectra are present, is indicated.
(adapted from Payne-Gaposchkin, 1957)

of a dust shell or by the heating of a preexistent envelope of dust.

The more detailed classification of nova light curves given by Duerbeck (1981) is based on about 100 galactic novae.

Table 6.2 from Duerbeck gives his classification scheme, and Table 6.3 applies this scheme to the galactic novae with sufficiently known light curves. Figures 6.7-6.11 from Duerbeck give some examples of light and color curves of the various classes.

Of the novae with well observed light curves, about 3/4 (73 objects) are type Na-fast-novae- (t_3 < 100 d), and about 1/4 (27 objects) are type Nb-slow novae- (t_3 > 100 d).

The distribution among the light curve types (Duerbeck, 1981) is as follows:

A. 39%, among them 2% Ar, 29% A, 8% Ao.

B. 29%, among them 10% Ba and 11% Bd, the rest is unclear.

C. 18%, among them 6% Ca, 11% Cb, the rest is unclear.

D. 12%, among them 1% DR.

E. 2%, this low percentage is also due to the fact that some type E novae are counted among the symbiotic stars.

Note that 18% of all novae are novae with noticeable dust formation (type C).

Duerbeck gives the following relations:

$M_V = -12.25 + 2.66 \log t_3$ (valid only for light curves of type A)

$M_V = -6.4 +/- 0.5$ (light curves of type B, C, D,)

Table 6-2(*)
A Classification Scheme for Nova Light Curves

type	description	examples	classification of Woronzow-Weljaminow (1953)
A	smooth, fast decline without major disturbances	CP Pup, V1500 Cyg	Rs - rapid, smooth star (CP Pup)
Ao	smooth, fast decline without major disturbances, oscillations in the transition stage	GK Per, V603 Aql	Ro - rapid, oscillating star (GK Per)
Ar	smooth, fast decline, recurrent nova	T CrB, RS Oph	Rd - fast star with a drop in the light curve (T CrB)
B	decline with minor or major irregularities		
Ba	decline with standstills or other minor irregular fluctuations during decline	V533 Her, LV Vul	Sss - slow, smooth star (V841 Oph)
Bb	decline with major fluctuations (e.g. double or multiple maxima)	DN Gem, NQ Vul	
C	extended maximum, deep minimum in transition phase, with		Sd - slow star with a drop in the light curve (DQ Her)
Ca	small variation of visual brightness at maximum (< 2^m)	T Aur, DQ Her	
Cb	stronger brightness decline during maximum	FH Ser	
D	slow evolution, extended premaximum, delayed maximum, often with several brightness peaks	HR Del, RR Pic	So - slow, fluctuating star (RR Pic)
DR	recurrent nova with slow evolution and delayed maximum	T Pyx	
E	extremely slow nova with irregular light curve	V99 Sgr, V711 Sco	Sss - extremely slow star (RT Ser)

(*) from Duerbeck (1981)

Although it is impossible to say at the first recorded outburst if a nova will be recurrent or not, a few distinct points of difference in the light curve were identified by McLaughlin (1960). The recurrent novae return to minimum in less than one year, while classical novae remain usually brighter than their preoutburst magnitude for several years. Of the four recurrent novae classified by Duerbeck, three belong to his class A, i.e., show a smooth, fast decline, while only one—T Pyx—belongs to his class D, i.e., shows a slow evolution and a delayed maximum, like the very slow classical novae HR Del or RR Pic. The number of known recurrent novae is too small for this 3 to 1 ratio of fast to slow novae to have statistical significance.

Duerbeck derives the absolute magnitudes for 31 classical galactic novae (Table 6.4) by means of different methods: 1) nebular expansion parallaxes; 2) differential galactic rotation (the stellar radial velocity, based on the hypothesis that it is mainly due to the motion in a circular galactic orbit, and the galactic longitude, permit us to derive the distance; 3) the interstellar line strengths; and 4) the interstellar reddening. Figure 6.12 gives the relation M(V) at maximum vs log t(3). The existence of two well-separated groups is evident: the higher luminosity group includes only fast novae and the other slow and very slow novae. We will come back to this result in Chapter 7. Duerbeck shows that Group I can be interpreted by a quasi-instantaneous mass-loss at a lumi-

Table 6-3(*)
Classification of Light Curves of Galactic Novae

type A:	X Cir	(6.6)	Q Cyg	(22)	V476 Cyg	(16)	V1500 Cyg	(3.6)
	V446 Her	(16)	CP Lac	(10)	CP Pup	(8)	V630 Sgr	(6)
	V909 Sgr	(7.6)	V1059 Sgr	(<24)	T Sco	(21)	V697 Sco	(<15)
	V723 Sco	(17)						
type Ao:	V528 Aql	(35)	V603 Aql	(8)	DK Lac*	(32)	GK Per	(13)
	LU Vul	(21)						
type Ar:	T CrB	(6.8)	RS Oph	(18)	U Sco	(5.2)		
poss.A:	V368 Aql	(30)	V604 Aql	(24)	QZ Aur	(<34)	DM Gem	(22)
	HR Lyr	(80)	GI Mon	(37)	FL Sgr	(32)	KP Sco	(42)
type Ba:	EL Aql	(25)	V500 Aql	(42)	OY Ara	(83)	IV Cep	(37)
	V465 Cyg	(104)	V1668 Cyg	(23)	DM Gem*	(22)	V533 Her	(44)
	DK Lac*	(32)	V400 Per	(43)	V441 Sgr	(106)	V787 Sgr	(45)
	RU UMi	(140)	LV Vul	(37)				
type Bb:	DN Gem	(37)	DI Lac	(43)	V840 Oph*	(36)	V849 Oph	(175)
	V1016 Sgr	(176)	V1017 Sgr	(160)	FS Sct	(86)	V373 Sct	(85)
	NQ Vul	(65)						
poss.B:	V1229 Aql	(38)	V1301 Aql	(78)	RS Car	(?)	RR Cha	(?)
	IL Nor	(108)	V841 Oph	(112)	HS Pup	(65)	FM Sgr	(30)
	V363 Sgr	(80)	V1275 Sgr	(30)	V4021 Sgr	(100)	V368 Sct	(31)
type Ca:	T Aur	(100)	V450 Cyg	(100)	DQ Her	(94)	HZ Pup*	(70)
	V732 Sgr	(64)	V720 Sco	(17)				
type Cb:	V606 Aql	(34)	V726 Sgr*	(90)	V707 Sco	(49)	V719 Sco	(24)
	EU Sct	(42)	FH Ser	(62)	Ser 1978	(50)	XX Tau	(42)
	CQ Vel	(53)						
type D:	DO Aql	(900?)	EL Aql	(?)	V356 Aql	(~170)	HR Del	(230)
	RR Pic	(150)	X Ser	(?)	CN Vel	(800)		
type Dr:	T Pyx	(88)						
type E:	η Car	(?)	AR Cir	(415)	V794 Oph	(?)	HS Sgr	(?)
	V999 Sgr	(?)	V711 Sco	(?)	RR Ser	(?)	RR Tel	(?)

Note: the t_3 time is given in parentheses. Novae with uncertain light curve classification are marked with an asterisk.

(*) from Duerbeck (1981)

nosity far above the Eddington limit and Group II by continued radiation at the Eddington limit from a bloated white dwarf.

This finding is based only on galactic novae, because too few data are available for the Magellanic Clouds. Actually, the large extent of the Magellanic Clouds requires very long programs of surveys with "time resolution" sufficient to record the maxima and the time of decline. The surveys made by Arp (1956) and by Rosino (1964, 1973) would be suitable for a comparison with the galactic relation. However, novae of Duerbeck Group II can be classified only by a small fraction of their light curves, which is not sufficient for an accurate determination of t(3). Moreover, no very bright novae have been found in M 31, and the maxi-

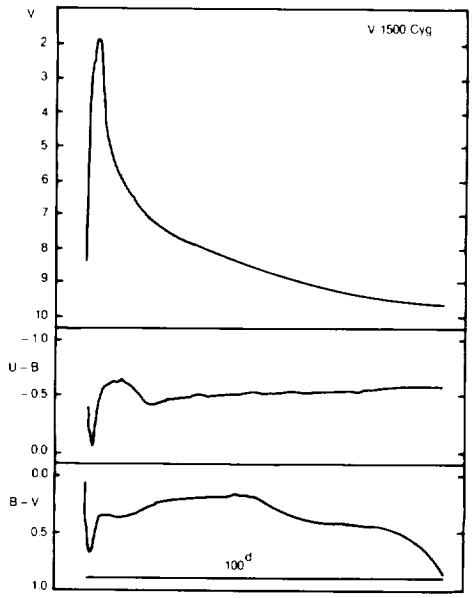

Figure 6-7. Light and color curves of V1500 Cyg (type A, Duerbeck classification)
(from Duerbeck, 1981)

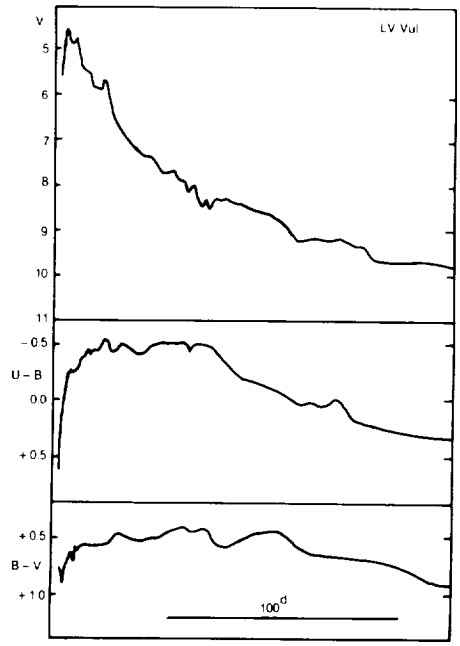

Figure 6-8. Light and color curves of LV Vul (type B)
(from Duerbeck, 1981)

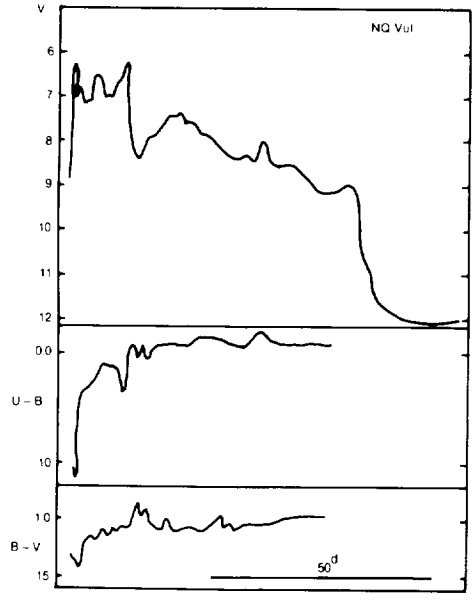

Figure 6-9. Light and color curves of NQ Vul (type Bb)
(from Duerbeck, 1981)

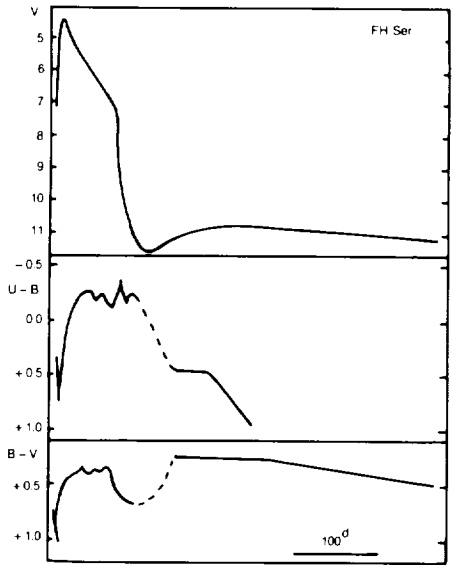

Figure 6-10. Light and color curves of FH Ser (type Cb)
(from Duerbeck, 1981)

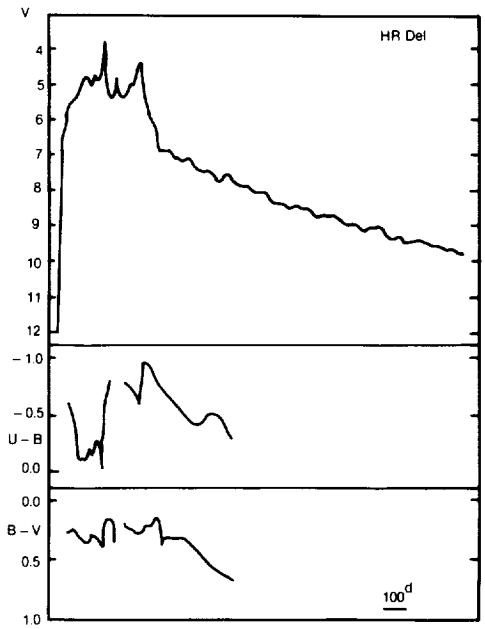

Figure 6-11. Light and color curves of HR Del (type D) (from Duerbeck, 1981)

mum brightness of novae of Duerbeck Group I is generally fainter than for galactic novae of Group I. A recent work by Van den Bergh and Pritchet (1986) discusses the observations of 73 novae in M 31 and the possibility of using novae as extragalactic distance indicators, if novae in all galaxies should turn out to have the same luminosity function at maximum light.

From a study of the nucleus of M 31 in the light of H Alpha, Ciardullo et al. (1983) have detected four novae and observed that the decay time of H Alpha emission was much longer than the decay time in the continuum. Hence, H Alpha emission of novae might represent a standard candle for extragalactic measurements. To be applicable, all these methods need disponibility of a very large number of observations of novae in nearby galaxies.

Van den Berg and Youngh (1987) have collected all the published UBV photometric data

Table 6-4(*)
Distances, Absorption Values, and Absolute Magnitudes of 35 Novae

object	a	b	m_{max}	m_{min}	M_{max}	M_{min}	type	t_2	d(pc)	A_v	source
V356 Aql	037.42	-04.94	7.0p	17.7p	-6.5	+4.0p	D	212	1700	2.04	N
V528 Aql	036.68	-05.90	7.2p	18.1p	7.6	+3.3p	Ao:	35	2400 - 600	2.6-0.6	N
V603 Aql	033.46	+00.84	-1.1p	11.6v	-9.6	+3.5v	Ao	8	330	0.5	UV
V1229 Aql	040.54	-05.44	6.5p	19p	-6.8	+5.7p	Ba?	38?	1730	1.6+0.4	D,N
T Aur	177.14	-01.71	4.1p	14.9v	-6.7	+4.4v	Ca	100	600	1.25+0.25	D,N
IV Cep	099.61	-01.64	7.5v	17.5v	-5.8	+4.3v	Ba	37	2050 + 150	1.65+0.1	D,N
T CrB	042.38	+48.17	2.0v	9.9v	-8.5	-0.6v	Ar	6.8	1250 + 600	0.08	N
V450 Cyg	079.12	-06.46	7.0p	17p	-5.9	+4.1p	Ca	100	1800 + 400	1.4+0.1	D
V476 Cyg	087.37	+12.42	2.0v	17.1v	-9.5	+5.2v	A	16	1650 + 50	0.85+0.4	D,N
V1500 Cyg	089.82	-00.07	1.85v	21B	-10.1	+10.1B	A	3.6	1350	1.25+0.25	App.
V1668 Cyg	090.84	+06.76	6.1v	20B	-6.2	+7.9B	Ba	23	2300 + 500	1.10	D,N
HR Del	063.43	-13.97	3.8v	11.9v	-6.5	+1.6v	D	230	880	0.56	D,N
DN Gem	184.01	+14.70	3.6p	15.6v	5.3	+7.0v	Bb	37	450 + 70	0.27+0.1	D,N
DQ Her	073.16	+26.44	1.3v	14.7v	-5.9	+7.5v	Ca	94	260	0.16	N
V446 Her	045.41	+04.71	3.0p	18.8p	-8.5	+6.8p	A	16	790 + 170	1.7+0.5	D,N
V533 Her	069.19	+24.27	3.0p	15.6v	-6.7	+6.2v	Ba	44	680 + 250	0.25	N
CP Lac	102.14	-00.84	2.1p	15.6p	-9.6	+3.9p	A	10	1000 + 100	1.5+0.1	D,N
DK Lac	105.23	-05.35	5.0p	15.5p	-7.2	+3.3p	B?Ao?	32	1500 + 200	1.2+0.2	D,N
BT Mon	213.86	-02.63	4.5:p	16p	-6.3:	+5.2p	?	42	1000 + 200	0.63	D
RS Oph	019.80	+10.38	5.0v	11.4v	-8.7	-2.3v	Ar	18	1800:	2.4:	App.
V849 Oph	039.23	+13.49	7.3:p	15p	5.9:	+1.8p	Bb	175	3100	0.72	N
GK Per	150.95	-10.11	0.2v	13.0v	-9.2	+3.7v	Ao	13	5250.7 +	0.15	D,N
RR Pic	272.36	-25.67	1.2p	12.0v	-6.9	+3.9v	D	150	400	0.04	N
CP Pup	252.92	-00.84	0.5p	14.3p	-11.5	+2.3p	A	8	1500	0.8+0.2	D,N
T Pyx	257.20	+09.70	7.0p	14.9v	-7.4?	+1.4v	Dr	88	3000 + 2000	0.35+0.05	N
V630 Sgr	357.77	-06.06	4.0p	14.4p	-9.3	+1.1p	A	9	2000	1.6+0.8	D,N
V1275 Sgr	355.07	-06.17	7.5p	13p	-6.2	?	B??	30?	3200 300	1.0+0.5	D,N
T Sco	352.67	+19.47	6.8v	12v	-9.2	?	A	21	12000	0.6	
U Sco	357.67	+21.88	8.5p	19.2p	-8.7	+2.0p?	Ar	5.2	17000?	0.95?	N
EU Sco	029.72	-02.97	8.0p	17.0p	-7.0:	+0.9:p	Cb	42	5060 + 1700	2.6+0.6	N
V368 Sct	026.67	-02.63	6.9v	18.6v	-5.8	+5.9p	B?	31	1750 + 350	1.6	N
FH Ser	033.91	+05.78	4.5v	15.1v	-6.9	+3.7v	Cb	62	650	2.3	N
Ser 1978	012.86	+06.04	8.3p	?	-7.0	?	Cb	50	4800	1.2	N
LV Vul	063.30	+00.85	9.5v	16.9B	-6.3	+5.4B	Ba	37	820 + 50	1.2:	D,N
NQ Vul	055.35	+01.28	6.1v	18.3p	-6.6	+4.6p	Bb	65	1200:	2.5+0.6	N

source of the extinction data: d=Deutschman, Davis and Schild (1976), N = Necket (1967)

(*) from Duerbeck (1981)

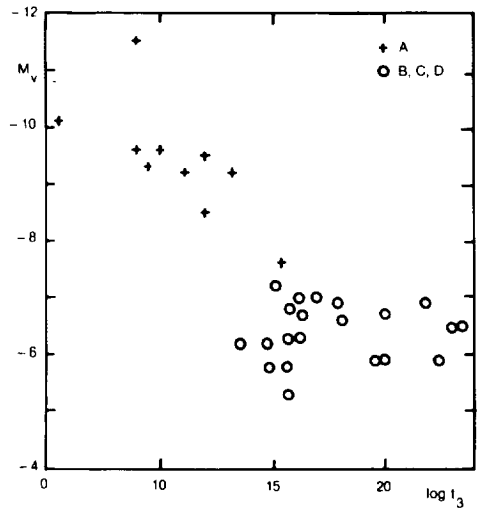

Figure 6-12. Absolute magnitude M_V vs. log t(3) for classical galactic novae.
(from Duerbeck, 1981)

on novae up to November 1, 1986. They have obtained two main results from this study:

1) The intrinsic color of novae two magnitudes below maximum is found to be $(B-V)_0$ = -0.02 +/- 0.04 with an internal dispersion σ (B-V) < 0.12 mag. At maximum $(B-V)_0$ = + 0.23 +/ - 0.06. The $(U-B)_0$ colors at maximum, on the contrary, present a large intrinsic scatter.

2) Novae with smooth light curves become redder both in B-V and U-B centered within one day of maximum light. This reddening lasts about 5 days for fast novae to 14 days for slow novae. That novae are reddest at maximum can be understood because at maximum they have maximum photospheric radius (and therefore minimum surface temperature).

III. SPECTROSCOPIC PROPERTIES

III.A. QUIESCENT PHASE.

For understanding the reason of the outburst, it would be extremely important to know the physical state of the star before and after the eruption. Unfortunately, very few data are available, especially for the phase preceeding the outburst. Low-resolution spectra obtained with objective prism in the photographic region from before outburst are available only for V 603 Aql 1918 (Cannon, 1920), V 533 Her 1963 (Stephenson and Herr, 1963) and HR Del 1967 (Stephenson, 1967).

V 603 Aql: all the spectra were underexposed. The best pre-eruption spectrum was obtained on July 1, 1899. The spectrum appears to be nearly continuous, but the Balmer series is detectable in absorption. The energy distribution resembles that of Class B or A, and Class G can be clearly excluded.

V 533 Her: the spectrum was recorded nearly two years before outburst, on June 16, 1961. The image is underexposed, and only a faint continuum is observable, with no detectable spectral lines, either in emission or in absorption. However, since the image is so weak, the only positive indication about the absorption lines is that there can be neither hydrogen lines as strong as those of an A-type star, nor H and K lines of Ca II as strong as in a normal G-type star, nor any of the several absorption features that would be seen in a spectral type later than G. The energy distribution between 4800 and 3300 A is very similar to that of a little reddened O star or early B.

HR Del: two well-exposed spectra were recorded on objective prism plates seven years before outburst, on July 16, 1960. The spectrum is continuous without any definite absorption or emission feature (at dispersion 580 A/mm at H Gamma), and the energy distribution is clearly that of an unreddened O or very early B-type star.

Like photometric observations, also the spectroscopic ones, although limited to these three cases, suggest that pre and post-outburst characteristics remain almost the same. However, for V 603 Aql, no absorption lines are observed—at the dispersion of 18 A/mm—in the postnova spectrum (Greenstein, 1960) while the prenova spectrum, according to Cannon, showed H I absorption lines observable at the much lower dispersion of her spectrograms.

Spectroscopic observations of old novae generally indicate that they present very blue continuous spectra with some weak emission lines. A complete review of data on postnova spectra was given by Greenstein (1960); see Table 6.5 from his paper. In addition to broad H I emissions, He I and He II emissions are observable in several cases, and , when relatively close to the epoch of the explosion, nebular lines are still observable; in all cases the excitation decreases with time after outburst. For instance, in the spectrum of Nova Her 1963 in 1967 when the nova was 1.5 mag above its minimum, the nebular lines of [O III] were strong, while in 1969 they were barely visible; in 1976 He II 4686 was fainter than the H I lines, and there was no trace of the nebular lines.

No definite evidence for the presence of absorption lines has been found in the spectra of past novae. The spectra of all novae at minimum are sensibly alike and do not appear to be correlated with the characteristics of the explosion. The emission line intensity and width are often variable, as indicated, for instance, by the extended series of observations made by Williams (1983). The lines are generally broad with widths of several hundreds of km/s, sometimes more than 1,000 km/s (Williams, 1983).

The spectra of five old novae (two slow and three fast novae) and one quiescent recurrent nova are shown by Wyckoff and Wehinger (1977). They present some differences that one can imagine to be related to their type: the two slow novae have Balmer lines much weaker than the three fast novae; the slow recurrent nova also has weak Balmer emissions and, moreover, does not present the 4640 emission, which is a blend of C III and N III (Figure 6.13). It is not clear if these differences are imputable to different physical conditions (temperature and density), or to a different chemical composition (i.e., a different evolutionary stage) or consequence of different conditions of the thermonuclear runaway, see chapter 7. By adding to these observations the data given by Greenstein (Table 6.5) we observe that generally the spectra of past novae of class Na have hydrogen lines stronger than helium lines, while the reverse is true for past novae of class Nb. The only exception is CP Pup 1942, which was an exceptionally fast nova and one of the brighter ones. This star showed also [O III] lines whose Doppler shift indicated that the original ejection velocities were still present. However, an extended series of spectroscopic observations of past novae, quiescent recurrent novae, dwarf novae and nova-like stars made by Oke and Wade (1982) and by Williams (1983) do not give evidence of systematic differences in the spectra of different classes of novae. The differences between spectra of single objects seem rather due to different physical conditions in the region where the spectrum is produced at the moment of the observations, and not to the characteristics of the outburst.

Panek (1979) has compared the energy distribution of the old nova V 603 Aql with that of one nova-like star and two dwarf novae at both quiescent and active phase. All spectra are similar, except that the old nova shows a very small Balmer discontinuity and stronger emission lines, especially 4686 He II. Panek shows the position of these objects (the old nova V 603 Aql, the dwarf novae VW Hydri, and UZ Ser just after outburst and in quiescence, and the nova-like star V 3885 Sgr) in a two-color diagram u-b, b-v (where u, b, and v were formed by averaging the linear fluxes measured at 3448 and 3636 A (u), 4210 and 4566 A (b), and 4990, 5556, 6055 A (v) and compares them with the position of black bodies at temperatures included between 50,000 K and 10,000 K and of model atmospheres with log g = 8 and effective temperatures between 50,000 K and 8,000 K. The four objects fall either on the black body line or between the black body and the model atmosphere curve. But we cannot generalize these results based on very few objects. A more extended sample of spectra of CV's has been collected by Williams (1983). He studies the spectra of 69 CV's including 13 old novae, (8 fast and 5 slow novae) and 4 quiescent recurrent novae, 29 dwarf novae, and 23 nova-like stars. This study indicates important differences in the spectra of the various old novae both in energy distribution and emission

line strength (Table 6.6 and Figure 6.14 a, b, c, and d), but no correlation with the subclass is apparent. Using his data, we have compared the line intensities of H alpha, H beta, 6678 and 5876 He I and 4640 C III+ N III, and their widths (in km/s) for the different classes of CV's. The line widths in general, (but there are exceptions) are an indication of the inclination of the system: all CV's show a loose correlation between *i* and the line width (Figure 6.15 a, b): the broader the emission lines are the closer to 90° the inclination of the accretion disk is. Warner (1986c) also found a correlation between the equivalent widths of H alpha, H beta, and 4686 He II and the orbital inclination (Figure 6.16). It is interesting to add that by using this correlation, Warner was able to estimate the effect of the orbital inclination on the magnitude of old novae, confirming the expectation given from the spectral characteristics that their main source of brightness at minimum is the disk. In fact, from the best available determinations of $M_{v(max)}$ and from the range $m_{v(max)}$-$m_{v(min)}$, he derives $M_{v(min)}$ and finds the correlation $M_{V(min)}$ vs cos i (Figure 6.17). The frequency distribution of the observed $M_{V(min)}$

Table 6-5

Characteristics of the Spectra of Old Novae

Nova	Spectrum and Other Data	Type
V603 Aql 1918	H>He II (Hu 1938; Mc 1950; and G 1957); He I, λ 4650 A present; Δλ=7A; no absortion lines at 18 A/mm	Na
T Aur 1891	Weak He II>H (Hu 1933, 1937)	Nb
T Crb 1866, 1946	Symbiotic, red companion, spec. binary; dwarf blue object is nova; recurrent U?	RN
Q Cyg 1876	Em. weak (Hu 1936); sharp and weak (G 1957)	Na
V476 Cyg 1920	H=He II (Hu 1936, Mc 1938); H>He II, broad > H (G 1958)	Na
EM Cyg	H>He II, broad (Burbidge); never seen at bright max; U?	—
DM Gem 1903	Continuous? (Hu 1933)	Na
DN Gem 1912	H weak (Hu 1933); He II=H (Mc 1933); He II broad > H (G 1958)	Nb
DQ Her 1934	He II>H, broad, Δλ=20 A, double em. lines (G 1956); variable in 4^{hr} period (Kraft); ratio of high-low series members changes at quadratures; eclipsing binary; shell still contributes	Nb
DI Lac 1910	Continuous (Hu 1936); broad absorption lines, like white dwarf, emission H>He II, sharp (G 1959)	Na
HR Lyr 1919	Continuous (Hu 1936); weak He II (G 1959)	Na
MacRae + 43 1	H>He I, variable ratio to continuum; Δλ=7 A(G 1953); never seen at bright maximim	—
V841 Oph 1848	Continuous (Hu 1936); He II>>H, He I weak (G 1956); lines sharp	Nb
RS Oph 1898, 1933, 1958	Symbiotic red star; complex em.; atypical; recurrent	RN
GK Per 1901	He II>H, He I, Δλ=16 A (Hu 1937); H>He II, He II = He I; Δλ=17 A (G 1953)	Na
CP Pup 1942	He II>>H, He I weak; [O III] persists in shell and shows original ejection velocities still present (G 1956); velocity structure absent in H and He II	Na
T Pyx 1890, 1902, 1920, 1944	He II>H, [O III] (Hu 1934); He II>>H, sharp (G 1956, 1958)	RN
V Sge	He II>H, *V/R* variable; Δλ=40 A; shortward-displaced core (Elvey and Babcock); never seen at bright maximum; (U?)	—
WZ Sge 1913, 1946	Continuous (Hu 1934); white dwarf absorption lines; Be type, H emission (G 1956)	RN
V1017 Sgr 1901, 1919	Continuous (Hu 1936)	RN

* G = Greenstein; Hu = Humason; Mc = McLaughlin. Dates given are those of observations of spectra. U? = Object may be related to U Gem stars or other nova like stars; Δλ = width of emission at half-intensity.

agrees with the theoretical distribution expected for randomly orientated disks (Figure 6.18).

The Figures 6.14 a, b, and c, give the equivalent widths for H alpha, H beta, 6678 and 5876 He I, 4686 He II and 4640 C III+ N III for all classes of CVs. When several measurements for a same star have been made, we have plotted the average values. The values are generally dependent from the state of the object (quiescent or in outburst for dwarf novae, while several old novae and nova-like stars may present line variability). In order to judge the degree of variability, we have given in the Table 6.6 the mean value and, in parenthesis, the standard deviation s, both for the line intensities and the line widths. We also report the intensity ratios H alpha/6678 He I, H beta/4686 He II, H alpha/H beta, and 4686 He II/5876 He I, in order to ascertain if the spectra of the members of the different classes present some systematic characteristics permitting us to distinguish one class from the other. As shown from the Figures 6.14, no clear systematic difference is evident. The comparison may be biased by the fact that the number of individuals among novae is much lower than among dwarf novae and nova-like. Hence the samples are not comparable. Anyway, we can say that 6678 and 5876 He I are generally stronger in dwarf novae and nova-like than in novae and recurrent novae. The intensities of H alpha and H beta are in large part included in the same interval of values for all classes, although very high values (W > 80 A) are found only among dwarf novae and nova-like stars. The same can be said for 4686 and 4640, although very high values for 4686 (W > 30 A) are found only among the nova-like stars. The 4640 line is

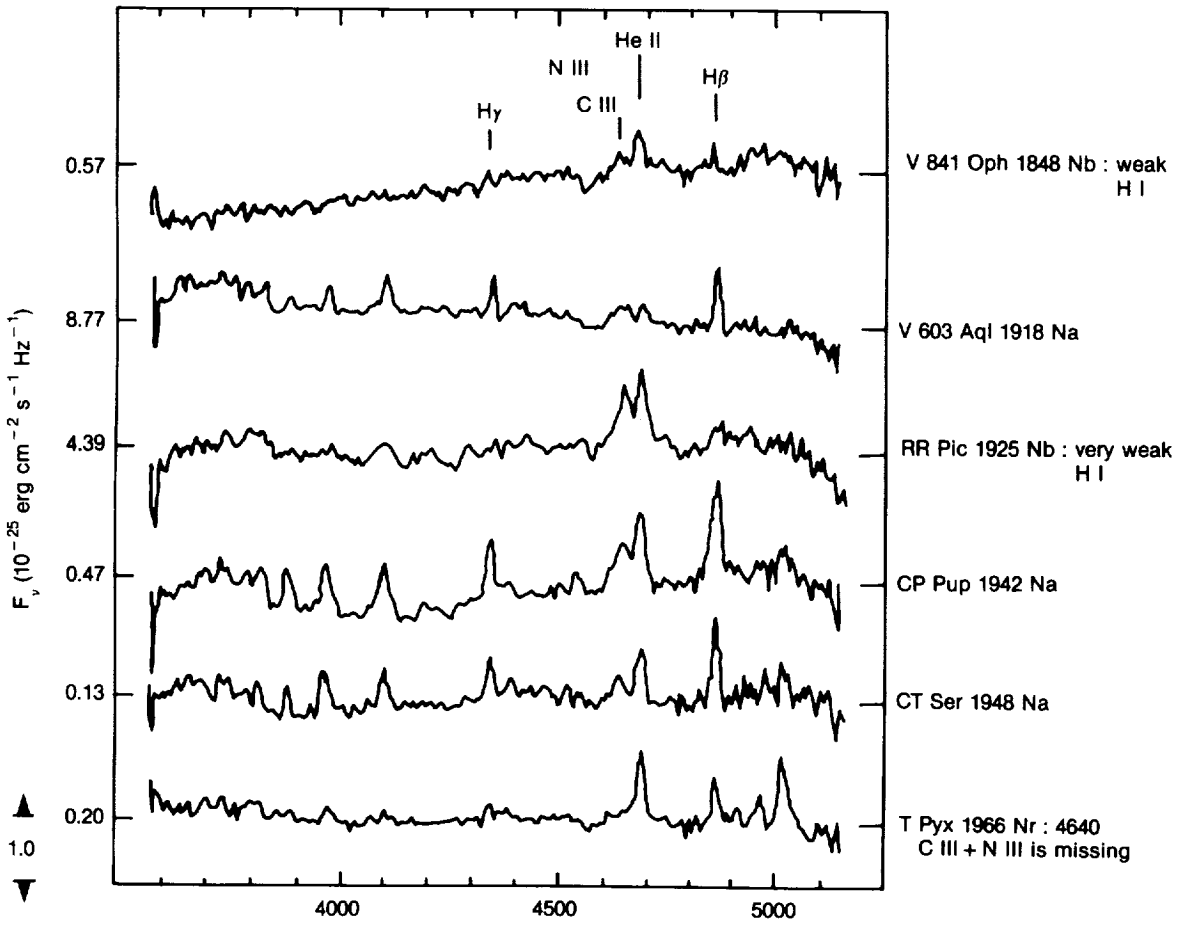

Figure 6-13a. Spectra of old novae (from Wyckoff and Wehinger, 1977)

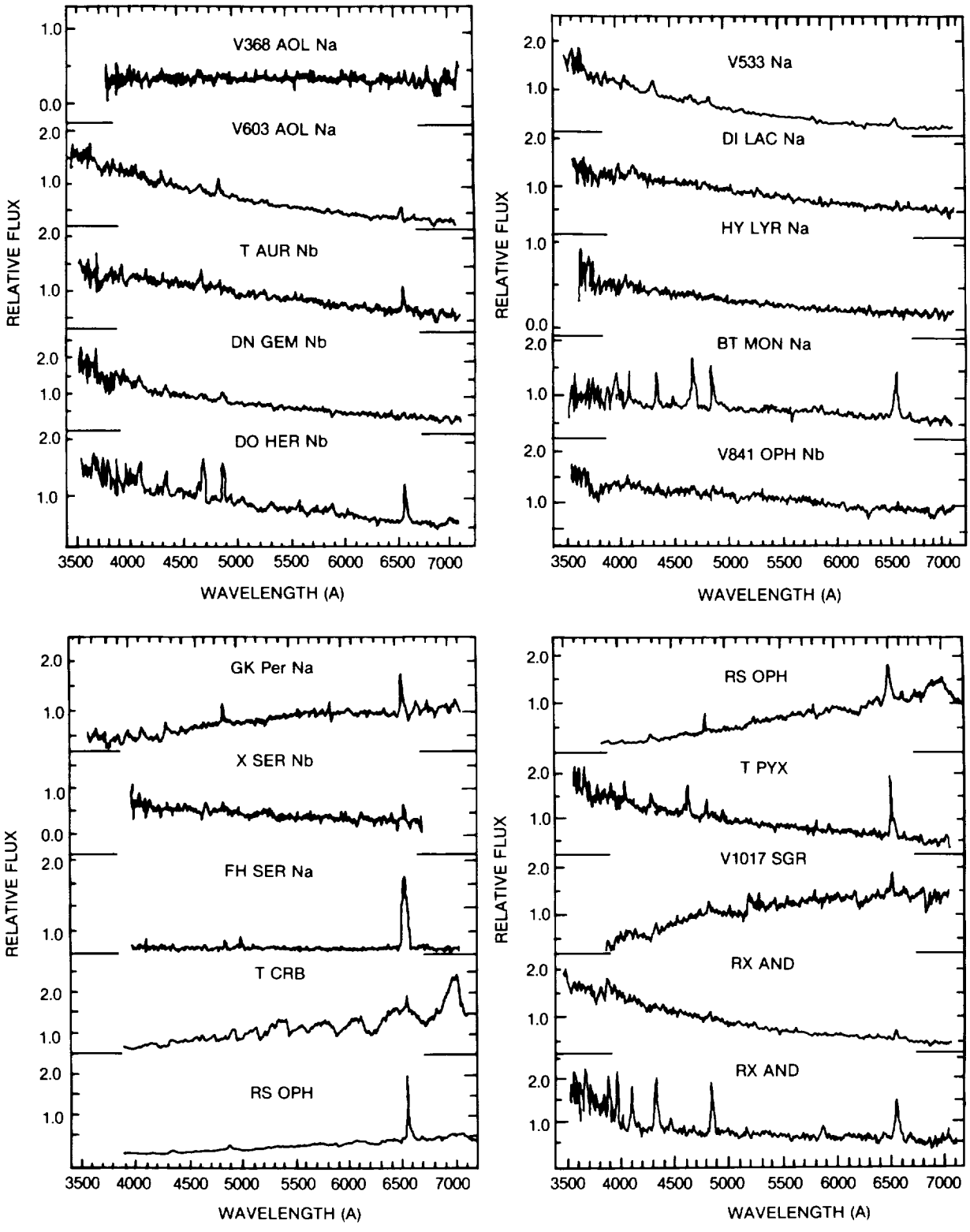

Figure 6-13b. Spectra of old novae (from Williams, 1983)

Table 6-6

Mean Equivalent Widths, Line Widths and Line Ratios for Novae, Recurrent Novae, Dwarf Novae and Nova-Like Stars. (Data from Williams, 1983).

Name	Class		Hα	Hβ	6678	5876	4686	4640	Hα/Hβ	Hα/6678	Hβ/4686	4686/5876 or (4686/6678)
V 603 Aql	N	Wλ(A)	13.3	6.9	2.7	2.4	4.4	3.3	1.9	4.9	1.6	1.8
i = 16		s	3.3	1.1	1.1	1.25	0.7					
		Δλ(Km/s)	210									
		s	87									
T Aur	N	"	24.1	6.7	5.7		10.1		3.6	4.2	0.7	(1.8)
i = 68°			5.4	1.8	-		-					
			467	583	474		1066					
			26	255	-		-					
DN Gem	N	"	9.3	8.4			4.4		1.1		1.9	
i = 30°		-	-			-						
			329	562			619					
			-	-								
DQ Her	N	"	70	23	3.4	4.8	15.3	5.9	3	20	1.5	3.2
i = 89°			40	8.7		1.9	2.4	1.3				
			547	495	366	290	513	425				
			50	31		170	63	47				
V533 Her	N	"	22.2	4.9	4.3				4.5	5		
i = 62°			-	-								
			653	396	600							
			-	-	-							
DI Lac	N	"	3.6		2.0	3.5				1.8		
i = 30°			-			-						
			81			282						
BT Mon	N	Wλ(A)	47	28	5.3	5.6	25	9	1.7	8.9	1.1	4.5
i = 84°		s	7.5	6		1.3	4.5	3				
		Δλ(Km/s)	438	545	312	235	424	495				
		s	158	136		49	32	85				
V 841 Oph	N	Wλ	2.6									
i = 0												
GK Per	N	Wλ	19	10.8	5.2	3.9	2.4		1.8	3.7	4.5	0.6
i = 75°		s	1.3		1.8	0.25						
		Δλ	323	309	344	149						
		s	57		40	110						

Table 6-6 (continued)

Mean Equivalent Widths, Line Widths and Line Ratios for Novae, Recurrent Novae, Dwarf Novae and Nova-Like Stars. (Data from Williams, 1983).

Name	Class		Hα	Hβ	6678	5876	4686	4640	Hα/Hβ	Hα/6678	Hβ/4686	4686/5876 or (4686/6678)
X Ser	N	Wλ	23.4	7.1	6.2		9.3		3.3	3.8	0.76	(1.5)
		Δλ	317	259	70		609					
FH Ser	N	"						9.4	1.5		3	
i = 40°		54.2	37.3			12.5						
		749	378			289						
T CrB	RN	"	5.35	3.5					1.4			
			1.2	0.4								
RS Oph	RN	Wλ	53.2	12.7	3.9	2.1			4.2	13.6		
T Pyx	RN	Wλ	74.6	9.7	5.5	3.4	13.7	3.5	7.7	13.6	0.71	4
		Δλ	687	554								
RX And	DN	Wλ	23.3	17.3	7.1	7.75			1.35	3.3		
i = 65°		s	24.3	27	8.3	8.4						
		Δλ	304	353	283	350						
		s	204	215	191	284						
AR And	DN		56	38.8					1.4			
		"	22	0.4								
			581	540								
			1	228								
UU Aql	DN		60	65.6	4.2	8.0			0.9	14.3		
		"	9.4	21		2.5						
			401	562		272						
			35	153		-						
Z Cam	DN	"	11.3	4.5	0.9				2.5	12.5		
			4.2	0.7								
i = 60°			421	359								
			-	-								
SS Aur	DN	Wλ(A)	109	108	10.2	26.2	13		1.0	10.7	8.3	0.5
i = 32°		s	6.5	13.5	1.3	4.5						
		Δλ(Km/s)	444	639	396	435	767					
		s	41	114	111	113						
FS Aur	DN	"	30.9	48	5.3	5.7	8.2		0.64	5.8	5.8	1.4
		"	4.7	18	-	-	4.4					
			358	737	230	125	907					
			30	235	-		-					

Table 6-6 (continued)

Mean Equivalent Widths, Line Widths and Line Ratios for Novae, Recurrent Novae, Dwarf Novae and Nova-Like Stars. (Data from Williams, 1983).

Name	Class		Ha	Hb	6678	5876	4686	4640	H_α/H_β	H_α/6678	H_β/4686	4686/5876 or (4686/6678)
HT Cas	DN	"	204	107	33	38.6	12.1	16.8	1.9	6.2	8.9	0.3
i = 76°			4	13.6	15	14	-	-				
			831	987	935	1206	1437	1407				
			18	63	354		-	-				
WW Cet	DN	"	32.6	34	2.7	6.0			0.96	12		
i = 40°			6.3	12.2	-	0.7						
			538	761	247	412						
			155	124	-	81						
1E 0643.0	DN	"	47.4	46.9	6.15	15.5	18.6	4.3	1.01	7.7	2.5	1.2
			19.6	30	3.5	6.2	9.0	0.7				
			478	594	351	425	1142	310				
			65	207	179	107	474	26				
SY Cnc	DN		13.2	13.7	9.5	5.1			0.96	1.4		
i = 50°		"	13	-	-							
			327	498	671							
			172	-	-							
YZ Cnc	DN		65.5	54.5	15.9	28.5			1.2	4.4		
			74.5	62.4	10.5	14.2						
		"	449	737	485	612						
			243	360	4	18						
SS Cyg	DN	Wλ(A)	48.9	55.6	6.3	9.0	6.9		0.88	7.8	8.0	0.77
i = 30°		s	12.5	22	1.1	2.3	1.6					
		Δλ(Km/s)	456	592	394	134	995					
		s	151	169	71	61	531					
EM Cyg	DN	Wλ	5.0	2.6			4.8		1.9		0.5	
i = 63°												
AB Dra	DN	Wλ	31.3	19.6	3.7	3.6	3.2		1.6	8.4	6.1	0.9
		Δλ	564	973		370	947					
U Gem	DN		58.3	15.4		12.8			3.8	(4.4)		
i = 67°		"	626	579		648						
IR Gem	DN	"	117	80.6	18.7	29	15.2		1.5	6.2	5.3	0.5
i = 50°			478	554	392	332	1209					

Table 6-6 (continued)

Mean Equivalent Widths, Line Widths and Line Ratios for Novae, Recurrent Novae, Dwarf Novae and Nova-Like Stars. (Data from Williams, 1983).

Name	Class		Hα	Hβ	6678	5876	4686	4640	H_α/H_β	H_α/6678 (H_α/5876)	H_β/4686	4686/5876 or (4686/6678)
AH Her	DN	Wλ	26.4	26.5		3.2			1.0	(8.2)		
i = 46°		Δλ	427	682								
EX Hya	DN	Wλ	98.4	70	10.4	19.6	14		1.4	9.0	5.0	0.7
i = 75°		s	0.3	14	3.1	1.9	3.9					
		Δλ	860	1192	570	770	1282					
		s	48	279	219	52	165					
T Leo	DN	Wλ	203	115	22.7	38.7			1.76	8.9		
i < 50°		Δλ	500	457	321	472						
X Leo	DN	"	30.8	22.3	2.5				1.4	(12.3)		
i=45°			564	919								
CN Ori	DN	"	14									
i = 50°			550									
CZ Ori	DN	"	87.7	43.5						2.0		
			758	503								
RU Peg	DN	Wλ	10.9	4.5	3.1	2.2	2.9		2.4	3.5	1.6	1.3
i = 32°		s	3.9	0.3								
		Δλ	175	516	201							
		s	156									
KT Per	DN	Wλ	14.5	18.6					0.8			
i = 65°		s	-	-								
		Δλ	544	871								
		s	-	-								
WZ Sge	DN	Wλ	123	27.8	8.5	4.1			4.4	14.4		
		Δλ	893	725	404	325						
SW UMa	DN	Wλ	129	67.9	12.6	19.8			1.9	10.2		
i = 50°		s	17	5.2		1.9						
		Δλ	506	741	249	583						
		s	8	119		8						
TW Vir	DN	"	72.5	80	14	20	13.7		0.9	5.2	5.8	0.7
i = 43°			16	14	9	5	5					
			497	695	529	447	1044					
			63	103	139	85	163					

Table 6-6 (continued)

Mean Equivalent Widths, Line Widths and Line Ratios for Novae, Recurrent Novae, Dwarf Novae and Nova-Like Stars. (Data from Williams, 1983).

Name	Class		H_α	H_β	6678	5876	4686	4640	H_α/H_β	H_α/6678 (H_α/5876)	H_β/4686	4686/5876 or (4686/6678)
Z And	NL	Wλ	174	43					4.0			
		Δλ	187									
AE Aqr	NL	Wλ	34	21.6	1.5				1.6	23		
i = 64°		s	14									
		Δλ	369	369	264							
		s	35									
TT Ari	NL	"	26	13	4	5.8			2.0	6.5		
i = 23°			17	9	1	5.9						
			248	118	115	166						
			32	145	76	80						
KR Aur	NL	Wλ	12.1	5.3					2.3			
		Δλ	254	400								
G 61-29	NL	"			50.5	73	35.1					0.5
					808	852	1845					
YY Dra	NL	"	124	129	9.8	24.9	12.7		0.96	12.7	10.1	0.5
			596	739	424	389	1059					
2A 0311-227	NL	"	20.8	43.9	1.9	5.9	33.7		0.5	10.9	1.3	5.7
			686	901		457	1192					
VV Pup	NL	"	123	93.9	18.6	19.4	69.2	15.9	1.3	6.6	1.4	3.6
			661	513	478	311	435	551				
AM Her	NL	W_λ(A)	55	34	7.7	7.5	15.6		1.6	7.1	2.2	2.1
		s	24	20	2	6.4	2.3					
		Δλ(Km/s)	307	333	266	297	298					
		s	126	135	68	202	49					
V 426 Oph	NL	Wλ	31.3	14.9	2.8	1.6			2.1	11		
i = 60°		Δλ	659	813	184							
V 442 Oph	NL	"	12.5	4.8	4.3		3.9		2.6	2.9	1.2	(0.9)
			322	469	269		354					
V 2051 Oph	NL	"	193	124	24.8	35.3	9.9		1.6	7.8	12.5	0.3
			787	853	532	517	999					

Table 6-6 (continued)

Mean Equivalent Widths, Line Widths and Line Ratios for Novae, Recurrent Novae, Dwarf Novae and Nova-Like Stars. (Data from Williams, 1983).

Name	Class		H_α	H_β	6678	5876	4686	4640	H_α/H_β	H_α/6678 (H_α/5876)	H_β/5686	4686/5876 or (4686/6678)
HK Sco	NL	Wλ	334	113	7.6	12.7	47.1		2.95	44	2.4	3.7
		s	173	65								
CL Sco	NL	Wλ	427	58	9	12.5	7.5	7.6	7.4	47	7.7	0.6
		s	194	11	2	2	1	2.7				
		Δλ	305	150	110	23	186	280				
		s	178	183	27			80				
V Sge	NL	"	166	59			111	7.6	2.8		0.5	
			2	5			6	3.2				
			785	724			720	342				
			55	73			83	136				
V 3890 Sgr	N or NL	Wλ	379	59.6	14.1	35.5	16.7	18.0	6.35	27	3.6	0.5
		Δλ	514	208	81	171	227	462				
RW Tri	NL	Wλ	16.6	6.0	1.3		5.0		2.8	12.8	1.2	(3.8)
i = 72°		s	6	2.8	0.6		0.8					
		Δλ	636	442			555					
		s	215	145			201					
UX UMa	NL	"	16	6.5		3.2	4.5		2.5	(5)	1.4	1.4
i = 72°				4.9			0.8					
			384	516			559					
			71	180			280					
AN UMa	NL	W_λ(A)	33	26	11.4	3.4	12.3	3.3	1.3	2.9	2.1	3.6
		s	3	2.8		0.9	0.5					
		Δλ(Km/s)	366	722	266		321					
		s	114	86			103					
2H 2215-086	NL		68.6	23.5	6.6	5.8	17.2	4.2	2.9	10.4	1.3	3
		"	17	5	1.3	2.7	1.5	1.9				
			442	469	351	418	396	381				
			43	205	212	148	129	222				
2H 2252-0.35	NL		20.2	9.2	3.5	2.7	4.7	3.0	2.2	5.8	2.0	1.7
		"	5	1.2	1.3		0.6					
			398	449	204	327	311	631				
			78	119	93		89					
0623+71	NL	Wλ	6.5									

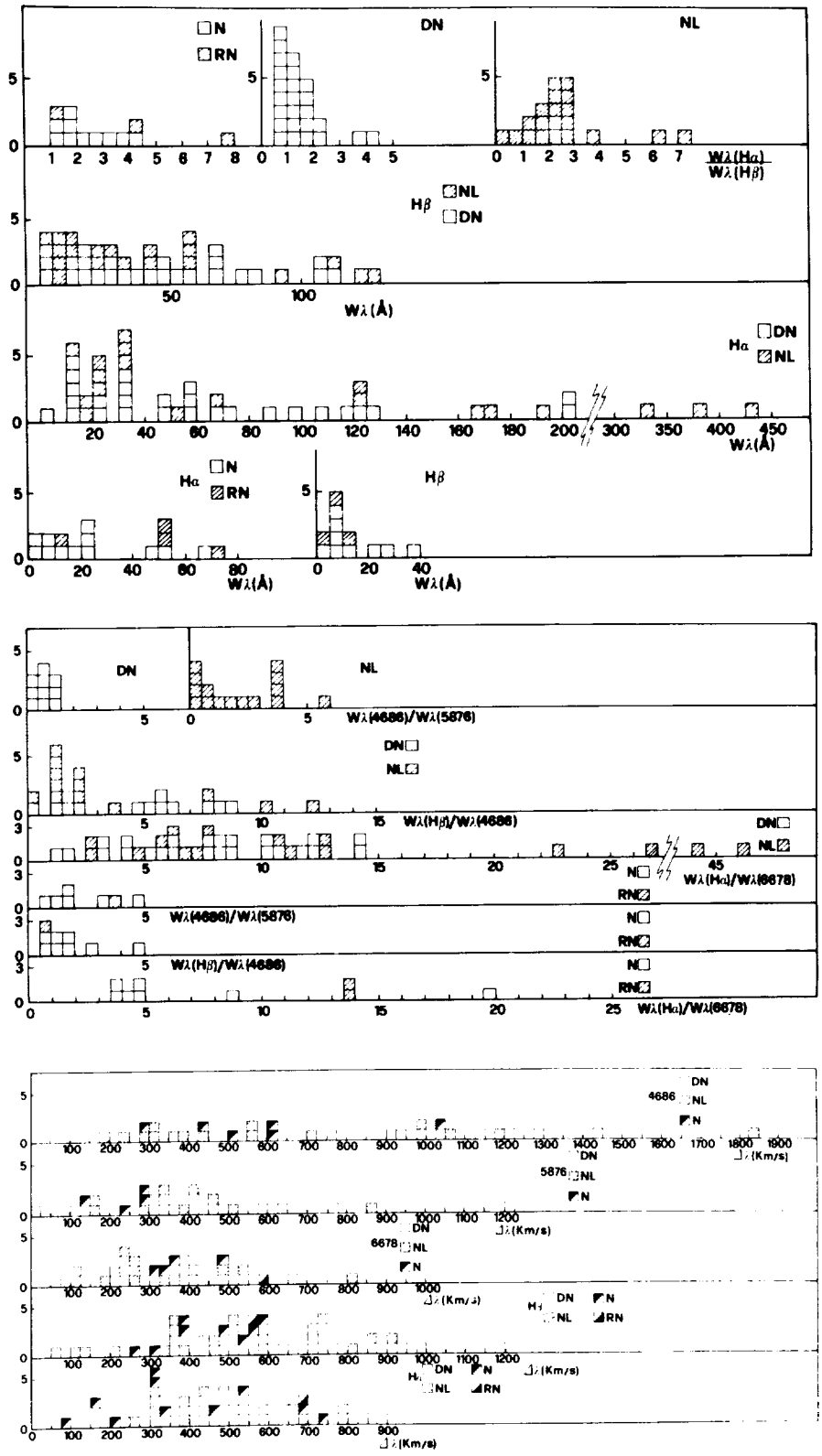

Figure 6-14 -a) The equivalent widths of Hα, Hβ and the ratio Hα/Hβ for classical and recurrent novae, dwarf novae and nova-like stars. b) Ratios of the equivalent widths Hα/6678, Hβ/4686, 4686/5876. c) Widths (km/s) of Hα, Hβ, 6678, 5876, and 4686 for classical and recurrent novae, dwarf novae and nova-like stars.
(data from Williams, 1983)

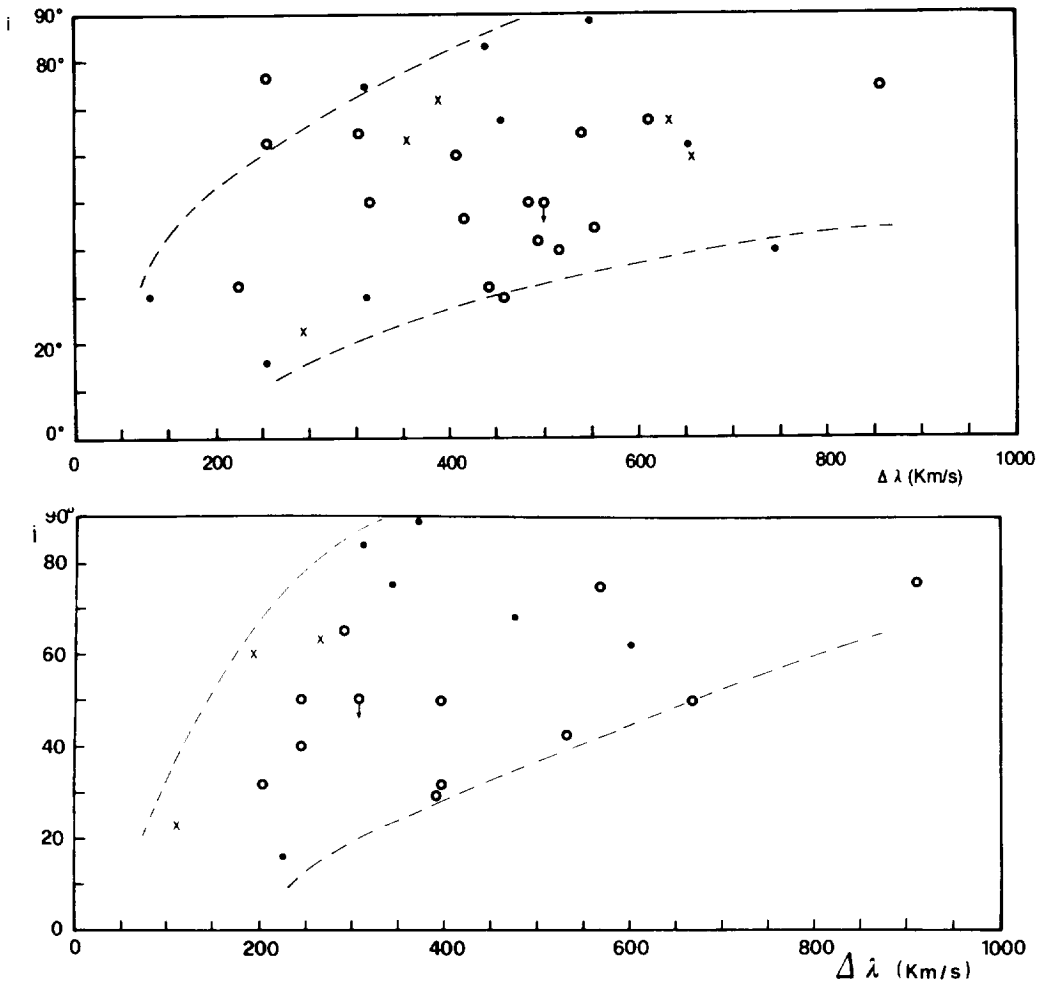

Figure 6-15 -a) Orbital inclination of the system versus the line width (km/s) of H α for classical novae (black dots), dwarf novae (circles) and nova-like systems (crosses). b) same as a) for 6678 He I.
(data from Williams, 1983)

generally absent or not measurable in dwarf novae. The ratio H alpha/H beta for the majority of novae and dwarf novae is included between 1 and 2, and few have values between 2 and 5. About 50% of nova-like stars on the contrary, have values between 2 and 3. This value is a measure of the Balmer decrement, which is a well-known indication of the physical mechanisms at work in the gas, depending on the physical conditions of it (optical thickness and temperature).

The line widths for novae are included in the same range of values as those for dwarf novae and nova-like (but the highest values—ΔV > 1000 km/s—are found among dwarf novae and nova-like stars.

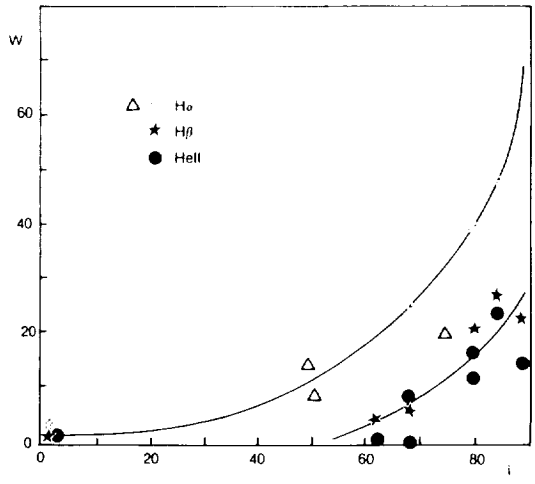

Figure 6-16. Correlations between emission-line equivalent width and orbital inclination. The triangles are data from Williams (1983), the others from Warner (1986).
(adapted from Warner, 1986)

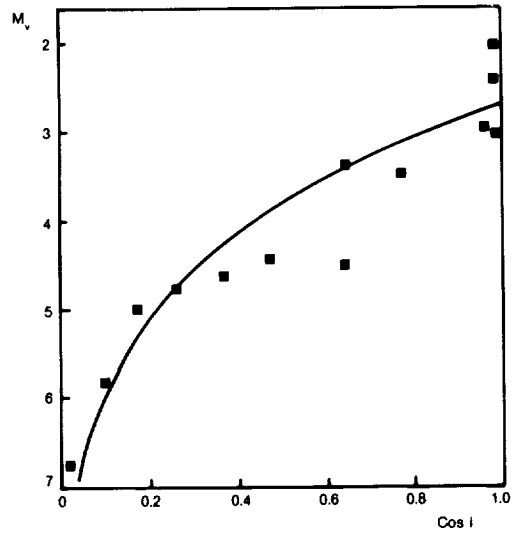

Figure 6-17. Correlation between absolute magnitude M_v and orbital (or disc) inclination for old novae. (from Warner, 1986 c)

WY Sge 1783 also shows a typical old nova spectrum with a faint blue continuum and strong emission of H I, He I and He II, C III+ N III, variable with the orbital phase (Shara and Moffat, 1983; Shara et al. 1984) (Figure 6.19 a, b). The central object of the very old nova CK Vul 1670, on the contrary, is too faint to be detectable. Only the nebulosities ejected from the nova are observable, and they present a spectrum characterized by a strong H alpha emission (Shara et al., 1985).

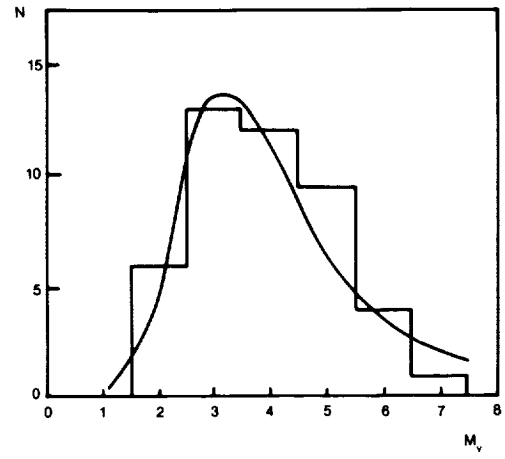

Figure 6-18. Frequency distribution of absolute magnitudes (histogram) compared with theoretical distribution (continuous curve) for randomly orientated discs broadened by a Gaussian with 1 mag dispersion. (from Warner, 1986 c)

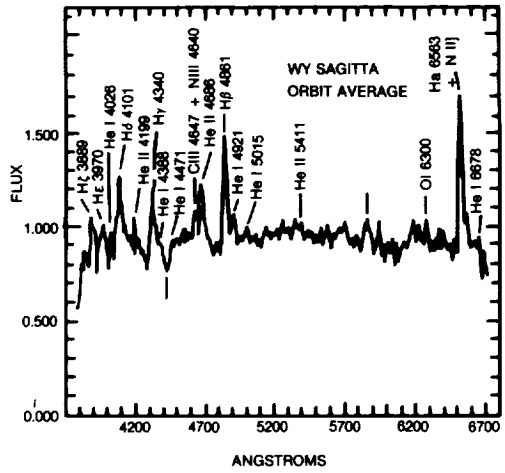

Figure 6-19a. The spectrum of the old nova WY Sge (1783), orbit averaged. (from Shara and Moffat, 1983)

No trace of absorption lines and in particular of lines of a late-type companion is generally found in classical post-novae spectra, even in the case of GK Per, whose color is that of a K-type star and whose orbital period is exceptionally long among novae, 1.99 days.

Among dwarf novae, on the contrary, the spectrum of the late companion is generally visible when the orbital period is longer than about 6 hours, because then the orbital size is large enough to house a sufficiently bright red star. This rule is apparently not valid among old novae; beside GK Per, also the cool component of BT Mon - orbital period 8.01 hours - contributes only about 6% to the total luminosity of the system (Robinson et al. 1982). The other past novae with known orbital period larger than 6 h are V 1668 Cyg (P = 10.54 h) and Nova Lac 1910 (P = 13.05 h). No evidence of a late-type companion is found in the spectrum of the former, while no data are available for the latter.

Although the spectrum of GK Per in quiescent phase does not show the strong blue continuum and the strong flux at 4686 He II and at 4267 C II generally present in old nova spectra, during its minor recurrent outbursts the spectrum becomes more similar to those of the majority of old novae. Spectra obtained at different moments of the minor outbursts (Figure

6.20, Bianchini et al., 1982) indicate that the ratio 4686 He II/H beta increases regularly with increasing brightness. Hence, during these outbursts, the spectrum of GK Per becomes more similar to those of the other old novae. The line width measured at zero intensity in outburst and in quiescence has about the same value—40 A (Szkody et al., 1985).

In the case of DQ Her, which is a well-ascertained binary, as indicated by the occurrence of eclipses, Kraft (1959) was able to show that

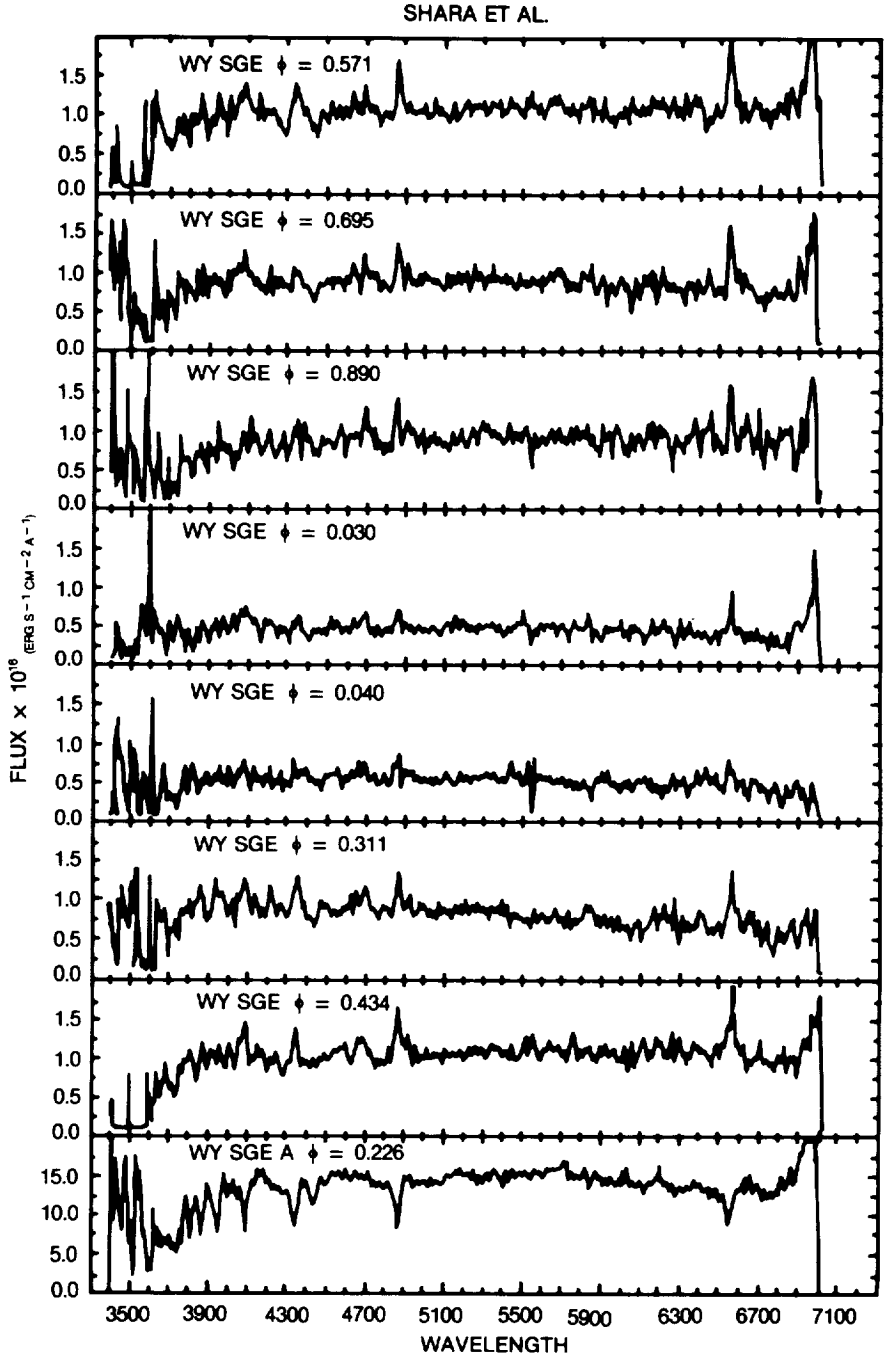

Figure 6-19b. The spectra of WY Sge at different phases. (from Shara et al., 1984)

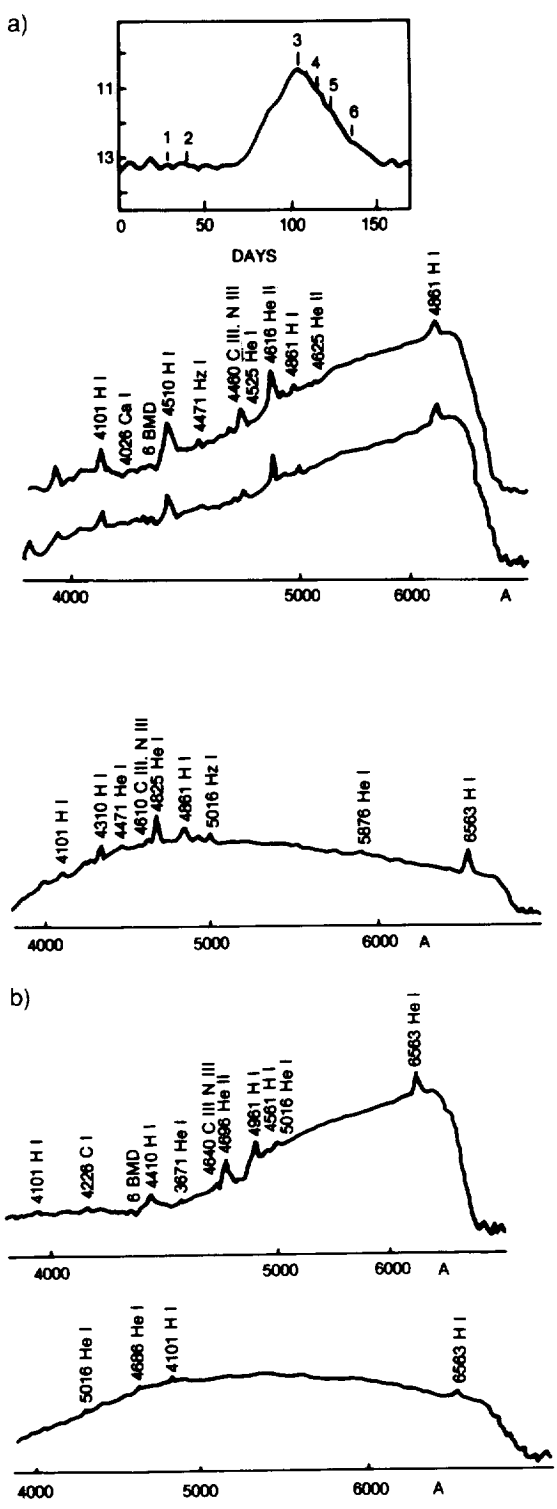

Figure 6-20a. Mean light curve of GH Per of the 1975 and 1981 outbursts. The positions when the spectra shown in b) have been taken is indicated. b) Density tracings of spectra obtained in vicinity and during the 1975 and 1981 outbursts.
(from Bianchini et al., 1982)

both the line and continuum emission arise mainly from a region near the compact component. In fact, the rotational disturbance(*) in the radial velocity curve of λ 4686 (Kraft, 1958) and the onset of the eclipse begin at the same moment, indicating that the He II emission and the continuum originate in the same region. From the Balmer jump, the He II intensity, and the observed colors, an electron density N_e = 3 x10^{13} cm^{-3} and a T_{color} 40,000 K are derived. These values support the picture that much of the light comes from a rather dense disk or ring surrounding the nova.

The very slow nova RT Ser (1909) is probably an exception among classical novae. Spectra taken in the red region in 1975 and 1978, in addition to the nebular emission lines, show TiO absorption bands. Spectra taken in the blue region in 1964 show only nebular emissions, but probably this is not due to a real variation of the spectrum but rather to the fact that the cool companion becomes more easily detectable in the red region (Fried, 1980). Another very slow nova—RR Tel—shows the presence of a red giant component as indicated by its spectral characteristics. The two recurrent novae T CrB and RS Oph also show a symbiotic spectrum with evidence of a red giant companion. Hence, it seems that the visibility of the two spectra and the luminosity of the red companion - class III - are characteristics common to symbiotics and to some recurrent novae and some very slow novae, which are often also called symbiotic novae.

III.B. SPECTRA DURING THE OUTBURST AND DECLINING PHASES OF NOVAE

Several indicators of nonthermal phenomena are observed in the spectra of the majority of novae during their explosive phases:

(*) We remind that the rotational disturbance consists in a deviation of the orbital radial velocity curve occurring just at the beginning and at the end of the eclipse. The radial velocity of the eclipsed star shows an excess of positive velocity at the beginning of the eclipse (when the part of the stellar disk, rotating toward us, is eclipsed; the reverse occurs at the end of eclipse (in the hypothesis that, for mechanical reasons, rotation and revolution occur in the same directions).

1) Anomalously high ionization, which probably requires nonradiative heating (e.g., presence of coronal lines).
2) Nonthermal widths of spectral lines (up to 3000-4000 km/s).
3) Nonthermal atmospheric extent (from less than 1 solar radius up to several hundreds solar radii as derived by the product of the expansion velocity by the time elapsed from outburst).
4) Mass-flow, as indicated by the line-shifts and the asymmetric line-cores and wings.
5) Simultaneous presence of high and low excitation + ionization features.

Hence, we have macroscopic evidence of mass-flux and mechanical heating of the atmosphere.

III.C. DEVELOPMENT OF THE SPECTRUM DURING THE OUTBURST

The spectra at maximum are generally similar to those of an A- or F-type supergiant. V 1500 Cyg 1975 had one of the earliest type, B2 Ia and V1148 Sgr 1943 the latest (K-type).

Although the absorption spectra of novae at maximum are similar to those of supergiants of Classes B, A, or F, they are not identical to them. However, if we consider the violence of the outburst, it is rather surprising that they are so similar.

The spectra are characterized by absorption and emission lines (P Cygni profiles).

Several typical absorption systems have been identified. Figure 6.6 shows schematically the shape of the light curves for fast and slow novae and indicates when the various spectral systems are present.

The PREMAXIMUM spectrum is observed during the light increase until just after maximum. It generally resembles a spectral type of a B or A supergiant. The PRINCIPAL spectrum replaces the premaximum within a few days after maximum and persists until the nova has faded by about 4 mag. The principal spectrum closely resembles the premaximum spectrum and it is often difficult to distinguish the one from the other. However, in general, the premaximum spectrum tends to be hotter than the principal spectrum. Generally, the latter is similar to that of an A or F supergiant with Ca II lines stronger than normal and strong lines of O I and C I. The Mg II line at 4481 A weakens rapidly, while the lines of Fe II, Ti II, and Mg I, with lower levels in a metastable state, persist along with the H I lines. Hence, there is evidence of increasing dilution of the radiation incident on the expanding principal shell. The expansional radial velocity is larger than that indicated by the premaximum spectrum. The DIFFUSE-ENHANCED spectrum appears later than the principal one; it reaches maximum strength at about two magnitudes below maximum. It presents strong and wide lines of H I, Ca II and usually Fe II, O I, and Na I. Slow novae have richer diffuse-enhanced spectra, with lines of Ti II and Cr II. In the later stages, the hydrogen lines can present several components. The expansional radial velocity is about two times larger than that indicated by the principal spectrum, and it is often variable with time. The ORION spectrum (so called because it is similar to the spectra of the B-type stars in the Orion nebula) appears when the diffuse-enhanced is strongest and reaches its maximum intensity at three magnitudes below maximum. It resembles that of an early-type star with O II and N II relatively strenghtened. Hydrogen lines can be either present or absent. The radial velocity is variable and equal or higher than that of the diffuse-enhanced spectrum.

These four systems account for all but a few absorption features. To each absorption system, a corresponding emission system is correlated. In fact, all the absorption and corresponding emission features form the characteristic P Cyg profiles, which are typical of the expanding envelopes. Moreover, another emission system—the NEBULAR system—appears when the nova has weakened by four magnitudes and is completely developed when the nova is still three magnitudes weaker; i.e., seven magnitudes below maximum. At first it

consists of lines typical of nebulae, like [NI], [OI], [NII], [OII], [OIII] and later on of coronal lines. We define "coronal lines" those with upper potential higher than 125 eV, corresponding to the ionization potential of Fe VII.

The nebular emission lines have the same width as the emissions associated with the principal spectrum: this means that when the shell is diluted enough to become optically thin in the continuum (and therefore when the absorption lines disappear), it is still optically thick in the lines and produces the nebular spectrum. In this sense, one says that the nebular spectrum "replaces" the principal spectrum.

The postnova system is observable when the nova envelope is dissipating in the interstellar medium. Nebular and coronal lines are present. The nebular spectrum is characterized by the permitted emissions of H I, He I, He II, N II, N III, N IV, O II, O III, O IV, C II, Si IV, and by the forbidden emissions of O I, O II, O III, N II, Fe II, Fe V, Fe VI, Fe VII, Fe XIV, Ne III, Ne IV, Ne V, A X, Ca V, S II, K V, Ni VIII, Ni XIII, Ni XVI, and Na IV, with ionization potentials ranging between 13 and 500 eV. Hence, the regions where the coronal lines are formed are similar to those observed in the solar corona. The temperature of these regions is much higher than that of the stellar photosphere (required electron temperature $Te > 10^6$) and still much higher than that of the dusty envelope surrounding the majority of past novae, and which is indicated by their infrared spectrum. Several mechanisms of heating of the "corona" have been proposed and will be discussed in Chapter 7.

The coronal lines become observable a few months after outburst and remain observable sometimes for years. A few examples are given by Malakpour (1980). Very slow nova HR Del 1967: the outburst occurred on June 6, 1967; the coronal lines were observed in November 1972, 4 years after the onset of the nebular phase. Fast nova V 433 Her 1960: the outburst occurred on February 26, 1960; the coronal lines became observable already on March 20, 1960, but became almost invisible in August 1960. Fast Nova Her 1963: the outburst occurred between the 19th and the 28th of January 1963. The coronal lines became visible on February 11, 1963, and were observed until July 1963. Slow Nova FH Ser 1970: the outburst occurred on February 11, 1970; only one coronal line, 5534.6 [A X], was observed in August 1970 and was not present on May 25, 1970. Slow nova V373 Sct 1975: the outburst occurred on April 4, 1975. The coronal lines were observable from July 14 to the end of August. Very fast nova V 1500 Cyg 1975: the outburst occurred on August 25; the coronal lines were not present on September 12, but they were present on September 29, and were still present in January 1976.

The mechanical energy liberated by mass-loss during the explosion is comparable to the radiative energy produced: both are of the order of 10^{44} ergs.

III.D. EXPANSION VELOCITIES

The expansion velocities are correlated with the speed class and with the spectral type at maximum. Moreover, the expansional velocities of the various absorption systems generally increase from premaximum to orion system. Figure 6.21 gives the relation between speed class and expansional velocity of the principal spectrum. The two recurrent novae for which these data are known are T CrB, which obeys to the general relation, and T Pyx, which deviates strongly. Too few data are available to say if recurrent novae do obey or do not to the same relation of classical novae. Typical expansional radial velocities of the various spectral systems are indicated in the following Table 6.7, based on novae representing various speed classes.

C. Payne-Gaposchkin (1957) has observed that spectral type and expansional radial velocity of the principal spectrum are correlated: the earlier the spectral type, the higher the radial velocity. Since we are dealing with a shock front, it is plausible that it is "the velocity which determines the spectrum" (C. Payne-Gaposchkin, 1957, in *The Galactic Novae*, p. 82).

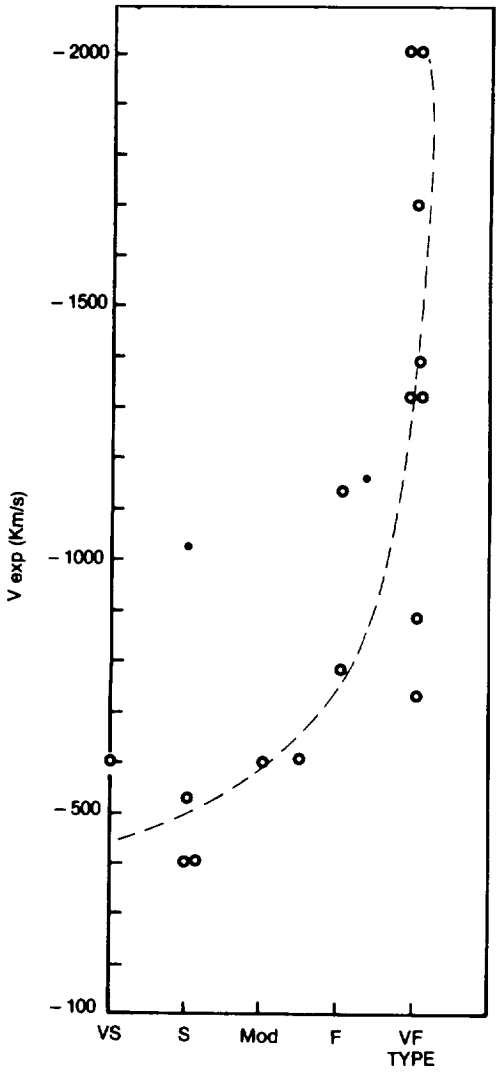

Figure 6-21. Relation between the speed class and the expansion velocity of the principal spectrum. VS=very slow; S=slow; Mod=moderately fast; F=fast; VF=very fast. Open circles: classical novae; black dots: recurrent novae (T Pyx and T CrB).

Similar relations exist also between spectral type at maximum and the radial velocity difference between the diffuse-enhanced and the principal spectrum.

The data by C. Payne-Gaposchkin are given in Table 6.8.

A loose relation also exists between the expansion velocity and the absolute visual magnitude at maximum (Figure 6.22). Data from Mustel (1978) shows that the expansion velocity of the "photosphere" (i.e., the layers where the continuum and absorption spectrum are formed, or where $\tau \approx 1$) grows with time, and the growth is particularly rapid in the latest periods of expansion, just before light maximum. For instance, in V 603 Aql, the expansion velocity during the day before t_{max} was twice that of the previous day; the same picture was shown by DQ Her. V 1500 Cyg 1975 had V exp of -1300 km/s on August 29, -1700 on August 30 (epoch of maximum) and -2200 on August 31. The slow nova RR Pic had the first maximum on June 7, 1925. From June 6 to June 7, the expansional velocity came up to 250 km/s, while between June 4 and 5 it was only 40 km/s. Hence, the rate of energy generation in the inner subphotospheric layers increases just before light maximum; the velocity of the gas on the photospheric level records a sharp increase due to a second shock wave that hits the first expanding layer. It is the accelerated matter that forms the principal envelope.

The spectra of recurrent novae seem to show a different behavior than that of classical no-

TABLE 6.7

EXAMPLES OF EXPANSIONAL RADIAL VELOCITIES.

Object	Type	Expansional velocity (km/s)			
		Premax.	Princ.	D-E	Orion
N Aql 1918	Fast	-1300	-1500	-2200	-2700
N Gem 1912	Average	- 400	- 800	-1400	-1600
N Her 1934	Slow	- 180	- 300	- 800	- 500
					-1000
N Cyg 1975	Very fast	-1300	-1700	-3000	
				-4000	

TABLE 6.8

CORRELATION BETWEEN SPECTRAL TYPE AT MAXIMUM AND EXPANSIONAL VELOCITY OF THE PRINCIPAL SPECTRUM.

Spectral Type	Corresponding Temperature	Average RV (km/s)	Number of Objects
F8	6,000 K	- 142	2
F5	7,000	- 168	2
F0-F2	8,000	- 268	4
A5	8,500	- 618	4
A2	9,000	- 560	3
A0	10,000	- 600	2
B9	11,000	- 600	2
B5	15,000	-1000	1
B1	25,000	-1210	1
N III lines	50,000	-1378	7
N V lines	200,000	-1950	3

These are mean values. We add here a few examples for some individual objects, which may deviate from the average values:

The very slow nova HR Del 1967: Sp. A, V = -625 km/s

The fast nova V1668 Cyg 1978: Sp. F, V = -600 km/s

The very fast nova V1500 Cyg 1975: Sp. B2 Ia, V = - 1,700 km/s

vae. We remind the reader however that only four of them have been observed spectroscopically, and among them T Pyx (the only known slow recurrent nova, which has been observed fragmentarily) behaves like classical novae. T Cr B and RS Oph do not show systems corresponding to the diffuse-enhanced and the orion spectrum, and during the light decrease present strong coronal lines of [Fe X], [Fe XIV]; U Sco, on the contrary, does not show highly ionized forbidden lines.

Details on the spectral behavior of single objects will be given in Chapters 8 and 9.

IV. INFRARED OBSERVATIONS OF NOVAE

A dozen novae have been observed from the ground in the infrared (from about 1 μm to 20 μm). Moreover, the infrared satellite IRAS has observed some recent, old and very old novae. Infrared observations are important because many novae are known to produce dust shell few weeks after outburst.

The first evidence for the formation of a dust cloud around a nova was given by Geisel et al. (1970) who observed the decline of FH Ser 1970 between 1 and 22 μm. They observed that when the visual light curve showed the dip typical of slow novae, infrared emission started to increase (see Figure 6.23 and 6.24). The infrared emission was very similar to that of a black body at temperatures varying between 1,300 to 900 K. Circumstellar dust was the natural candidate for interpreting this emission. The lack of any spectral feature at 10 μm suggested that silicate grains are absent and that the dust may be formed of graphite. McLaughlin (1935, 1937) was the first to suggest that the diminution of about 9 mag observed in the visual light curve of DQ Her was due to a cloud of dust formed from the ejecta. Now the recent infrared observations of novae confirm his prediction.

Bode and Evans (1983) review the evidence for the presence of dust in novae and classify them, according to their infrared development, in three classes, as follows:

"Class X: novae for which the infrared luminosity = luminosity of the underlying object. These novae invariably have a pronounced discontinuity in the visual light curve, which coincides with infrared flux rise. The temperature of the dust shell attains a minimum before rising to a plateau - the so-called isothermal phase. Typical member, NQ Vul" (see figure 6.25).

"Class Y: novae for which the infrared luminosity < 10 per cent that of the underlying object. The visual light curve is smooth and the dust shell temperature decreases

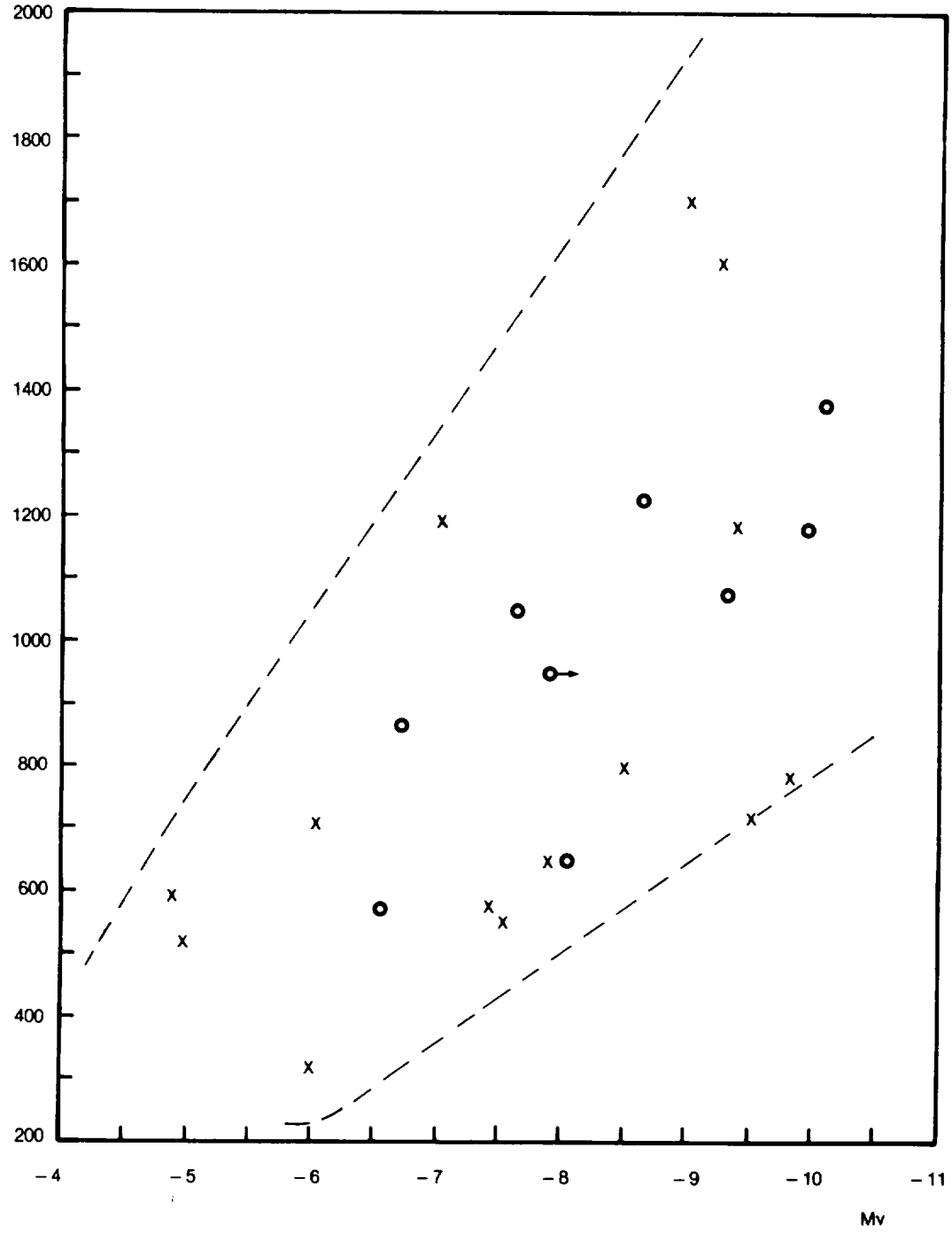

Figure 6-22. Relation between the expansion velocity of the principal spectrum and the absolute visual magnitude. Crosses: data from Cohen and Rosenthal, 1983; circles: data from Cohen, 1985.

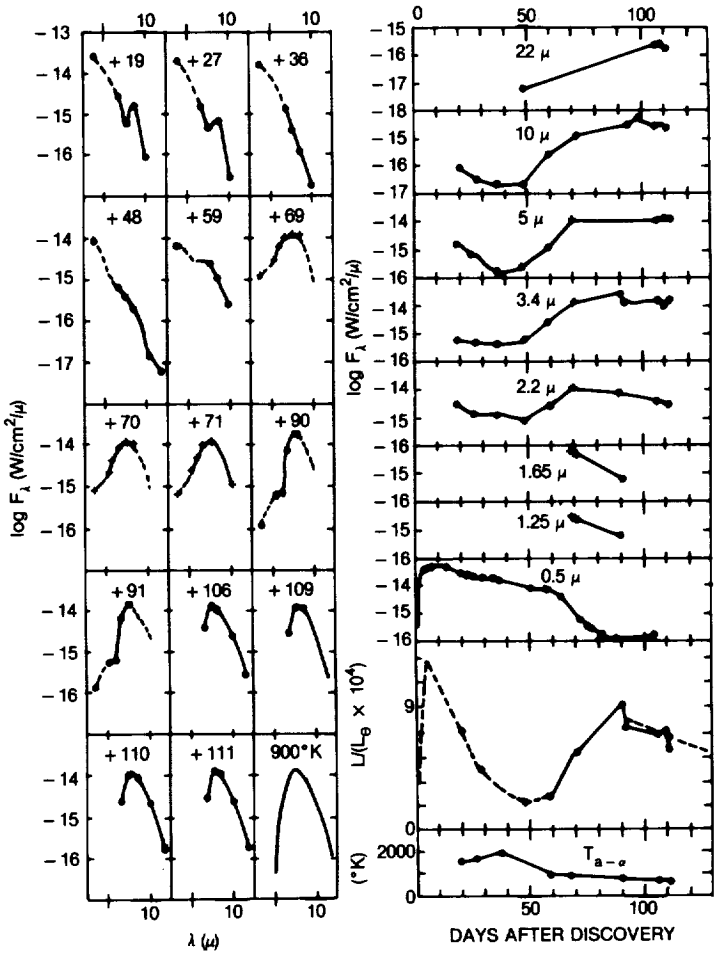

Figure 6-23. FH Ser 1970: left, Fλ vs λ on successive days after its discovery. A 900 K black body distribution is given for comparison. Right, light curves for different wavelengths, and total luminosity (at optical and IR wavelengths) in solar units. The color temperature T(K-N) is plotted to show the cooling of the dust as the luminosity of the system changes.
(from Geisel et al., 1970)

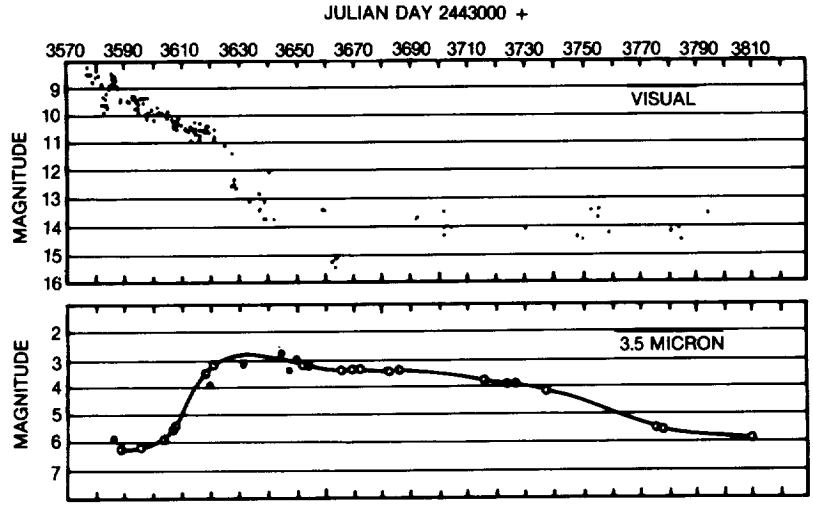

Figure 6-24-LW Ser 1978: visual light curve and 3.5 μm light curves. (from Gehrz et al. 1980 a)

monotonically. Typical member, V 1668 Cyg" (Figure 6.26).

"Class Z: novae with little or no infrared excess, i.e. little or no dust. The visual light curve is usually smooth. The only member known with certainty to date is V 1500 Cyg" (Figure 6.27).

It is important to note that these different infrared behaviors are correlated with the speed class: slow novae generally belong to

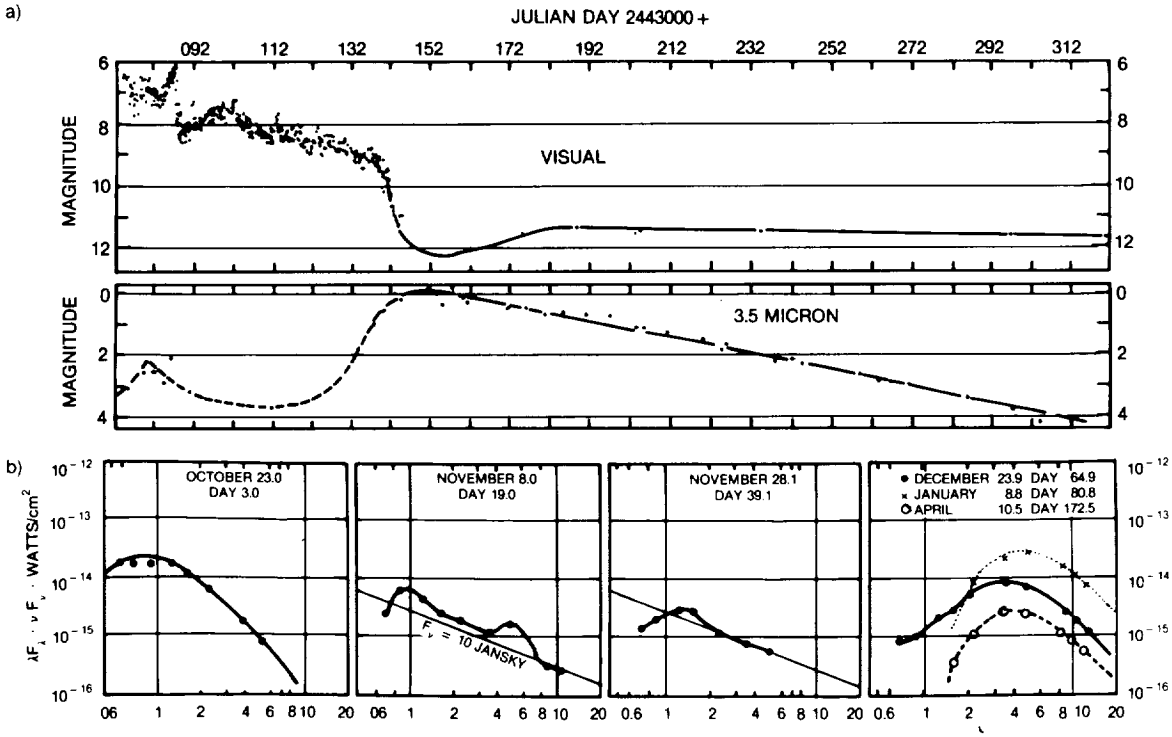

Figure 6-25a. NQ Vul: visual and 3.5 μm light curves. The visual magnitude dims as the 3.5 μm magnitude brightens, as the dust condenses. b) Distinct phases of the nova development: day 3.0 shows the initial pseudophotosphere; day 19.0 the free-free phase with an unidentified feature at 5 μm superposed; day 39.1 the free-free prior to dust condensation; days 64.9 to 172.5 the thermal reradiation by the condensed dust.
(from Ney and Hatfield, 1978)

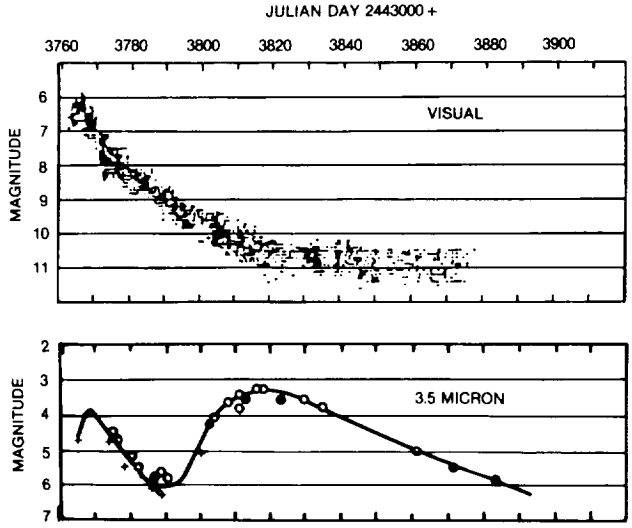

Figure 6-26. V1668 Cyg 1978: visual and 3.5 μm light curves. The visual light curve shows no transition phase as condensing dust causes the IR flux to rise. (from Gehrz et al., 1980 b)

C-5

Class X, intermediate novae, to Class Y, and very fast novae, to Class Z. Of course these conclusions are based on a relatively small number of observations, and exceptions could be revealed when a larger sample will be available.

More detailed description of the infrared behavior of some typical novae is given in the following.

The best studied novae are FH Ser 1970, V1301 Aql 1975, V 1500 Cyg 1975, NQ Vul 1976, V1668 Cyg, LW Ser 1978, Nova Aql 1982.

Slow novae of the DQ Her type, which exhibit a deep minimum in the visual light curve and then recover before starting their smooth decline (the visual transition stage), form a

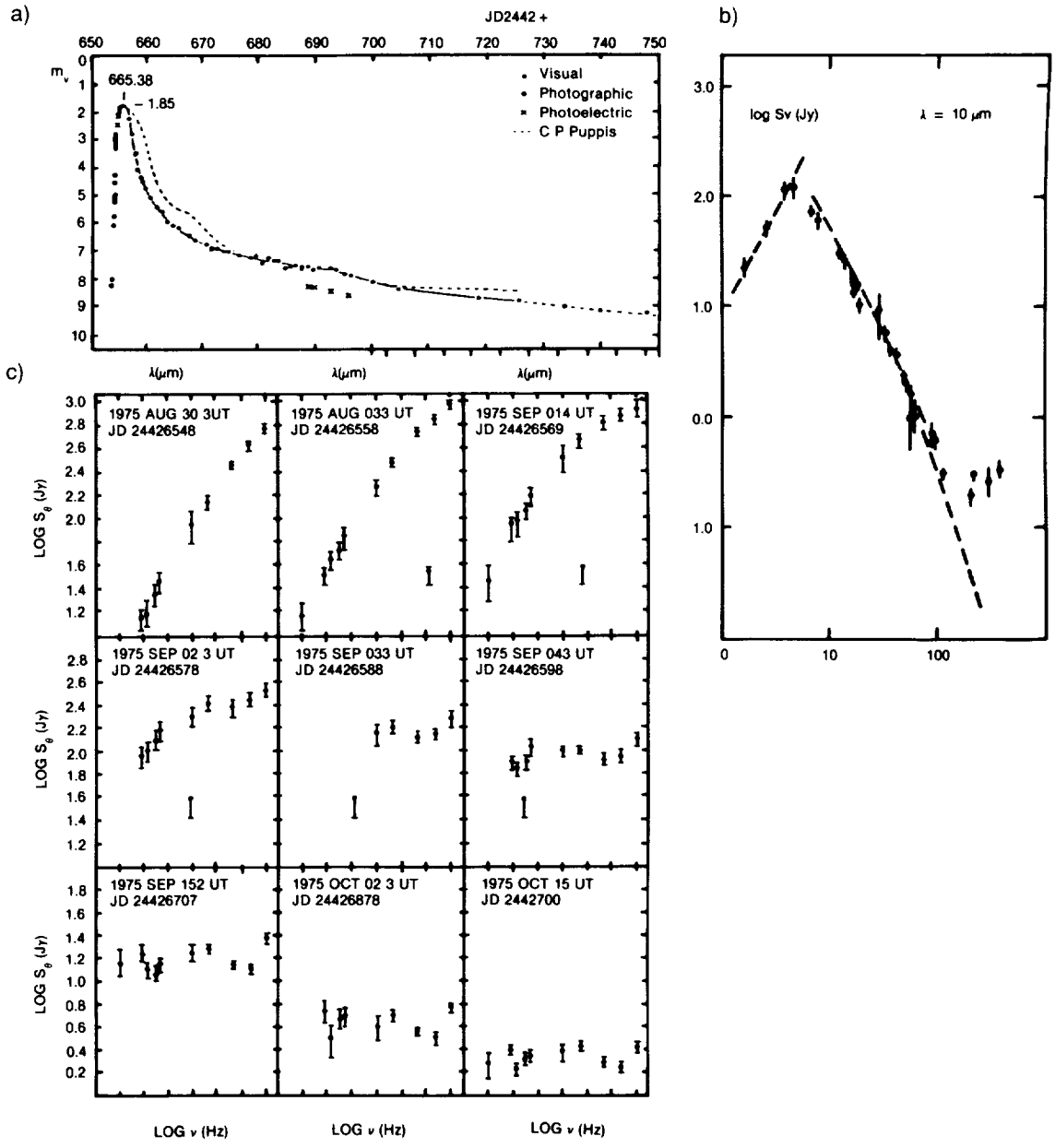

Figure 6-27a. Optical light curve for V1500 Cyg (1975) (from Wolf, 1977) b) IR (10 μm) light curve for V1500 Cyg 1975 (from Ennis et al. 1977) c) Energy distribution from 1.2 μm to 20 μm at various epochs of the outburst. The transition from black body to thermal bremstrahlung emission occurred on Sep. 2, 1975. (from Ennis et al., 1977)

thick circumstellar dust shell. They belong to the Class X. FH Ser, LW Ser, NQ Vul belong to this type. The very fast nova V 1500 Cyg, representative of Class Z, on the contrary, radiated like an optically thin expanding plasma for nearly one year; there is some weak evidence that a small amount of dust was formed after one year from outburst.

V 1668 Cyg, representative of Class Y, is a moderately fast nova. After an initial expansion of the hot gas shell, an optically thin dust shell was formed, and it reached its maximum visual optical depth of 0.1 about 60 days after outburst.

The very slow nova HR Del 1967 represents an exception to the correlation between speed class and infrared behavior. In fact, it has not formed a thick shell. When the dust shell remains optically thin or does not form at all, no deep minimum is observed. This is the case of HR Del, whose light curve presents a slow, smooth decline and no dip.

IV.A. COMPARISON OF INFRARED AND VISUAL LIGHT CURVES OF SOME TYPICAL NOVAE

The visual and infrared light curves of several novae are plotted in Figures 6.25, 6.26, and 6.27.

The visual and infrared (1.2 to 10 μm) light curves of the extremely fast nova V 1500 Cyg (Figures 6.27a, b) exhibit about the same behavior: all reach a maximum and then decrease smoothly. However, the maximum brightness is reached at progressively later epochs with increasing wavelength; e.g., the visual maximum was reached on August 30, 1975, and that at 10 μm on September 2, 1975. The energy distribution is typical of a black body with temperatures varying from 10,000 K to 5,000 K until day 3.2 after outburst; then the energy distribution changes gradually to that typical of free-free radiation (Figure 6.27 c). Only 300 days after outburst, a slight infrared excess, which can be attributed to the formation of dust, is observable at wavelengths equal to or larger than 3.6 μm. These data show the nova to present a thick "pseudophotosphere" until day 3.2 and then to consist of an expanding mass of ionized gas.

The visual and infrared light curves of FH Ser, LW Ser, and NQ Vul (Figures 6.23, 6.24, and 6.25) all have the common property that they are almost the mirror image of one another; when the visual brightness starts to decrease, the infrared curves show increasing brightness. The energy distribution in infrared is that of a black body at temperatures of the order of 1,000 K and decreases with time from the outburst (Figure 6.23) Hence, we have a clear example of the different behavior of V 1500 Cyg with its thin electron shell and FH Ser, LW Ser, and NQ Vul with their thick dust shell.

In the case of FH Ser, Hyland and Neugebauer (1970) and Geisel et al. (1970) observed the commencement of infrared emission about 60 days after discovery, coincident with the rapid decline in visual light. Ultraviolet observations up to day 57 and infrared observations by day 90 indicated that the total luminosity remained equal to that observed at outburst (see section 6.V on ultraviolet observations for more details).

Infrared observations were continued by Mitchell et al. (1985) and continued until day 529 after discovery. Figure 6.28 from Mitchell et al. shows the infrared light curves at 1.25, 1.65, 2.2, 3.5, 4.8, and 10 μm. It must be noted that the discontinuity in the light curves, occurred between day 111 and day 129; after that event, fading occurred in all bands (except at J=1.25 μm, where, however, the observations are very uncertain and data are lacking). The energy distribution at various epochs is shown in Figure 6.29, together with approximate black body fits. The temperature decreases from 960 K on day 70 to 760 K on day 91. The discontinuity in the light curves is reflected by the slight increase to 800 K on day 154. Later on, it is difficult to represent the observations by a single black body only. Instead, there is evidence for a cool black body component, responsible for the major part of the infrared luminosity, and an excess in the 1-3 μm region.

The cool component decreases in temperature from 700 K on day 210 to 400-500 K after day 400, while the short wave excess increases in relative strength and temperature.

The interpretation of these data will be discused in Chapters 7 and 8. We anticipate here that to explain these observations and especially the discontinuity in the light curves, we must assume that the dust grains grow from day 60 to day 111 and undergo a significant reduction in size between day 111 and day 129. The excess flux at the shorter infrared wavelengths may probably be due to increasing line emissions as the shell expands.

V 1668 Cyg differs from V 1500 Cyg, as well as from the three class X novae, because it shows two distinct phases in its infrared light curves: a first phase with a thin electron shell, when the infrared light curves decrease smoothly, as does the visual one, thus resem-

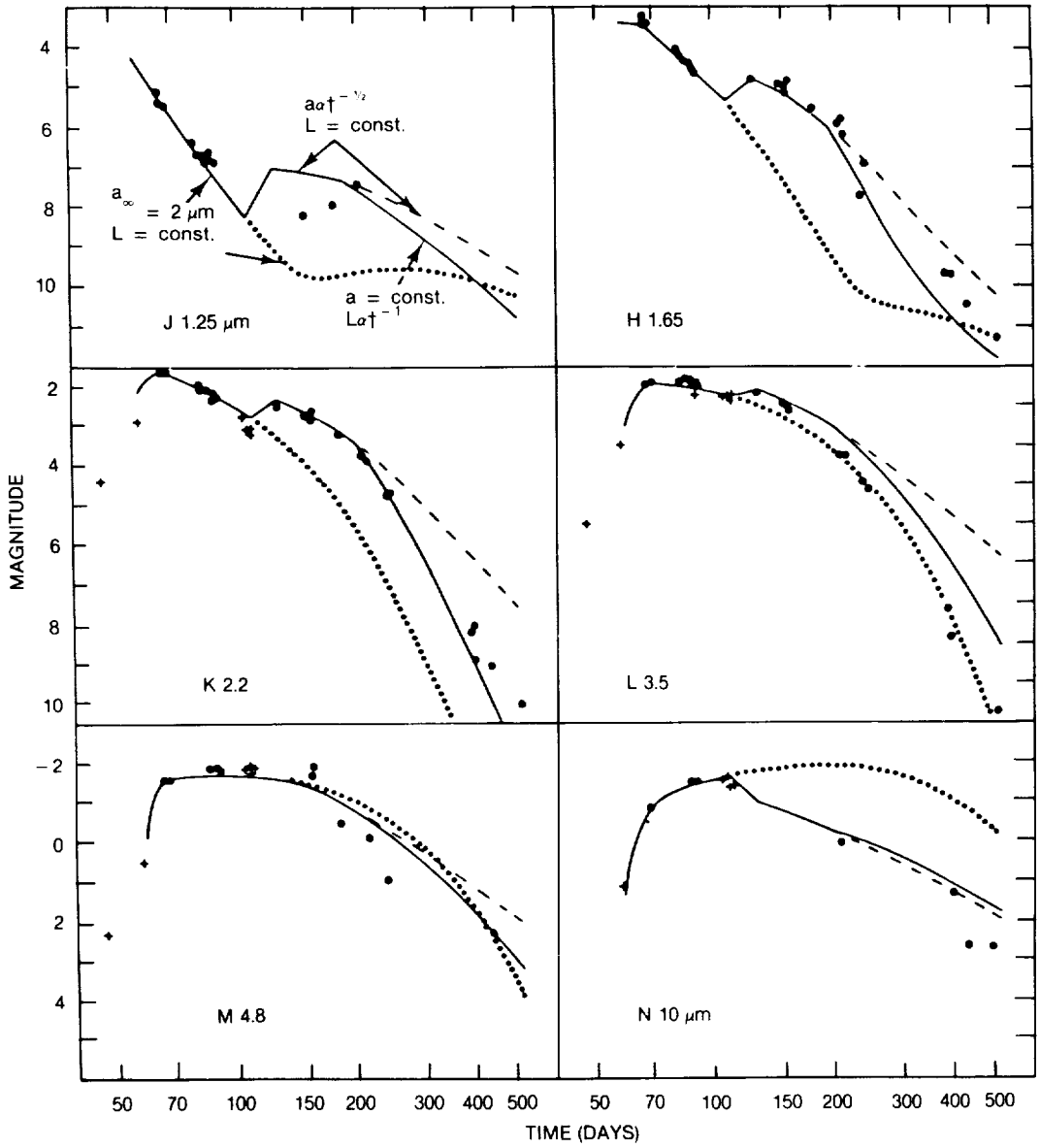

Figure 6-28. Infrared light curves of FH Ser. Dotted and dashed lines correspond to the predicted light curves for continuing grain growth beyond day 111, and for constant bolometric luminosity and continued grain size reduction beyond day 200 respectively.
(from Mitchell et al., 1985)

bling V 1500 Cyg (Figure 6.26) and a second phase with an optically thick dust shell, as indicated by the infrared increasing brightness reached when the visual brightness is almost gone back to the preoutburst magnitude.

A different case is represented by the fast Nova Aql 1982 (Bode et al., 1984). It was discovered by Honda (1982) on January 27, 1982. The initial decay was of 0.3 mag/day, typical for a fast nova, as well as the relatively smooth early light curve. On day 37, it had developed an infrared excess characteristic of a dust shell at T = 1100 K.

Figure 6.30 by Bode et al. shows the visual

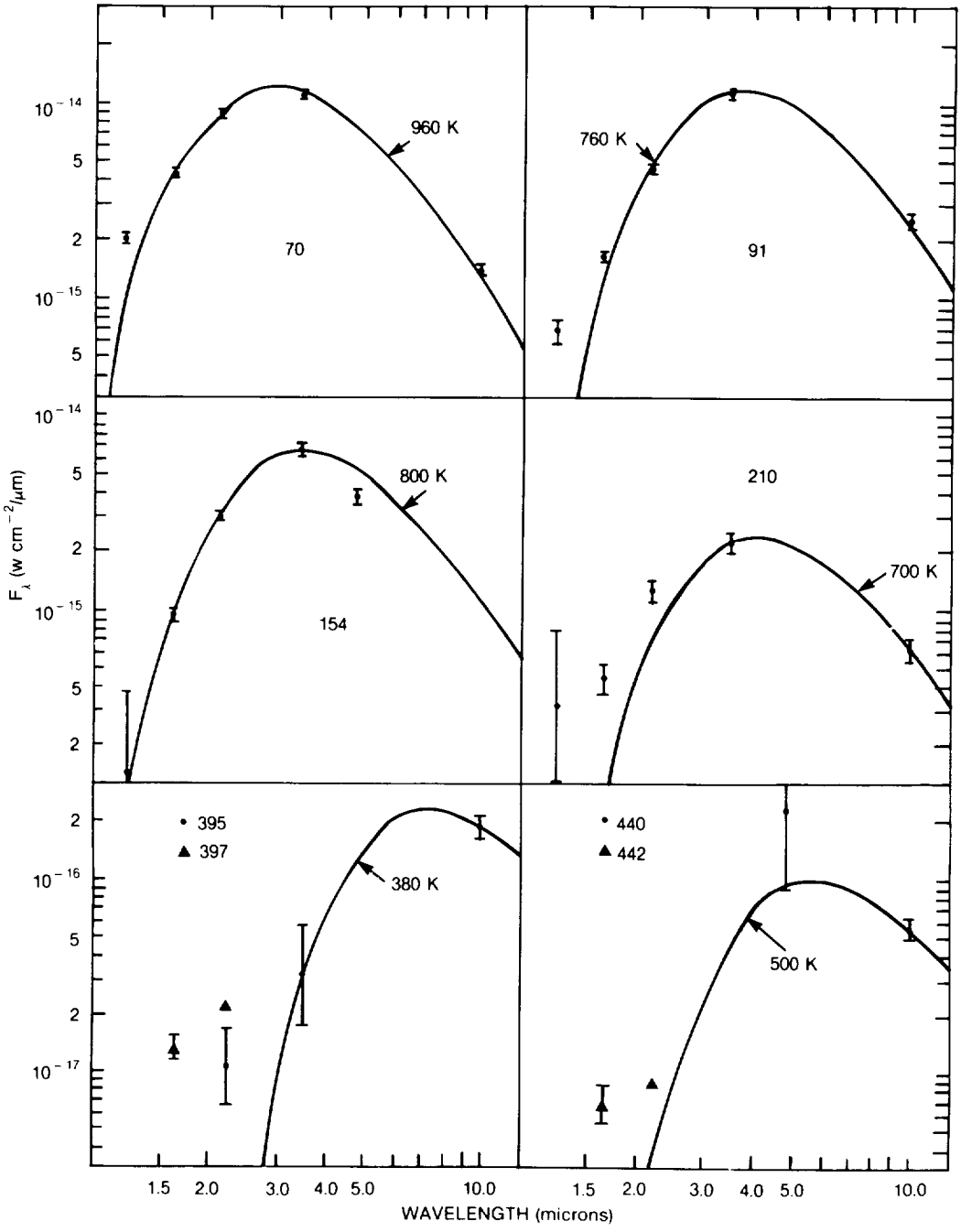

Figure 6-29. Energy distribution of FH Ser and approximate black body fits. Beyond day 210 the energy distribution broadens due to excess emission in the 1-3 μm region appearing above the cool dust emission component. (from Mitchell et al., 1985)

and infrared light curves: no dip in the visual light curve, a smooth brightness decrease in the infrared curve. Figure 6.31 shows the fit of the infrared flux to the black body curves. Ultraviolet observations suggest that the bolometric luminosity was not maintained (differently from FH Ser; see Section 6.V). A very interesting observation made on July 3-4, 1982, 156 days after discovery shows the presence of an emission feature peaking near 10 μm (Figure

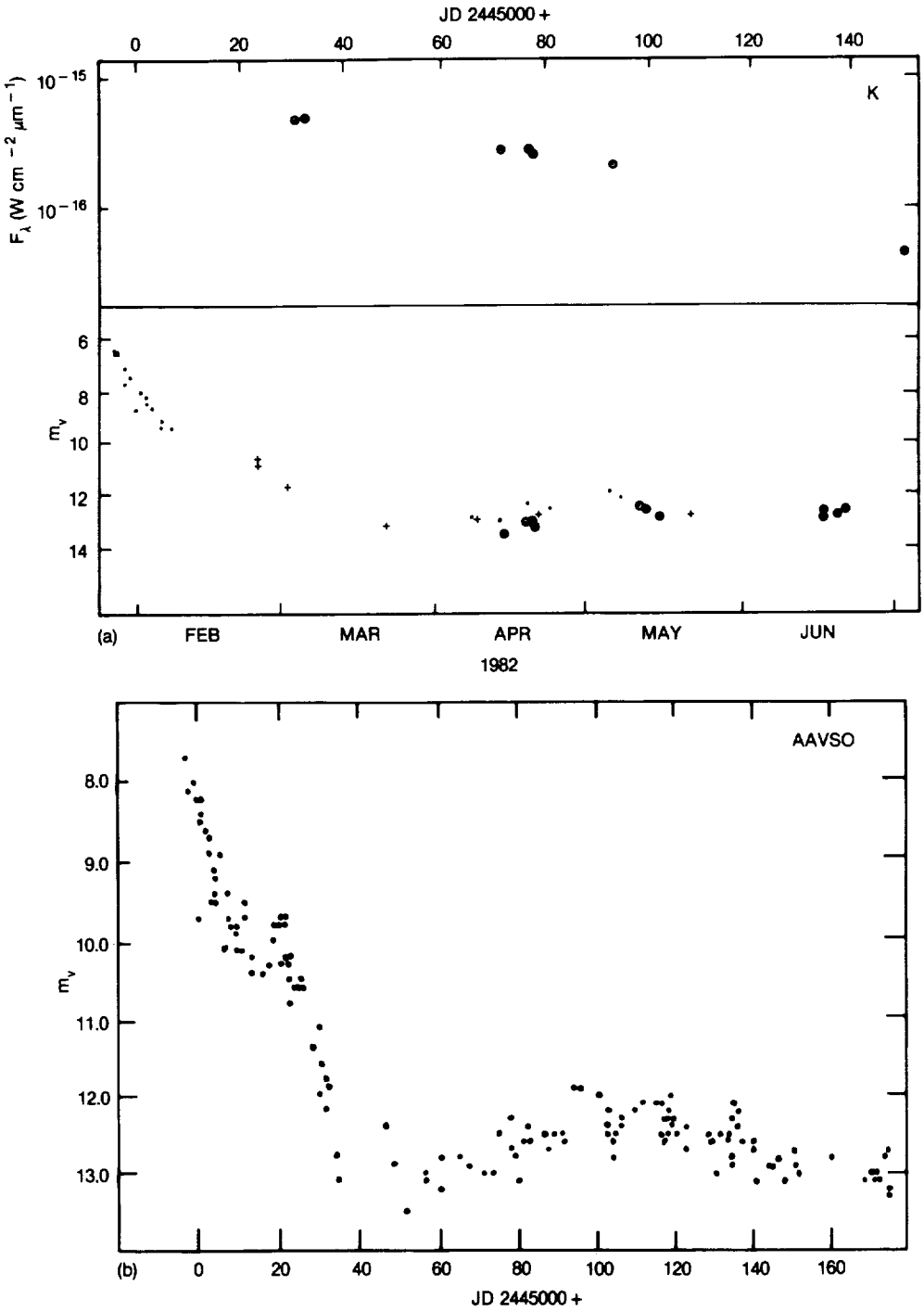

Figure 6-30. Nova Aql 1982: 1) infrared light curve from K band photometry; 2) Visual light curve obtained collecting visual estimated (dots), IUE FES measurements (plus) and V band photometric observations (circles); 3) Visual light curves from AAVSO observations.
(from Bode et al., 1984)

6.32), which can be attributed to SiC grains, and which has never been detected before in the other novae observed in infrared. It was the absence of this silicate feature that suggested that generally dust is formed of graphite grains.

Beside the emission feature, one spectrum observed on April 18, 1982, in the range 1 to 4 μm (Figure 6.33) shows one broad and shallow absorption at 3.9 μm, which is also often seen in the spectra of oxygen-rich stars (Rinsland

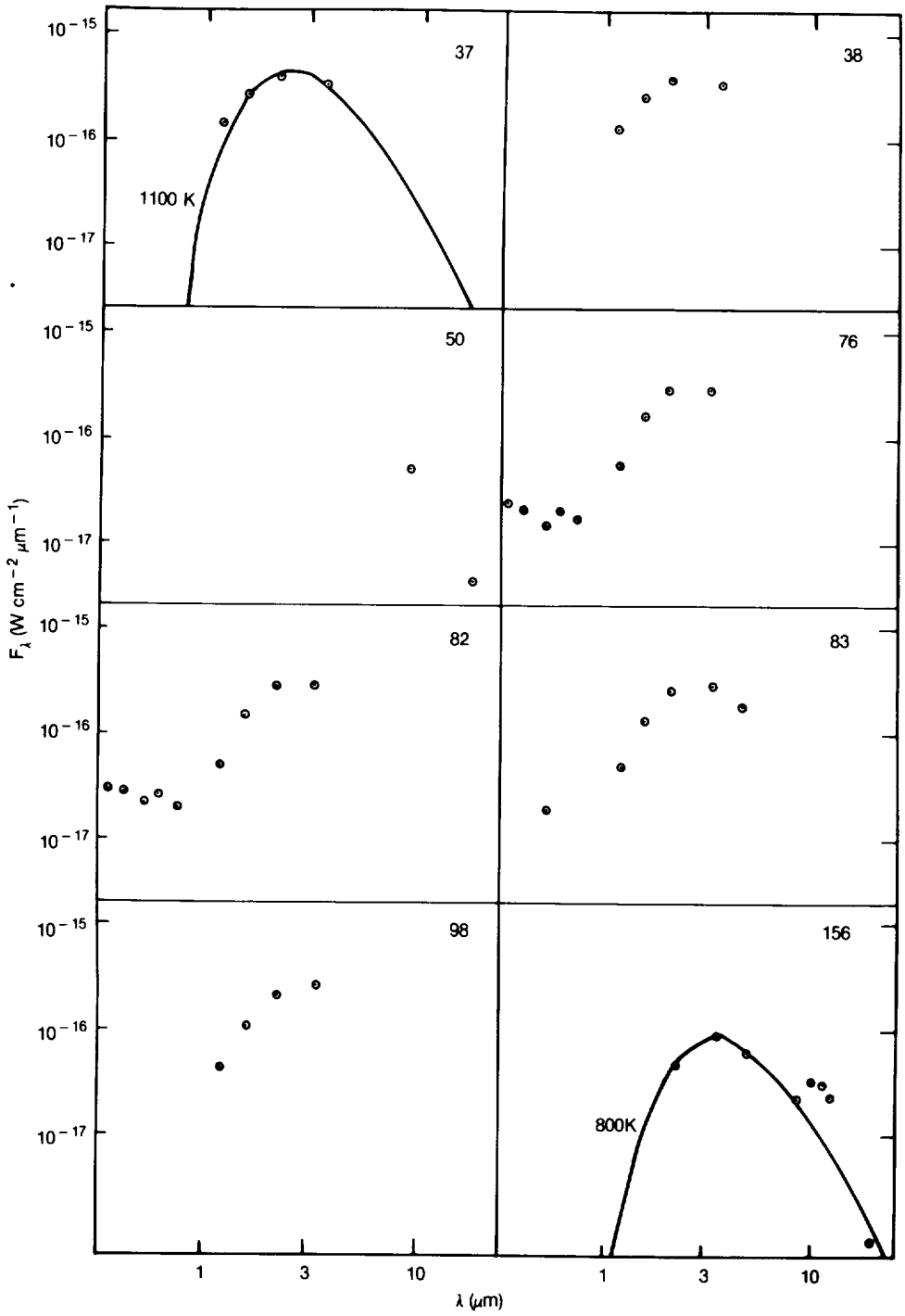

Figure 6-31. Energy distribution of Nova Aql 1982 and comparison with black body curves. The time in days after outburst is indicated.
(from Bode et al., 1984)

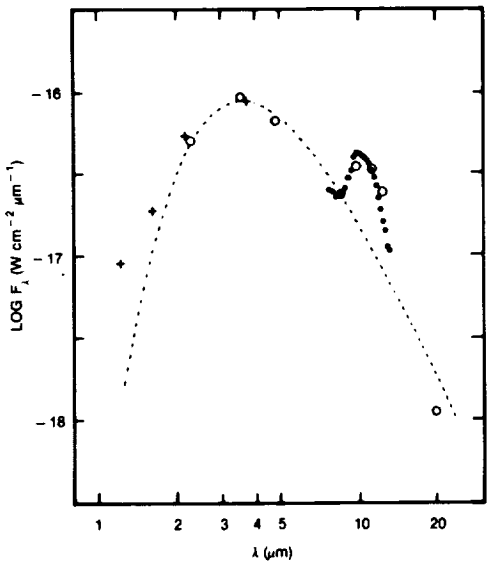

Figure 6-32. Near infrared flux distribution of Nova Aql 1982 on July 3-4. The broken line is an 800 K black body curve. A strong broad emission is present at about 10 μm.
(from Bode et al., 1984)

and Wing, 1982). It is identified with SiO in the gaseous phase. These emission and absorption features suggest that in this case, grains are formed in an oxygen-rich environment. Hence, the formation of graphite grains is improbable. It is more probable that dust grains are formed of iron composites. In fact, if carbon is slightly less abundant than oxygen, oxygen makes composites with the other elements and leaves no free atoms to combine with carbon. The composition of the dust grains in the shell of Nova Aql 1982 is unique among novae studied in the infrared. The sample, however, is still very small. Thermonuclear runaway models suggest that CNO are overabundant in nova ejecta and that C > O (Starrfield et al., 1978). In the case of Nova Aql 1982 it appears, on the contrary that O > C.

These kinds of observations are important because they can give a clue for deciding which is the origin of grains. Two main theories have been proposed. They are a), Grain growth in nova ejecta and b) Pre existing grains. In case a), we expect that grains reflect the composition of the interstellar medium.

Another emission line was observed in the infrared spectrum of nova Vul 1984 No 2, 140 days after outburst. A very strong emission was observed at 12.8 μm, which is identified with [Ne II].* It is the strongest 12.8 μm line ever observed in an astrophysical source (Gehrz et al., 1985, their Figures 1 and 2). A suggestion for the presence of the same line in the infrared spectrum of V1500 Cyg one year after outburst was made by Ferland and Shields (1978b) in order to explain the excess observed in the 10 μm band.

The Infrared Astronomical Satellite (IRAS) has observed the field of several novae (Table 6.9). The IRAS point source catalogue gives the opportunity to 1) search for emission from novae of different speed classes at various phases of their evolution, and 2) to search at longer wavelengths (12, 25, 60, and 100 μm) than is possible from the ground for finding evidence of very cool dust.

Search for infrared emission from CK Vul 1672, V 1370 Aql 1982 and MU Ser 1983 was negative (Callus et al., 1986).

The spectra of several novae, obtained by plotting the fluxes given in the IRAS Point Source Catalogue versus the wavelength are given in Figures 6.34a and 6.34b. The symbiotic nova RR Tel and the very slow nova V 605 Aql present a flux that is an order of magnitude higher than that from the other observed novae. The flux for V 605 Aql fits the black body curve for T=50 K, while that RR Tel fits the black body curve for T=290 K. The measurements at 60 and 100 μm for the other novae are not reliable. Their maximum flux falls at wavelengths shorter than 12μm indicating color temperature higher than 300 K. Dinerstein (1986) has performed a more detailed study of four classical novae (two relatively young—V 4077 Sgr 1982 and GQ Mus 1983—and two relatively old—FH Ser 1970 and HR Del 1967) with well-determined optical positions, which seem to have true infrared counterparts (Table 6.10 a and b). The criterion adopted for positive identifica-

* Ultraviolet observations have identified a few novae which are Ne-rich. They could belong to a subclass of novae where the white dwarf is a O-Ne-Mg star instead of a CO star.

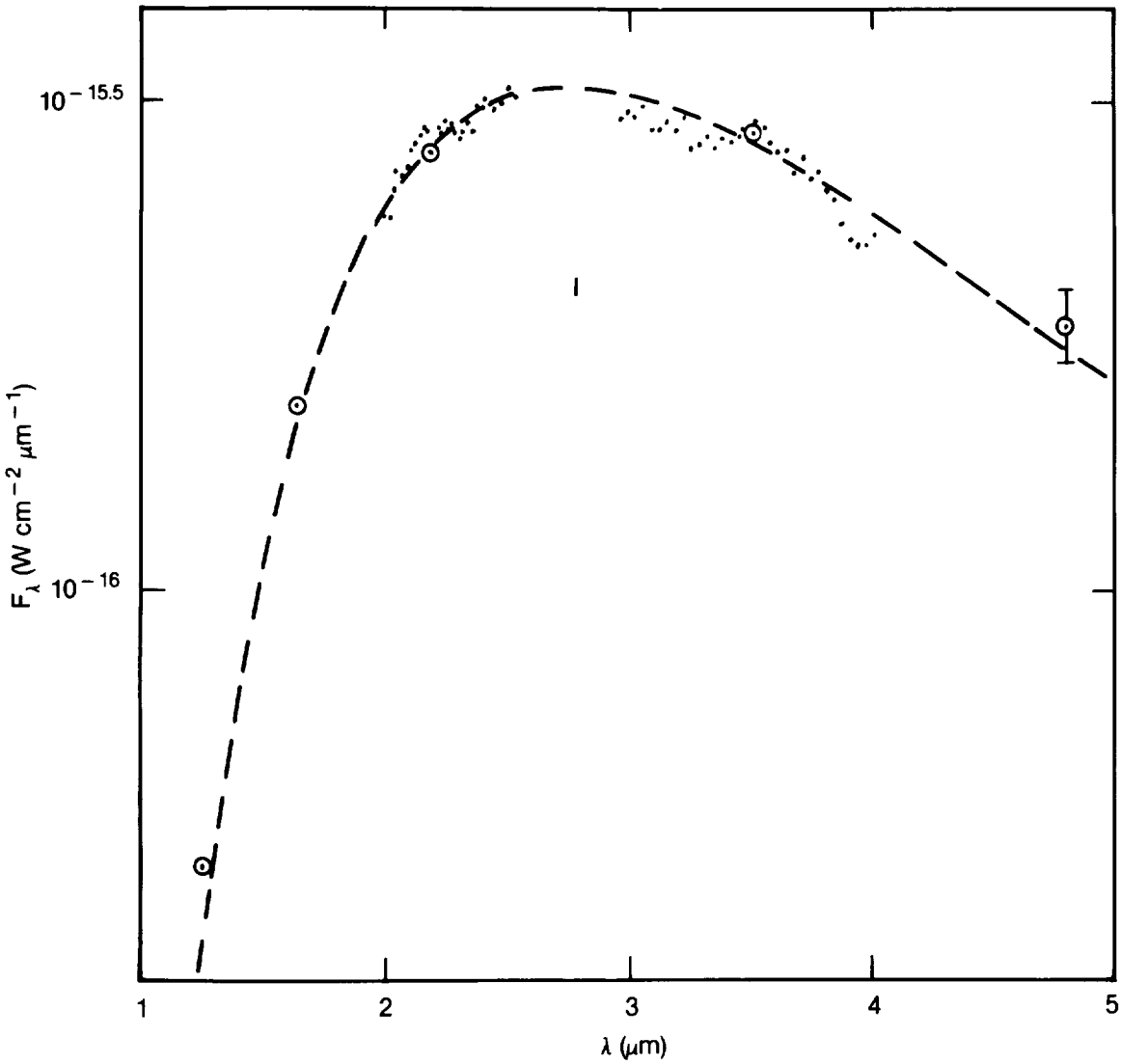

Figure 6-33. Near infrared flux distribution of Nova Aql 1982 on April 18.1, 1982. A broad shallow absorption is present at 3.9 μm.
(from Bode et al., 1984)

tion is that the difference between optical and infrared position is smaller than the quoted error ellipses for IRAS measurements. Search for infrared emissions from other novae was made by coadding the data from the original IRAS survey in order to increase the sensitivity. By this method, positive detection was obtained for DQ Her and for the recurrent nova T CrB. V 4077 Sgr was observed with IRAS 161, 169, and 357 days after maximum. Its spectrum fits the black body curves for T = 1000 K, except at 60 μm when the observed flux is lower (Figure 6.35 from Dinerstein, 1986). It is interesting to remark that the dust temperature apparently does not vary from 6 to 12 months after maximum. From the temperature and the observed flux, and the absolute luminosity derived from the speed class-luminosity relation (Duerbeck, 1981) a rough estimate of the mass of the emitting dust can be made: this one is found of the order of 10^{-16} solar masses.

The fast nova GQ Mus has a flux lower by two orders of magnitude than V 4077 Sgr. By using the technique of coadding fluxes, it is possible to see that its IR spectrum is flat, characteristic of free-free emission, in agreement with previous data obtained from the ground at 5 and 10 μm (Krautter et al., 1984;

TABLE 6.9

Novae observed by the Infrared Astronomical Satellite (IRAS).

NOVA	Outburst	Type of light curve (Duerbeck).	
CQ Vel	1940	Cb	
EU Sct	1949	Cb	
FH Ser	1970	Cb	(1986, Dinerstein)
HR Del	1967	D	(1986, Dinerstein)
KP Sco	1928	A	
LQ Sgr	1897	?	
RR Tel	1948	E	
RS Oph	Rec. N	Ar	
T Cr B	Rec. N	Ar	(1986, Dinerstein)
V 1016 Sgr	1899	?	
V 605 Aql	1919	D	
V 949 Sgr	1914	?	
NQ Vul	1976	Bb	(1985, Evans)
DQ Her	1934	Ca	(1986, Dinerstein)
V 4077 Nova Sgr	1982	Bb	(1986, Dinerstein)
GQ Nova Mus	1983	A	

Whitelock et al., 1984). There is no evidence for a dust component.

This result is a confirmation of the correlation between the speed class of a nova and the efficiency for the formation of a dust shell during its early phases of expansion: slow novae have generally dust shell, while fast novae do not. We remind that HR Del, however, is an important exception to this rule.

FH Ser was detected in the Point Source Catalogue at 12 μm only. Coaddition of the data permits detection at 25 μm too. The resulting color temperature is 500 K. However the dust appears much hotter than expected for an optically thin expanding dust shell of constant thickness. In fact, if the central luminosity source remains constant, the IR flux should decline with time as t^{-2} and the dust temperature as $t^{-1/3}$ (Gehrz et al., 1980a). Hence, for log t = 3.8, T dust should be one order of magnitude lower. It is suggested a contribution from IR fine structure lines.

HR Del was detected in the 25 μm band but not at 12 and 60 μm. This result suggests that we are not observing the thermal continuous spectrum, but rather line emission. We remind that [Ne II] emission at 12.8 μm was observed in Nova Vul 1984 N. 2 and probably also in Nova Cyg 1975. In the case of HR Del, candidate lines falling in the 25-μm band are [SIII] 19 and 34 μm, [NeV] 24 μm, [OIV] 26 μm, and [SiII] 35 μm.

DQ Her was detected at 60 and 100 μm by coaddition of data. A color temperature of 60 K was found consistent with the upper limit at 25 μm. Evans (1985) reports that non survey mode observations give a lower temperature, 34 K.

T CrB is detected in the Point Source Catalogue. However, coaddition of data gives more precise results (Table 6.10 c). The flux at 12 and 25 μm gives a dust temperature of 900 K.

The detection of such hot dust in a recurrent nova is interesting, because it cannot be the remnant of the last outburst that occurred in 1946, but rather an indication of continuous dust-rich mass loss. This is a plausible possibility, because T CrB is a well-known binary system where the M giant member is almost

Table 6.10

TABLE a) Data for nova Sgr 1982.

HCON	Date (1983)	Days after maximum	Uncorrected flux density (Jy) *Color-corrected flux density (Jy)* *IRAS* band [12 μm]	[25μm]	[60μm]	[100μm]	Mass of hot dust ($M_\odot$)
1	25 Mar	161	24.0±2.1 *18.9±1.6*	9.2±1.1 *6.9±0.2*	1.3±0.2 *1.0±0.2*	<2.8 <2.6	4.2 X 10^{6}*
2	1 Apr	169	21.8±1.6 *17.2±1.3*	7.5±0.7 *5.6±0.5*	0.94±0.13 *0.7±0.1*	<2.8 <2.6	3.4 X 10^{6}*
3	7 Oct	357	2.5±0.2 *2.0±0.2*	0.84±0.14 *0.63±0.10*	<0.4 *< 0.3*	<4.0 *< 3.7*	3.8 X 10^{7}

* Assuming d = 2.5 kpc (see the text).

TABLE b) Catalog and coadded fluxes for detected novae.

Object	λ(μm)	Flux density (Jy) Catalog[a]	Coadded[b]	Corrected[c]
GQ Mus	12	0.24 ± 0.06	0.26 ± 0.03	—
	25	0.31 ± 0.97	0.26 ± 0.03	—
	60	<0.30	0.30 ± 0.04	—
	100	<3.0	<0.72	—
FH Ser	12	0.32 ± 0.04	0.32 ± 0.03	0.29 ± 0.03
	25	<0.30	0.18 ± 0.03	0.14 ± 0.03
	60	<0.60	<0.29	<0.23
	100	<3.7	<1.2	<1.1
HR Del	12	<0.30	<0.08	—
	25	0.36 ± 0.06	0.34 ± 0.03	—
	60	<0.40	<0.11	—
	100	<1.0	<0.32	—

[a] Catalog values corrected for detection rate.
[b] Uncorrected coadded values.
[c] Coadded values corrected for color effects.

TABLE c). Additional coadded novae.

Object	Date	Optical position α(1950)	δ(1950)	Uncorrected flux density (Jy) *IRAS* band [12 μm]	[25 μm]	[60 μm]	[100 μm]
T Aur	1891	5^{h}28^{m}46^s	+30°24'36"	<0.10	<0.14	<0.16	<0.88
RR Pic*	1925	6^{h}33^{m}32^s	-62°47'17"	1.22 ± 0.05	0.29 ± 0.02	<0.40	<1.0
T Cor	recurrent	15^{h}57^{m}25^s	+26°02'32"	0.72 ± 0.03	0.26 ± 0.03	<0.12	<0.34
DQ Her	1934	18^{h}06^{m}05^s	+45°51'01"	<0.06	<0.05	0.58 ± 0.08	0.61 ± 0.07
V1370 Aql	1982	19^{h}20^{m}50^s	+02°23'35"	<0.10	<0.10	<0.15	<0.87
CK Vul	1670	19^{h}45^{m}32^s	+27°11'22"	<0.11	<0.10	<0.37	<3.7
E2000 + 223	?	20^{h}00^{m}39^s	+22°20'00"	<0.09	<0.09	<0.14	<0.77

* Source at nominal position of RR Pic as given by Wyckoff and Wehinger (1978); appears to correspond not to the nova, but rater to a field SAO star (see the text).

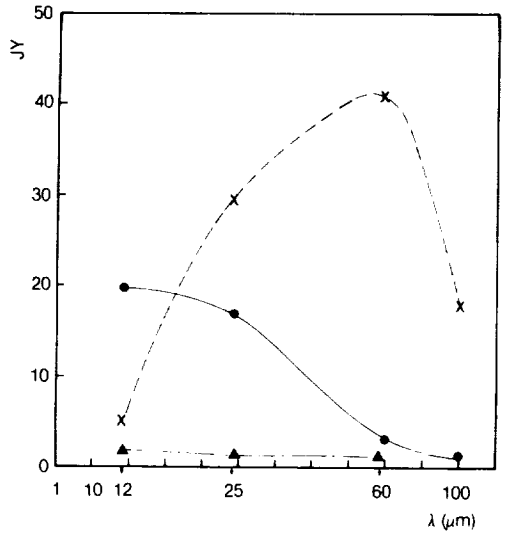

Figure 6-34a) Energy distribution curve for RR Tel (dots), V 605 Aql (crosses) and V1016 Sgr (triangles) from data of the IRAS Point Source Catalogue, 1984. b) the same as a) for CQ Vel (▲). T Cr B (•), T CrB (o, coadded data from Dinerstein, 1986), KP Sco (x). RS Oph (Δ), LQ Sgr (■), FH Ser (●), V 949 Sgr (♦). EU Sct (◊), HR Del( ). The data are from the IRAS Point Source Catalogue.

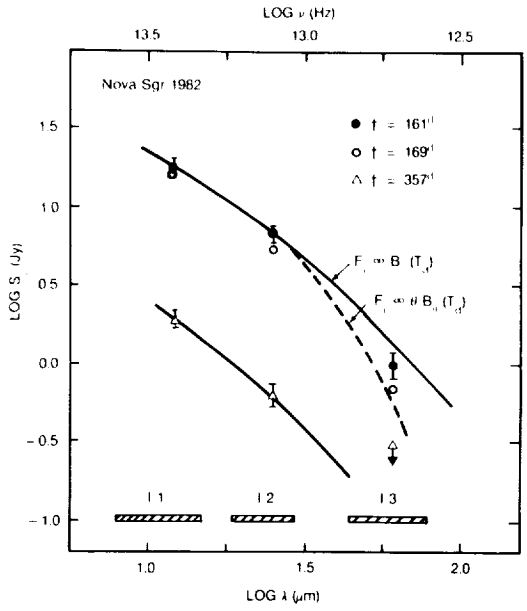

Figure 6-35. Energy distribution curve for Nova Sgr 1982 at three epochs. Black body curve for 1000 K (full line) are drawn through the IRAS data for days 161 and 357 from outburst. The dotted line shows the extrapolated curve for a grain emissivity varying as the frequency between 25 and 60 μm. The hatched horizontal bars indicted the passbands of the IRAS data. (from Dinerstein, 1986)

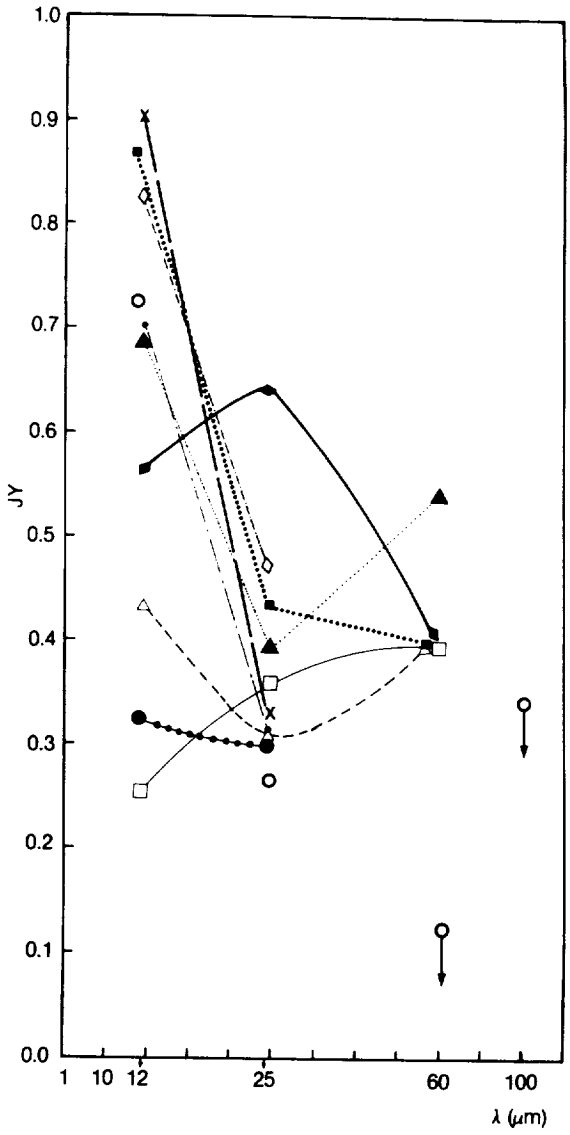

filling its Roche lobe. We can expect that dust will condense in the envelope produced by the M giant wind.

Evans (1985) reports the results of the observtions of NQ Vul 1976. This nova produced an optically thick dust shell 60 days after outburst. The expected temperature of the shell, derived by assuming that it decreases as $t^{-1/2}$ (case of free expansion, and constant luminosity of the remnant), is 240 K. The observed dust temperature, on the contrary, is 72 +/- 5 K. This result can be understood if we assume that the bolometric luminosity in 1983 was 7.6 x 10^{-3} times that of the constant bolometric luminosity, which was maintained during the first year after outburst.

V. ULTRAVIOLET OBSERVATIONS OF NOVAE AND RECURRENT NOVAE

(written by Selvelli)

V.A. INTRODUCTION

The far UV and X-ray radiation of novae originates from regions that are much hotter than those where the optical and infrared radiation is formed.

Thus, space observations of novae are complementary to the ground-based optical ones, and have given and are still giving a new, fundamental contribution to our knowledge on the nature of these objects.

The importance of UV observations of the continuum and line emission of CVs is manifold:

The bulk of the continuum radiation emitted by *quiescent novae* (QN) falls, with very few exceptions, in the satellite UV spectral region. The study of this radiation provides fundamental information about the physical processes that take place in the hot regions of the system, generally associated with the innermost disk part and the white dwarf surface. Estimates of T, L and of the mass accretion rate $\dot{M}$ in QN, a parameter of basic importance for the understanding of the nova phenomenon, are crucially dependent on the observations in this wavelength range.

For *novae in outburts*, observations of the UV continuum are essential for the determination of the bolometric luminosity and of its variations with time from the first outburst (OB) phases until the nebular stage.

In the satellite UV region of the spectrum, several important, strong resonance lines belonging to abundant elements (such as CIV λ 1550, SiIV λ 1400, NV λ 1240) are observed. Most of these ions lack strong lines in the optical region. High excitation lines produced by recombination such as He II λ 1640 or by fluorescence such as the OIII Bowen nebular lines near λ 3000 are also observed in CVs. Moreover, nebular lines (such as SiIII λ 1892, CIII λ 1909, OIII λ 1666, NIV λ 1486, etc.) are observed in novae during the nebular stage, in recurrent novae, and in a few old novae. The study of all these classes of lines provides valuable information on the excitation processes, the region(s) of line formation, the presence of outflow phenomena, and the intensity of the radiation field in the scarcely accessible EUV spectral range.

If semiforbidden or forbidden lines are present, they provide a useful tool for the diagnosis of the physical conditions (Ne, Te) in the low density regions of the system. In addition, in several cases, especially in novae in the nebular stage, the presence of lines of different ionization states of a given element has also allowed a careful determination of the chemical abundances in the ejecta, a parameter of paramount importance for testing the various theories on the processes that lead to the nova phenomenon and for understanding the evolutionary state of the system.

An accurate determination of the parameters above mentioned, together with the knowledge of their variations with time, can be used to set severe constraints on the various physical models of nova, both for the quiescent phase (Q), in which especially T and L are important, and for the eruptive one, where the dynamic, density, and chemical composition of the ejecta are concerned.

In the present section the behavior of novae in the UV is subdivided in two parts: 1) novae (classical and recurrent) in quiescence, and 2) novae (classical and recurrent) during outburst and post-OB phases. This subdivision might seem somehow artificial but it has a physical ground: UV observations of novae in Q provide important clues on the hot components of their radiation field and, therefore, on those processes that take place near the compact component. Little information is gained about the physical conditions in the outer regions since, with a few exceptions, the envelope ejected at the time of the outburst is no more detectable. On the other hand, observations made during the various OB and post-OB phases are related to the physical structure of the extended pseudophotospere formed in early OB phases,

and to the physical conditions (n_e, T_e, chemical composition, and velocity fields) in the ejected envelope.

V.B. ULTRAVIOLET OBSERVATIONS OF POST NOVAE

The launch of the IUE satellite (Boggess et al., 1978) has opened a new era in the UV observations of post novae, allowing the acquisition of about 200 UV spectra for a dozen objects with m_v up to 15.

Table 6.11 lists the postnovae observed with IUE until November 3, 1987.

Two comprehensive reviews on the UV observations of classical novae by Starrfield and Snijders (1987) and by Friedjung (1988) have recently appeared. The reader is referred to them for a detailed description of the OB phenomenology and for specific considerations on the abundances of the ejecta.

V.B.1. THE UV CONTINUUM

After correction for the interstellar reddening, which is usually determined from the λ 2200 absorption feature, a general characteristic of most objects is the presence of a hot continuum as indicated by the flux increase toward shorter wavelengths. The origin of this continuum is commonly attributed to the dissipation, through viscous processes in the accretion disk formed around the compact companion, of the gravitational energy released when mass is transferred from the companion onto the surface of the white dwarf.

A possible contribution from the white dwarf itself, still active and hot a long time after the OB, cannot be ruled out, and this possibility must be kept in mind when comparing data with the theoretical models.

The interpretation and modeling of the UV continuum is not a well established operation like, for example, that of fitting a stellar continuum with a model atmosphere. While a steeper slope toward shorter wavelengths is commonly interpreted as an indication of higher temperature, the actual value depends a lot on the details of the model chosen. The accretion disk spectrum is calculated as the sum of the contributions of the individual surface elements (annuli), each one emitting with a different temperature. Generally these models are based on sums of emissions of Kurucz's models or on sums of black bodies. A deeper criticism on the

TABLE 6.11

NOVAE and RECURRENT NOVAE Observed with IUE during Optical Quiescence.

OBJECT	R.A. (1950)			DECL (1950)		
GK Per	03	27	47	+43	44	05
T Aur	05	28	46	+30	24	36
RR Pic	06	35	10	-62	35	49
BT Mon	06	41	16	-01	58	09
CP Pup	08	09	52	-35	12	04
T Pyx	09	02	37	-32	10	47
T Cr B	15	57	25	+26	03	37
V 841 Oph	16	56	42	-12	48	59
RS Oph	17	47	32	-06	41	39
DQ Her	18	06	05	+45	51	02
V 533 Her	18	12	46	+41	50	22
V 603 Aql	18	46	21	+00	31	36
HR Del	20	40	04	+18	58	52

assumptions and limitations of the models and on the advantages and disadvantages of the various methods can be found in Wade (1984) and in Chapter 4.IV.B.

Generally, the power-law UV continua can be better reproduced using sums of contributions of stellar atmospheres. It is rather difficult, however, to produce a good agreement of the models with data that include both the UV and the optical continuum.

Wade (1984) has pointed out that a disk model with a range of temperatures has the same slope, for a given wavelength range, as a model with a single temperature. In other words, it is possible to associate with the flux ratio at, say, 2880 Å and 1460 Å, a corresponding temperature of a model atmosphere. The slope of the classical Lynden-Bell (1969) distribution ($F(\lambda) \propto \lambda^{-2.33}$) is the same as that of a Kurucz model with T=17.000° K, while that of a power-law distribution with α=2.0, quite common for cataclysmic variables (CVs), corresponds to a model with T=14.000° K.

In practice, in several cases, the observed continuum has been fitted equally well by a single component (i.e., a power law or a black body) or by two components (i.e., two black bodies or a black body and a power law). As a consequence, it is not surprising that different authors have proposed for the same objects fits with quite different temperature components; compare, for example, the determination of the temperature in HR Del made by Hutchings (1979a), Krautter et al. (1981), Rosino et al. (1982), Dultzin-Hacyan et al. (1980), and Wargau et al. (1983) (Table 6.12).

It is remarkable that with few exceptions (Verbunt, 1987) the slope of the continua of the different classes of CV s (dwarf novae, novae, nova-like) is rather similar. In the more luminous and best studied old novae (i.e., V 603 Aql, RR Pic, HR Del), the continuum slope in the UV (after correction for reddening) is very close to the slope of an $F(\lambda) \propto \lambda^{-2}$ distribution, in fair agreement with the "standard" $\lambda^{-2.33}$ distribution. (Figure 6.36)

It is not clear, on the basis of the IUE observations alone, how correct it is to extrapolate toward shorter wavelengths the continuum slope found from the IUE observations. Voyager data on V 603 Aql (Figure 6.37) led Carone et al. (1985) to conclude that for this object (but its trend is common to all other CVs observed with Voyager), the rising IUE flux distribution does not continue into the EUV.

It is remarkable that the EUV region (900-1200 Å) is rather flat (flattening begins near λ 1300 Å) for almost all CV s observed, while the EUV continuum (500-900 Å) is extremely weak ($< 5 \times 10^{-13}$). Carone et al. (1985), on the basis of these data, conclude that models that fit the IUE UV fail to fit the EUV region. Exceptions to the general trend $F(\lambda) \propto \lambda^{-\alpha}$ with $\alpha \sim 2$ are GK Per, DQ Her, BT Mon and T Aur.

GK Per (Rosino et al., 1982) is quite peculiar, since its UV continuum, unlike that of other old novae, shows an energy distribution curve that is not peaked toward the extreme ultraviolet but around λ 3600 (figure 6.38), an indication of a lower temperature. However, high excitation and ionization lines are present. Even from the IUE low-resolution spectra, a larger line width than in other old novae can be appreciated. Moreover, unlike in other old novae, there is some contribution in the UV from the K2 IV-V companion. GK Per is also a copious hard-x-ray emitter, and this emission shows a strong coherent modulation with a period of 351 s (Watson et al., 1984). This is a signature of the "intermediate polars" or DQ Her class of CVs, characterized by the presence of a rather strong magnetic field, of the order of 10^5 - 10^6 gauss. Probably, the magnetic field causes the disruption of the innermost disk part, where the missing UV continuum would otherwise be produced. (See Chapters 4.III.F.2.) Another intermediate polar is DQ Her, a system seen at quite high inclination, which shows periodic eclipse phenomena. Its far UV continuum is nearly flat and can be represented by a power law with spectral index α close to zero over the whole UV spectral range.

TABLE 6.12

Temperature Estimates in HR Delphini

		E(B-V)	
Rosino et al.	(1982)	0.1	35000+20000 BB'S
Duerbeck et al.	(1980a)	0.19	28000°K BB
Andrillat et al.	(1982)	0.17	$\lambda^{2.33}$ and BB with T=47000°K.
Friedjung et al.	(1982)	0.17	$F(\lambda) \propto \lambda^{-2.33}$
Hutchings	(1980)	0.10-0.15	16000°K model atmosphere.
Dultzin-Hacyan et al.	(1980)	(0.18)	40000°K BB plus power-law (far UV)
Krautter et al.	(1981)	0.15	45000°K+25000°K BB or power law with α=-2.09
Hutchings	(1979a)	0.23	15000°K or 50000°K BB plus power-law at λ 1500 A.
Wargau et al.	(1982)	0.15	80000°K plus 15000°K BB's.
<u>The same for V 603 Aql.</u>			
Dultzin-Hacyan et al.	(1980)	0.07	50000°K plus 8000°K BB's.
Duerbeck et al.	(1980a)		30000°K BB
Krautter et al.	(1981)	0.07	45000°K plus 25000°K BB or power-law with α=-1.99.
Wargau et al.	(1982)	0.00	200000°K plus 11000°K BB's.
Lambert et al.	(1980)	0.07	Thick disk
Ferland et al.	(1982a)	0.07	Power-law: $\nu^0 \div \nu^{0.5}$.
<u>The Same for RR Pic</u>			
Krautter et al.	(1981)	0.01	Power-law with α=1.81 or 40000°K plus 28000°K BB's.
Wargau et al.	(1982)	0.03	90000°K plus 14000°K BB
Rosino et al.	(1982)		33000°K plus 22000°K BB's.
Duerbeck et al.	(1980a)		27500°K BB.

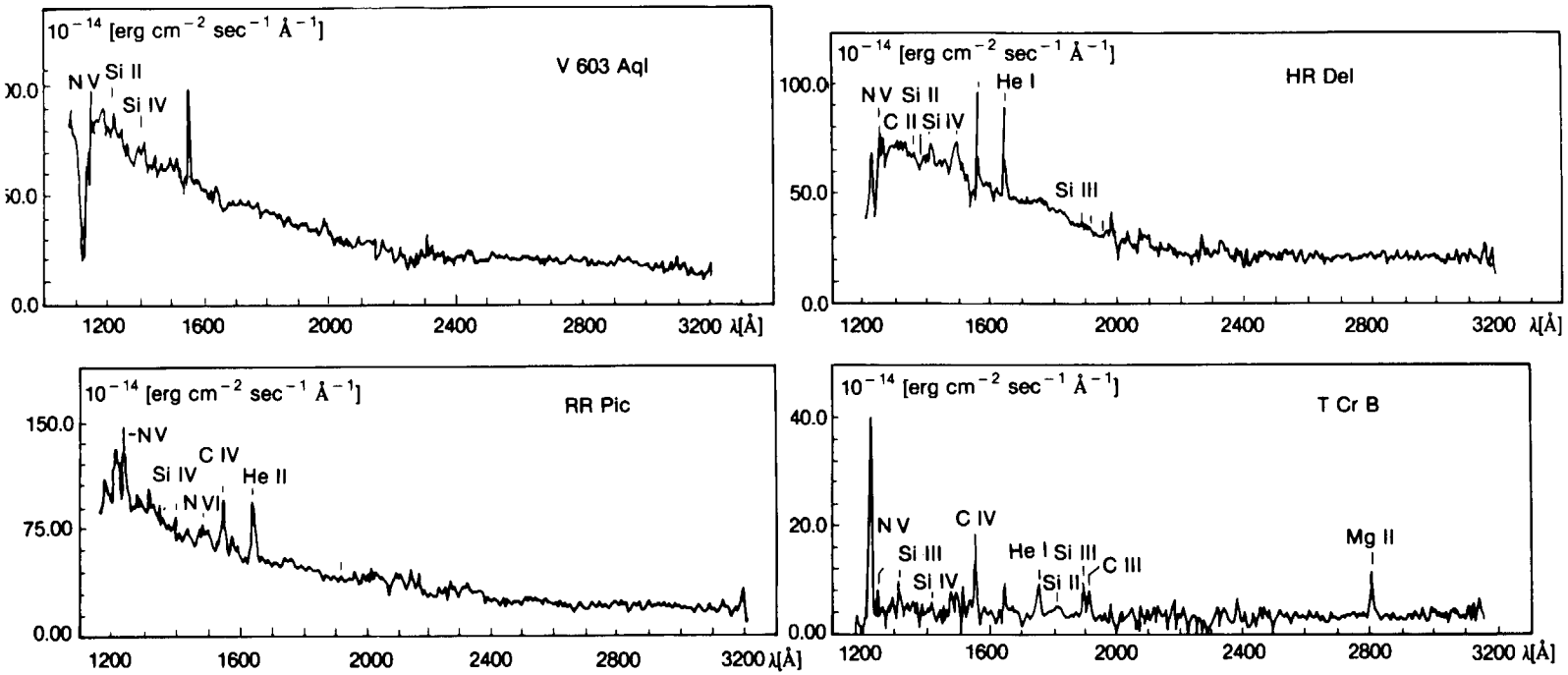

Figure 6-36. The UV continua of the brightest old novae V 603 Aql, HR Del, RR Pic, and of recurrent nova T Cr B. (from Krautter et al., 1981)

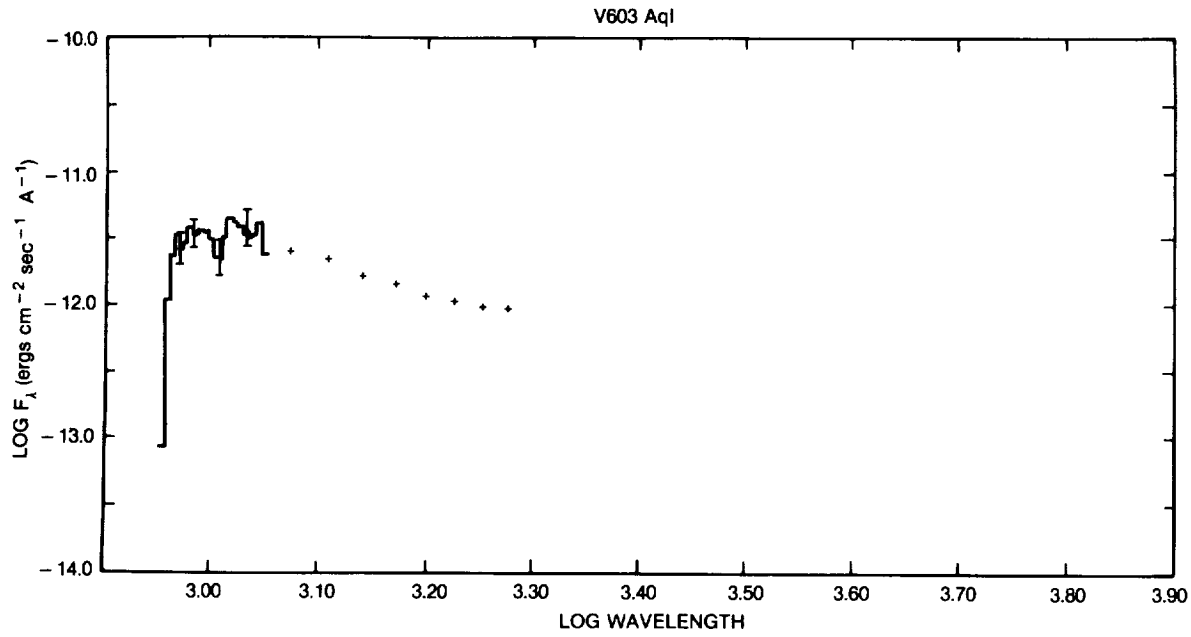

Figure 6-37. Voyager observations of V 603 Aql, dereddened by 0.07. (from Carone et al., 1985)

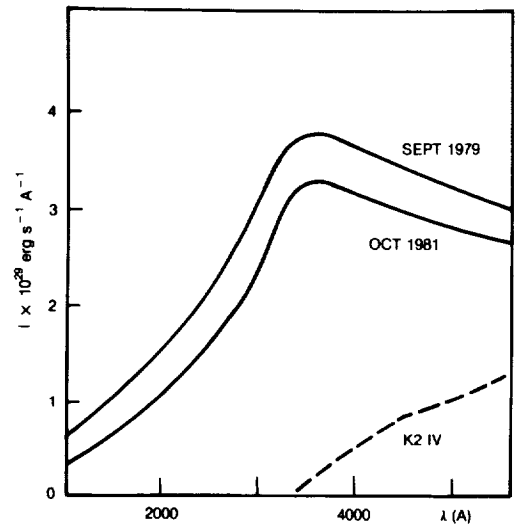

Figure 6-38. The continuum distribution of GK Per at quiescence. (from Rosino et al., 1982)

It is tempting to ascribe this peculiarity in the continuum slope in DQ Her to an inclination effect that causes the disk to be seen in its outermost coolest components. This suggestion is supported by the nearly flat continua of BT Mon (i~84°) (Figure 6.39) and T Aur (i~68°), and is in agreement with an optical study of Warner (1986c) who has found a strong correlation between the absolute visual magnitude and the inclination of the system. Warner has interpreted this result in terms of darkening of the disk limb when viewed at different inclination angles. Verbunt (1987), however, from a statistical study of the UV spectra of several CVs has concluded that the continuum slope does not show a definite dependence on the system inclination; his disk models show instead that the slope of the continuum depends strongly on the white dwarf mass.

V.C. THE MASS ACCRETION RATE AND LUMINOSITY OF OLD NOVAE

The disk luminosity is linked to the mass accretion rate $\dot{M}$, a quantity whose knowledge is essential for understanding the evolution of the system and physics of the outburst. In principle, $\dot{M}$ can be determined after a comparison of the slope of the continuum with theoretical models: a steeper UV slope indicates an higher $\dot{M}$. Unfortunately, as pointed out by Verbunt (1987), theoretical disk models show that the slope of the continuum depends also, and critically, on the white dwarf mass. Because of this, the $\dot{M}$ values reported in the literature might be affected by this uncertainty if the white dwarf mass was not previously well determined.

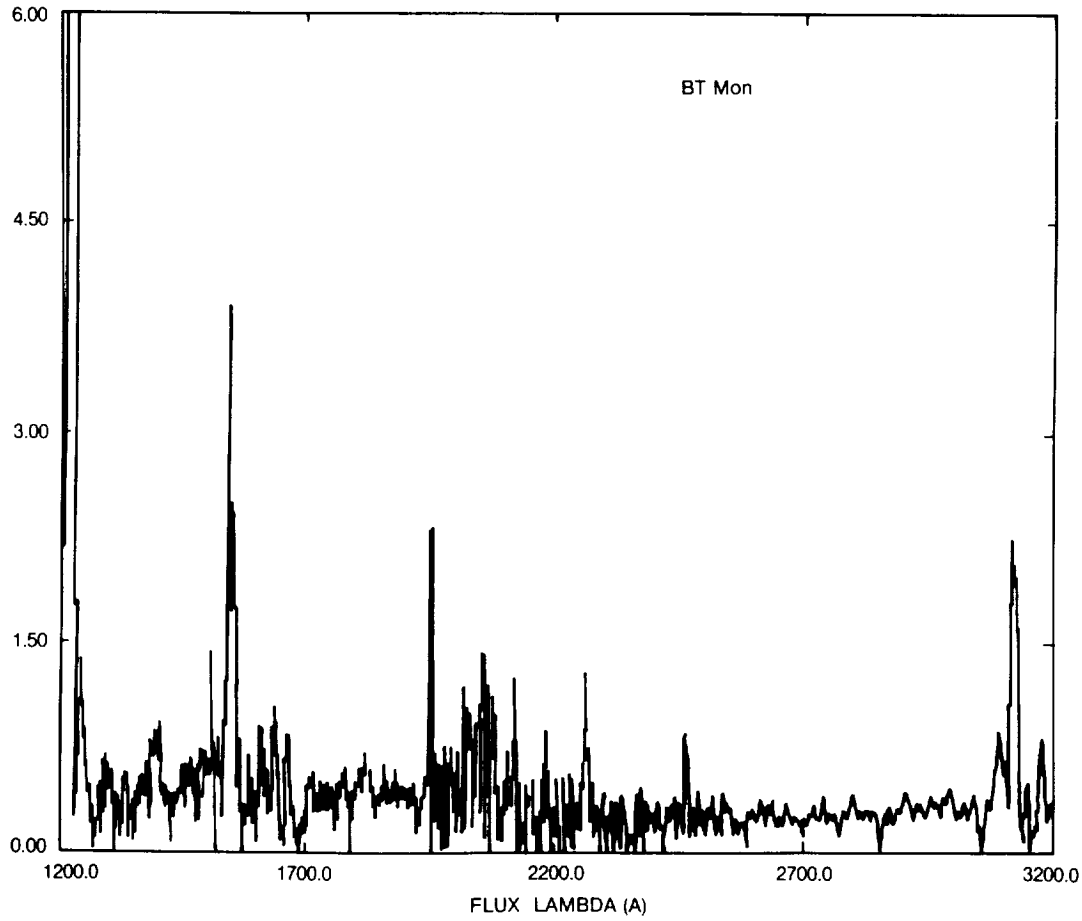

Figure 6-39. The flat continuum of BT Mon (i=90°).

An alternative, less model-dependent method for the determination of $\dot{M}$ is simply based on an estimate of the accretion luminosity from the observed UV (mainly) and optical fluxes. Once the luminosity is known, a lower limit for $\dot{M}$ can be assigned from the relation $L(disk)=1/2\ G\dot{M}M\ R^{-1}$ where $M \sim M_{\odot}$. (See also Chapter 4.II.C.2.)

The considerable differences in the L(UV) estimates for the same object by different authors are due to two main reasons: 1) uncertainties with the distances, and 2) uncertainties in the fitting of the observed continua with models. Wade (1984) has shown that luminosities deduced from fits with stellar atmosphere models are much lower (by factors from 10 to 100) than those obtained from blackbody fits to the same data.

The uncertainties in L are reflected in the uncertainties in $\dot{M}$, and quite serious discrepancies between the $\dot{M}$ values proposed in the literature for the same objects are present. Thus, for HR Del, Friedjung et al. (1982) derived $\dot{M} \sim 10^{-8}\ M_{\odot}\ yr^{-1}$, while Krautter et al. (1981) found $\dot{M} \sim 4.6\ 10^{-8}\ M_{\odot}\ yr^{-1}$, and Hutchings (1979a) gave indication of a value in excess of 10^{-8}. Kenyon and Webbink (1984) have suggested determining $\dot{M}$ by fitting the observed flux at different wavelengths to models of disks seen at different inclinations and emitting like the sums of blackbodies. With this method, they obtained for HR Del a $\dot{M}$ of the order of $4 \times 10^{-8}\ M_{\odot}\ yr^{-1}$ in fair agreement with Krautter's et al. (1981) value, which is a lower limit based on the "observed" UV luminosity only.

A compilation of mass accretion rates can be found in Verbunt and Wade (1984).

V.D. THE LINE SPECTRUM OF OLD NOVAE

A common characteristic of the line spectrum of cataclysmic variables in quiescence is the presence of strong emission lines of high excitation character like NV 1240, SiIV 1400, CIV 1550, and HeII 1640.

Intercombination lines like NIV 1486, NIII 1750, SiIII 1892 and CIII 1908; or lines of low excitation like OI 1303, CII 1335, and resonance lines of SiII are generally much weaker or absent except in the case of the recurrent novae T Cr B and RS Oph and in the case of those few old novae who still show evidence of the shell ejected at the time of the outburst. Table 6.13 lists the most common emission lines usually found in old novae.

TABLE 6-13

List of common UV Lines in Post-Novae.

λ	ION		λ	ION	
1240	N	V	1640	He	II
1260	Si	II	1750	N	III
1300	Si	III	1815	Si	II
1335	C	II	1860	Al	III
1400	Si	IV	1892	Si	III
1486	N	IV	1909	C	III
1550	C	IV	2800	Mg	II
1575	Ne	V			

V.D.1. P CYG PROFILES IN OLD NOVAE

Krautter et al. (1981) have reported the presence of P Cyg profiles in the spectra of the old novae HR Del, RR Pic, and V 603 Aql. Although the presence of some of the P Cyg profiles is questionable (e.g., λ 1640 in HR Del, CIV in RR Pic, etc.), they are clearly present in HR Del at CIV (Figure 6.40). The presence of such profiles indicates that material is still outflowing a long time after the outburst, and this poses several questions about the nature of the mechanism that originates the wind and the duration of the processes related to the outburst. Hutchings (1979a) has reported marked differences in the P Cyg profiles in the several spectra available. He suggested the presence of two absorption components of varying strength that could be consistent with mass loss in the form of a spiralling wind.

A more complete set of observations was obtained by Friedjung et al. (1982) who related the variations to the orbital phase of the observations. (See also the next section.)

Krautter et al. (1981) estimated the mass loss rate in HR Del by fitting the absorption component of the CIV doublet with the grid of theoretical profiles of Castor and Lamers (1979). Assuming a spherically symmetric wind and all carbon=CIV and taking V edge = 4,000 km s^{-1}, they derived $\dot{M} \sim 2.6\ 10^{-11}\ M_{\odot}\ yr^{-1}$. The uncertainty in this value is due to the rather crude assumptions that have been made. The

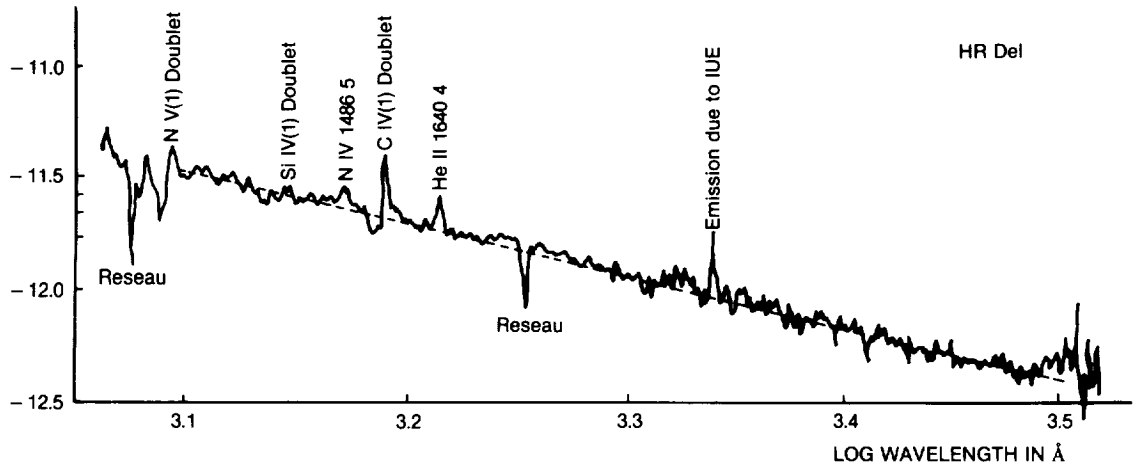

Figure 6-40. The P Cyg profiles in the spectrum of HR Del.

terminal velocities in the HR Del wind are of the order of 3 x 10^3 kms^{-1} for CIV. Hutchings (1979) and Rosino et al. (1982) give 2320 km s^{-1}, while Dultzin-Hacyan et al. (1980) give 2,900 and 3,500 km s^{-1} and Krautter et al. (1981) give 4,000 km s^{-1}. For NV Hutchings gives 2,800 km s^{-1} and Rosino gives 2,900 km s^{-1}. It must be pointed out, however, that in the low resolution IUE mode, a wide Ly α absorption of circumstellar or interstellar origin, which can extend up to λ1230, could mimic a shortward displaced absorption for the NV doublet, thus contaminating the true one.

In a study of dwarf novae, Cordova and Mason (1982) have suggested the presence of a conical outflow, perpendicular to the disk plane. They have also suggested that the mechanism responsible for the wind is radiation pressure in the resonance lines, as in hot-star winds. It is not clear, however, if this model might be applied to HR Del and why among old novae such P Cyg profiles have been clearly detected only in HR Del. (See also Chapter 4.IV.D.)

A marginal wind detection has been claimed by Cordova and Mason (1985) in the CIV doublet of DQ Her also. A comparison of the eclipse profile of CIV with the out of eclipse one showed that the latter is fairly symmetric, while the former appears to be skewed to the red. They suggest that a wind may be present but contributes only part of the total line emission.

If the wind geometry in old novae is similar to that of dwarf novae in OB, this result seems to contradict the indication by Cordova and Mason (1985) that P Cyg profiles in dwarf novae are more common in objects with low inclination (unlike DQ Her).

Recent observations of V 841 Oph (Cassatella et al., 1988), indicate the presence of P Cyg profiles in its UV spectrum also (Figure 6.41).

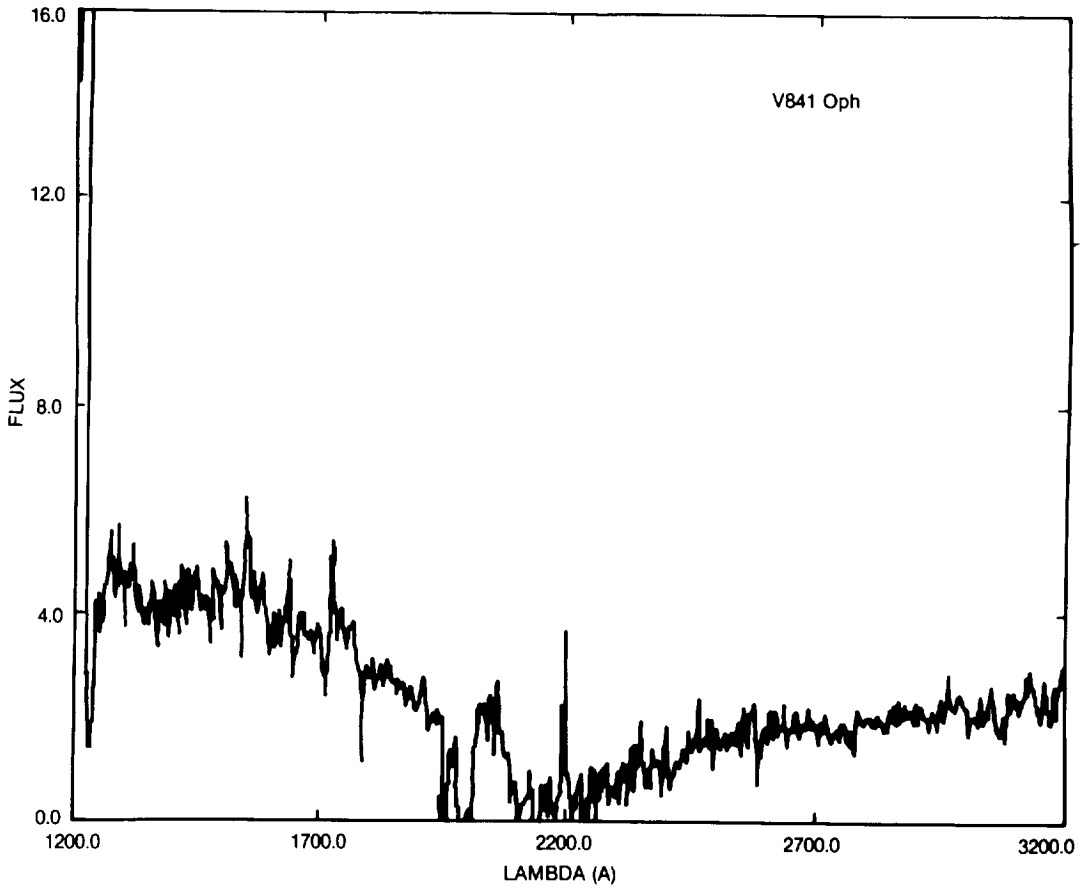

Figure 6-41. The UV spectrum of the post-nova V 841 Oph.

V.D.2. HIGH-RESOLUTION LINE PROFILES

Observations of emission line profiles in the UV spectra of old novae in quiescence are limited by the IUE performance. These objects are fainter than m_v 11.5, and although very hot, their far UV flux does not permit IUE observation in the high-resolution mode. Such observations would be of invaluable importance for the acquisition of high-resolution profiles, which would allow a deeper study of the region where the lines are formed and of their dynamical structure. V 603 Aql, the brightest nova remnant, is the sole object in this class that has been just barely observed in the high-resolution mode (Selvelli and Cassatella, 1981). The two spectra, (SWP + LWR) although at about 50% of the optimal exposure, clearly show emission lines of Si IV, CIV, and He II. These emissions are wide and shallow and centered on the nominal wavelength (Fig. 6.42). There is no trace of any P Cyg absorption. Their FWHM indicates v~1,800 km s^{-1} and FWZI give, v ~ 4,000 km s^{-1}. These profiles and velocities are those expected by lines formed in the innermost region of an accretion disk orbiting a white dwarf.

It is notable that over the whole spectrum, there is no evidence of sharp (and more easily detectable) nebular lines. This indicates that the envelope ejected at the time of the outburst has by now vanished.

V. E. THE UV SPECTRAL VARIATIONS

The time resolution between successive IUE spectra has an intrinsic lower limit of about 20 minutes also if the exposure time is much shorter, because of the cameras read-preparation times. However, even when the proper exposure time (typically 20 minutes for the brightest old novae) is added, still a rather satisfactory time resolution as compared with the orbital period can be achieved.

V603 Aql. Rahe et al. (1980) and Drechsel et al. (1981) have detected variations of the emission intensities and of the continuum both in the optical and in the UV range. These variations seem to be related to the orbital period. The intensity of the CIV, SiIV, and HeII emissions is

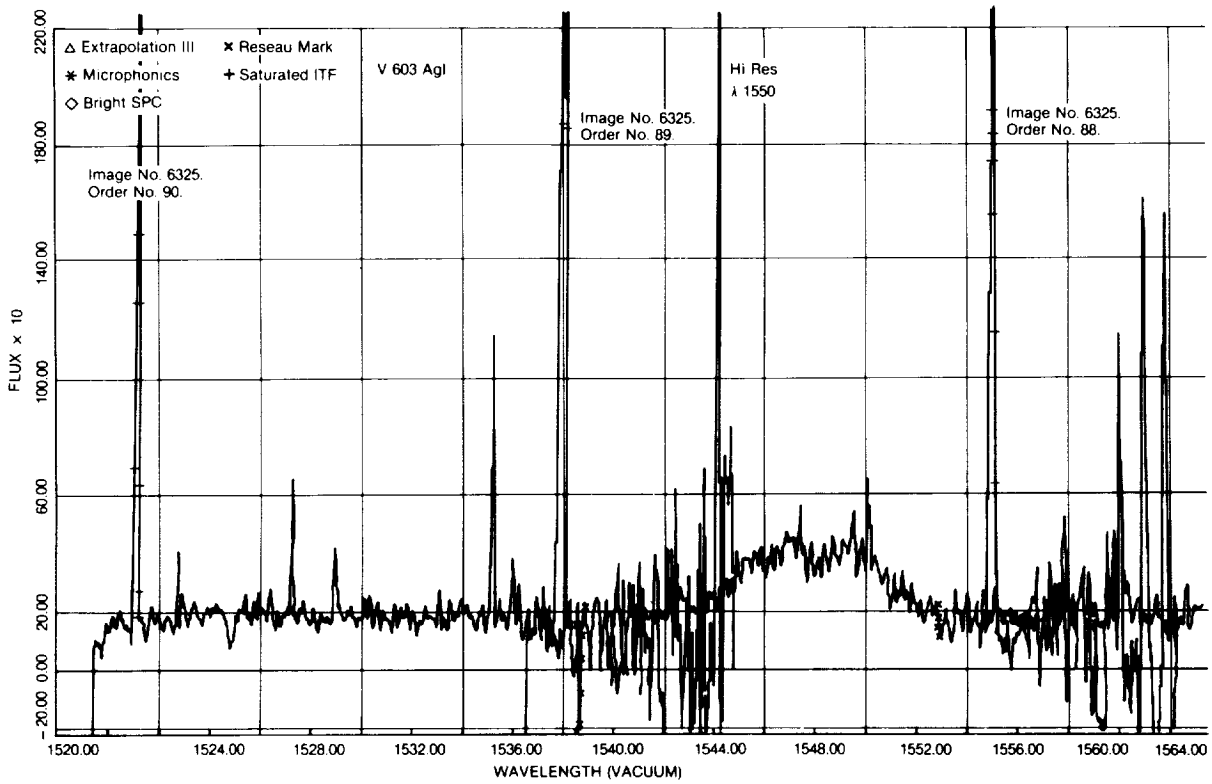

Figure 6-42. The high-resolution profile of the C IV 1550 dublet in V 603 Aql.

highest during maximum light at phase 0.5, and lowest near orbital phase 0.0. Similar results were found by Selvelli and Cassatella (1981) on less homogeneous material. Both Drechsel et al., and Selvelli and Cassatella have resorted to occultation or partial eclipse effects to explain the variations, but the small inclination of the system sheds serious doubts on this hypothesis.

Selvelli and Cassatella (1982) have also studied the variations in the λ 2000 – 3200 region. Maxima in the line emission and continua occur near phase 0.0, in disagreement with the previous results. This all suggests that the variations might be due to transients, and not to phase-related phenomena.

The results of Hutchings (1979a) suggested UV spectral variations in *HR Del*, although a quite large scatter is shown in his graphs. Andrillat et al. (1982) have considered these effects as phase-related. They found minima near phase 0.0 both in the 1200 - 2000 and in the 2000 - 3200 regions. In a study based on more homogeneous material, Friedjung et al., (1982) detected clearly phase-related variations both in the continuum and in emission and absorption lines. Fig. 6.43 (from Friedjung et al.) gives the observed variations. Inspection of this figure shows a periodic variation in the NV emission with a minimum around phase 0.9. The CIV emission seems to vary in antiphase with respect to NV, but possibly, its variations are more complex. A minimum seems to be present in all cases, except for CIV, around phase 0.9 both for lines and continuum. Note that phase 1.0 is that of maximum radial velocity.

The authors interpret the minimum as due to an occultation of the central part of the disk by a splash where the stream of accreted gas reaches the disk. The wind, which is responsible for the P Cyg profile variations, has evidently more complex variations.

A behavior similar to that of V603 Aql and HR Del is also present in *RR Pic*. Significant variations, both in the lines (by a factor up to six) and in the continuum (by a factor 1.5) are clearly

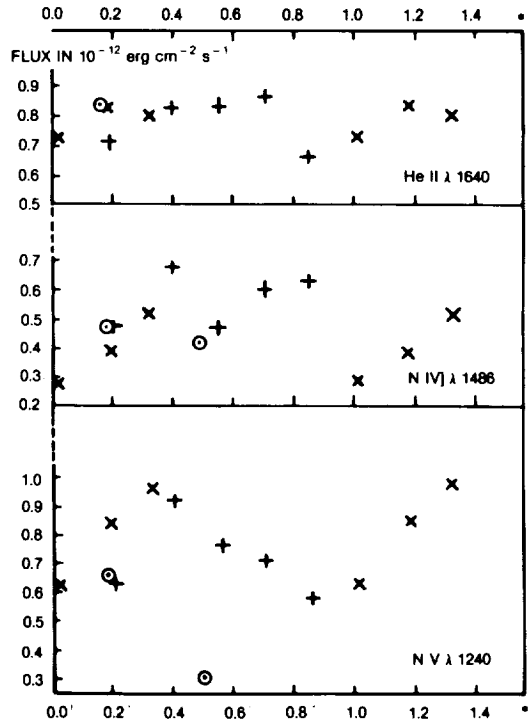

Figure 6-43. The variations with phase of the emission line intensities in a series of successive IUE spectra of HR Del.
(from Friedjung et al., 1982)

evident in spectra taken by Selvelli (1982) in a close sequence of alternate exposures with the SWP and LWR cameras during a 6-hour monitoring. The observed variations are in disagreement with the photometric behavior in the optical, reported by Vogt (1975) and by Haefner and Metz (1982). In addition, UV spectra taken at nearly the same phase in two different cycles show very different characteristics, thus confirming the reality of transient phenomena. It seems reasonable to suppose that both phase-related and transient phenomena contribute to the observed spectral variability, and that the transient phenomena are more evident in the UV region since the three best studied objects present this behavior. These results are in agreement with the conclusion of Verbunt (1987) that all systems for which time-separated observations are available show UV variability with time scale of the order of hours. He also suggests that these variations are probably not of orbital origin, since observations at different periods but at the same orbital phase show significant spectral changes.

V.F. CONCLUDING REMARKS

To conclude this section on classical old novae, it is important to emphasize that of the dozen old novae that are accessible to IUE, only a few have been studied in some detail. Selection effects could be very serious, considering the scarceness of the sample, and thus we might risk drawing general conclusions (for example, on L , T, $\dot{M}$, etc.) based on the behavior of the more luminous members of the class. It is therefore mandatory to improve these rather poor statistics by observing carefully all objects that are accessible to IUE.

V.G. THE UV SPECTRUM OF RECURRENT NOVAE IN QUIESCENCE

Recurrent novae represent a small class of objects whose recurrence time between outbursts is intermediate between classical novae and dwarf novae.

The major problem for the understanding of recurrent novae is the nature of their outbursts and the nature of the accreting objects. Recently, Webbink et al. (1987) have reviewed the properties of the rather different members of the "class" and have suggested the existence of two subclasses on the basis of their OB mechanisms:

1)Those powered by TNR on a white dwarf (T Pyx and U Sco) as in classical novae. In this case theoretical consideration (Starrfield et al.,1985) show that in order to produce outbursts with recurrence time scales compatible with those of T Pyx , the white dwarf must be very massive (M_{wd}~1.38 $M_\odot$) and the accretion rate must exceed $2x10^{-8} M_\odot$ yr^{-1}, that is, much higher than accepted for classical novae.

2) Those powered by the transfer of a burst of matter from the red giant onto a main sequence companion (T Cr B and RS Oph). In this case, the inter outburst accretion rate is expected to be rather low.

T Pyx. This regularly recurrent nova (P_r 20 ±1 years) has been observed by Bruch et al. (1981). Because of its faintness and of the severe reddening (0.35), the IUE spectrum was underexposed. However, a hot continuum is clearly evident, together with emission lines of CII, CIV 1550, HeII 1640, and NIII 1750. It is notable that, unlike in other recurrent novae (T Cr B and RS Oph), the MgII doublet is absent. This is interpreted as indication of the absence of the red giant in the system.

The three existing sets of IUE data of T Pyx in 1980, 1986, and 1987, show that the UV continuum is very hot (Fig. 6.44) and practically constant, an indication of a very high accretion rate, which seems to support the thermonuclear powered model. The suggestion by Webbink et al. (1987) that the OB of T Pyx is nuclear powered is based mainly on the difficulty encountered by the accretion-powered model in explaining the behavior of T Pyx during the OB phases and the dominance of a hot continuum source during quiescence, although some unresolved problems remain with the luminosity and the unusually blue color at minimum.

The recurrent nova *T Cr B* has been observed from the early phases of IUE's life until very recently (Cassatella et al., 1986). The UV continuum distribution can be represented, at the various epochs by a single power-law spectrum $F(\lambda) \propto \lambda^{-\alpha}$ over the entire IUE range, α ranges from 0.7 to 2.2 with a mean value of about 1.3.

In general, when the flux is higher, the continuum is steeper. A distinctive peculiarity of T Cr B is that significant UV variations correspond to very small changes in the visible light. The UV emission line spectrum shows wide range of ionization and excitation with the presence of ions from OI to NV and HeII. Radial velocity studies of Kraft (1958), Paczinski (1965), and more recently by Kenyon and Garcia (1986) have indicated that the companion of the red giant is a main sequence star, since its mass is about 1.8 $M_\odot$. However, the UV and X-ray observations seem to suggest a white dwarf companion. In fact:

1) The disk luminosity is radiated mostly in the UV, with a negligible contribution to the optical, contrary to what is expected from a

main sequence accretor.

2) A quite strong HeII λ 1640 emission generally present, with an average luminosity of 1.3 x 10^{33} erg s^{-1}. This emission is an indicator of temperatures of the order of 10^5 °K

3) The x-ray luminosity in the range 0.16 to 4.5 Kev is of 5 x 10^{31} erg s^{-1}, with the same order of magnitude of the few other detections of "classical" novae in quiescence. (Cordova et al. 1981b).

4) A recent high-resolution spectrum (Selvelli et al. 1988) has shown that the CIV λ 1550 emission is wide and shallow. The half-width at zero intensity (HWZI) indicates a velocity larger than 1500 km s^{-1}, and the shape resembles that observed in the CIV λ 1550 emission in a high-resolution spectrum of V 603 Aql. See Chapter 9 for a more expanded discussion.

RS Oph. In the UV, it is quite faint because of the strong reddening E(B - V) = 0.73, and only underexposed spectra were obtained (Rosino et al., 1982). The continuum is quite flat (Fig. 6.45), and the only spectral feature that is clearly evident is the NIII λ 1750 semi-forbidden line. CIV, HeII, and the other common emissions are not detectable. (See next section for the UV spectrum in outburst).

V.H. UV OBSERVATIONS OF NOVAE AND RECURRENT NOVAE IN OUBURST

Unlike old novae, for which there is a substantial similarity in the UV spectroscopic signatures (a hot continuum and high excitation lines), the UV behavior of novae during the outburst phases can hardly be reconducted into a common scheme. In this respect, each nova outburst represents a unique phenomenon with its own specific characteristics.

Since the launch of IUE, a dozen novae have been observed in the UV during their decline after the visual maximum. Only in a few cases was the nova monitored in the various post maximum phases until the detection limit.

Table 6.14 lists all novae and recurrent novae in OB observed with IUE. The studies of these observations were generally aimed to obtain information on the physical and chemical parameters of the ejecta (from spectra in the nebular phase) and on the dynamic and energetic of the outflow

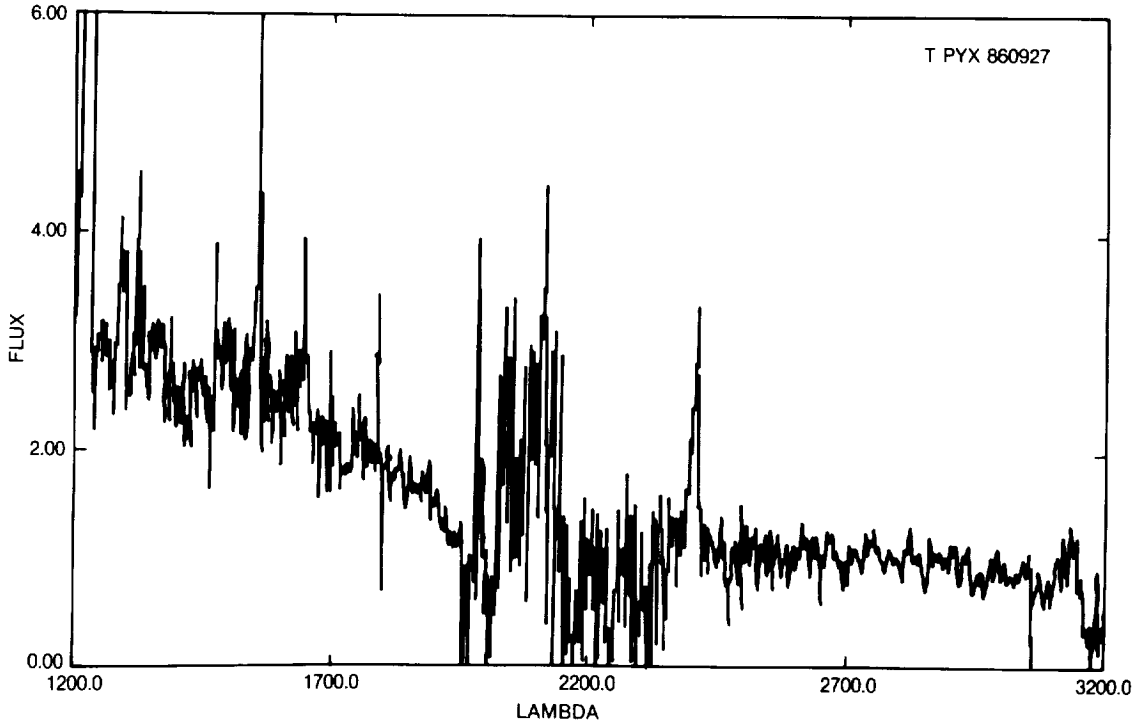

Figure 6-44. The UV spectrum of the recurrent nova T Pyx.

phenomenon.

For some of these objects enough IUE data have been available to permit an adequate study of their spectroscopic changes in the various phases following the OB. In particular, these data have made it possible to obtain reliable estimates of the bolometric luminosity and an accurate determination of the outflow velocities in the ejected envelope.

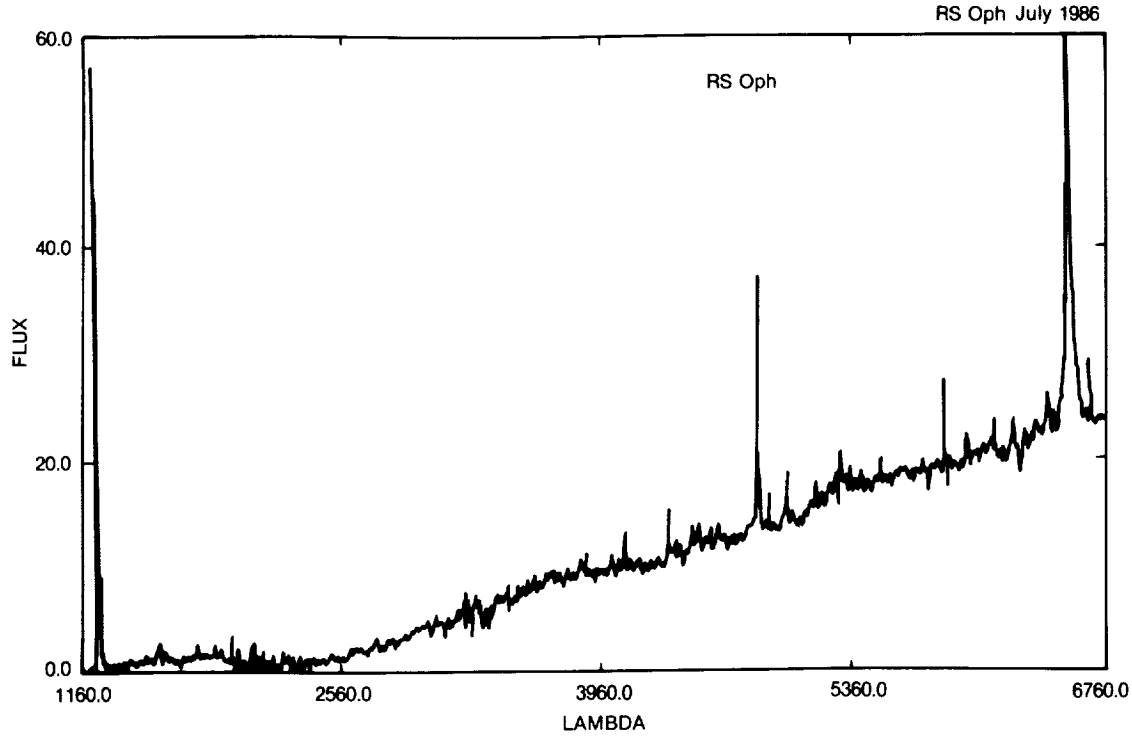

Figure 6-45. The spectrum of the recurrent nova RS Oph from 1200 to 6800 A. (from Cassatella et al., 1988)

TABLE 6.14

NOVAE and RECURRENT NOVAE in Outburst Observed with IUE until 1987.

OBJECT			R.A. (1950)			DECL (1950)		
NOVA	Mus	1983	11	49	35	-66	55	39
NOVA	Cen	1986	13	17	42	-55	34	30
U	Sco		16	19	37	-17	45	43
RS	Oph		17	47	32	-06	41	39
NOVA	Ser	1983	17	53	02	-14	00	56
V 394	Cr A		17	56	58	-39	00	27
NOVA	Cr A	1981	18	38	33.6	-37	34	09
V 4077	Sgr	1982	18	31	33	-26	28	27
NOVA	Her	1987	18	41	26.6	15	16	15
V 1370	Aql	1982	19	20	50.1	+02	23	35
PW	Vul	1984-1	19	24	03.5	+27	15	55
NOVA	Vul	1984-2	20	24	40.5	+27	40	48
NOVA	Cyg	1978	21	40	38	+43	48	10
NOVA	And	1986	23	09	47.5	+47	12	00

Moreover, observations made during the nebular stage have made possible a reliable determination of the chemical abundances in the ejecta. This parameter is of paramount importance for testing theories on the nova phenomenon and for understanding the evolutionary state of the system.

The physics of the nebular state is relatively simple and quite well understood. The methods and principles of the studies of gaseous nebulae have been successfully applied also to the study of the symbiotic stars, whose emission spectra are nebular-like; see the recent review by Nussbaumer and Stencel (1987) for details and the Section VII on the envelopes in this chapter.

The most important features of novae in outburst in the UV are reported here.

FH Ser, the first nova to be detected in the UV, was observed with OAO-2 over an interval of 53 days, starting about the time of visual maximum, and another observation was made about a year and a half later. (Code, 1971).

During the observed period, the spectrum changed from an absorption-like, spectrum, similar to that of an F star, to a strong emission-like spectrum. While the star in the optical was steadily fading in luminosity, both the UV continuum and the UV emission lines continued to brighten.

During the first 60 days after the OB, the energy distribution from 1000 to 6000 Å indicated an approximately constant integrated luminosity, where the decline in the optical was compensated by a progressive shift toward the UV. These results supported a model of nearly constant bolometric luminosity in novae after outburst.

V 1500 Cyg 1975 was observed with Copernicus just after maximum and was too cool to be detected at λ 2700 A (Jenkins et al, 1977). It became unobservable for Copernicus about 100 days after maximum. Measurements made after that date with ANS made it possible to derive that the bolometric luminosity at maximum and 100 days after outburst varied by a factor of 20, while the visual luminosity (measured in the y band) decreased by a factor of 6600, and the effective temperature increased from about 10,000 to 65,000 °K.

NOVA Cyg 1978 was the first nova observed with IUE: thanks to the capability of the IUE Observatory of a prompt reaction to any event considered worthy of observation, it was monitored from the first phases immediately following the outburst. The first IUE image was taken on September 14, 1978, by Cassatella et al. (1979) one day after visual maximum. The continuum looks like that of an F-type supergiant.

The main line features are FeII absorptions and emission of FeII, CrII, MnII and OIII (Bowen fluorescence mechanism). The MgII doublet consists of a P - Cyg profile with a strong emission component. A high-resolution spectrum taken two weeks later shows the same emission features with widths indicating expansion velocities of about 400 Km s^{-1} .

The OIII lines show larger (525 Km s^{-1}) expansion velocities, while the two components of the MgII 2800 doublet appear blended due to their broadness (FWHM 815 km s^{-1}). The narrow FeII and MnII absorptions of this high-resolution spectrum were studied also by Friedjung (1981b). He concluded that most of the absorption was circumstellar rather than interstellar and estimated the column densities.

A significant redistribution of energy toward the UV and IR is observed both in the continuum and in the lines during the phases of the decline in the optical. The maximum brightness at λ 2740 is reached about 20 days after OB and at λ 1450 about 45 days after OB. The total bolometric luminosity, obtained from UV + opt. + IR observations, reached its maximum about six days after the visual maximum with a value of about 3 times the Eddington luminosity for a 1 $M_\odot$ star (Stickland et al 1981). Between days 13 and 27 the total luminosity remained approximately constant at about 1 $L^{Edd} \sim 1.7 \times 10^4 L_\odot$ and then started to decline (Figure 6.46).

The behavior of Nova Cyg 1978 from the early OB phases until the nebular stage was monitored by Stickland et al. (1981) who provided the first

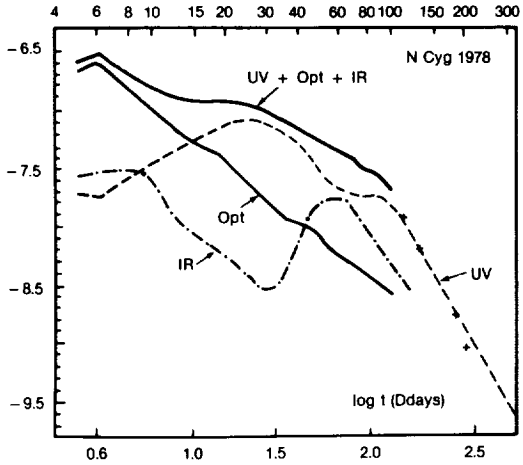

Figure 6-46. Light curves (UV, optical, IR and bolometric) of Nova Cyg 1978.
(from Stickland et al., 1981)

complete coverage of the UV outburst of a nova.

They performed a very detailed quantitative study of the physical conditions in the ejecta during the nebular phase by applying standard and original methods for the analysis of nebular spectra. The nebular spectrum in the UV shows emission lines of OV], NV, OI, OII, OIV, CII, OIV], NIV], CIV, HeII, OIII], NIII], CIII], and MgII. The nebular continuum is due to contribution of recombination and free-free processes of H and He mainly, plus a hot photosphere with T ~ 1.5 x 10^5 °K and R ~ 0.13 $R_\odot$.

The expansion velocity of the nebular shell, estimated by the widths of the nebular lines is 1270 Km s^{-1}, when deduced from the extreme widths, and 760 Km s^{-1}, when estimated from the widths of the flat-topped plateau regions in the centers of the line profiles.

Stickland et al. (1981) derived the electron temperature T_e in the nebula from the emission lines ratios CII 1335/CIII] 1908, CIII 2297/CIV 1550, and NIV 1718/NV 1240, where the first line in each pair is produced by dielectronic recombination via low-lying autoionizing states and the second line is produced by the more usual mechanism of collisional excitation. T_e values are around 9000 °K in the CIII region, around 11,500 °K in the CIV region and around 14,500 °K in the NV region.

The electron density N_e was determined from the ratios NII] 2140/[NII] 5755, and OIII] 1663/[O III] 5007, which yielded $N_e \sim 8 \times 10^7$ el. cm^{-3}. Abundances were then determined relative to H. The CNO abundances are enhanced, with respect to the solar ones, by a factor of 20 for total CNO and by 200 for N.

This indicates a TNR origin of the outburst. The value of the ionized ejected mass is of the order of 10^{29} g, and the corresponding kinetic energy is 6 x 10^{44} ergs, in agreement with the estimates for other classical novae.

Cassatella and Gonzalez-Riestra (1988) have included N Cyg 1978 in a study of the behavior of the FeII UV lines in novae in the early post maximum phases, using the extensive IUE material available.

During about one month after the maximum (near September 12, 1978), the object showed strong FeII lines, especially from multiplet UV 1, which appeared with a P Cygni structure particularly prominent in the low-resolution spectra of September 11. In the subsequent days, the violet shifted absorption components of FeII UV 1 progressively fainted, while the emission components became stronger, reaching a maximum probably near September 23. Finally, in the spectra of middle October, the emission component also disappeared, and FeII UV 1 was only visible in absorption, probably produced by the zero voltage lines 2599.4 and 2585.9 A. These changes were accompanied by the appearance, at the later date, of nebular lines and by a dramatic change of the UV energy distribution, as shown in (Figure 6.47.)

Nova Cr A 1981. IUE spectra of Nova Cr A have been obtained during 6 months on 11 dates beginning from the outburst in April 1981 up to mid-November 1981, when it entered the sun constraints of IUE (Sparks et al; 1982). These spectra cover the whole IUE range and are mostly at low resolution. It is noteworthy that the initial spectral evolution, immediately after the OB, is quite similar to that of Nova Cyg 1978. The strongest line in the first spectrum is OI 1303. The emission lines cover a range in ionization potential from

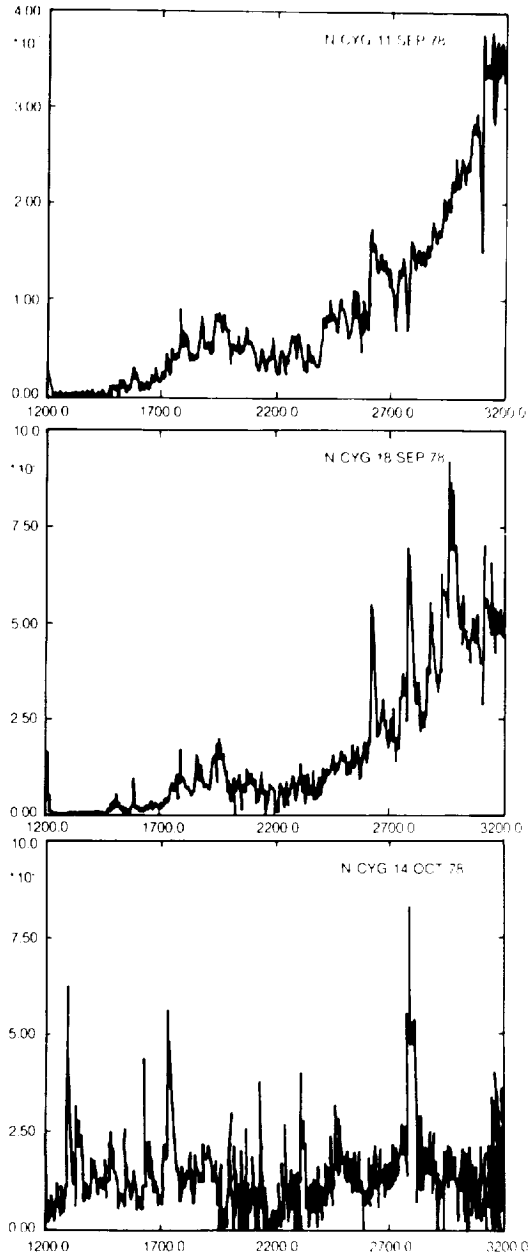

Figure 6-47. Observed UV spectra of N Cyg 1978 in outburst. In the spectrum of Oct. 14, 1978 the nebular lines have become strong and a hot continuum emerges in the short wavelength region.
(from Cassatella and Gonzales Riestra, 1988)

8 eV (MgII) to 80 eV (NV). Forbidden emission lines of high ionization character such as [MgVII] and [AlVI] were present for short periods in May and June 1981. (Figure 6.48) These lines seem to be produced by photoionization and not in a high temperature coronal region because of the absence of high excitation "auroral" emissions, which would be expected under coronal conditions.

On May 25, the FWHM of CIV emissions was 4500 km s^{-1}, a value quite uncommon for a moderately fast nova. At 200 days after maximum the nebular stage was not yet reached.

Williams et al. (1985) have made a quantitative study of the emission lines present in the spectra, with the purpose of determining accurately the physical conditions and the chemical composition in the gas ejected during the outburst. The ratio NIV 1719/NV 1240 yielded T_e~11,000 °K. Abundances relative to He have been determined for several elements by applying a quite elaborate method. (Figure 6.49) illustrates their results, which indicate that CNO elements are enhanced relative to He and, presumably, relative to H also. What is noteworthy is the very high enrichment of neon, together with that of Mg and Al. The study suggests N/C~20 and Ne more overabundant than CNO (!).

(The overabundance of neon is indicated by the strength of the [NeIV] 1602, [NeIV] 2422, and [NeIII] 1815 lines).

Nova Aql 1982 has been observed with IUE for the first time on February 24 and then on several dates up to June 30, 1982 (Snijders et al., 1984, 1987b).

Figure 6.50 (from Snijders et al., 1987) shows the estimated fluxes in the UV, optical, and IR. The total flux declined rather slowly with time, with a dominant contribution from the IR region. It is remarkable that the combined UV plus optical continuum [after correction for reddening: E(B-V)~0.55-0.60] varies at various epochs as $F(\lambda) \propto \lambda^{-2}$ from at least 1,400 to 6,000 A and that these fluxes vary approximately in *phase*, unlike in other novae. A dip in the UV flux was observed near d=77, probably because of absorption by dust internal to the nova shell, while the IR contribution becomes dominant.

Figure 6.51 shows IUE spectra at various epochs after the outburst.

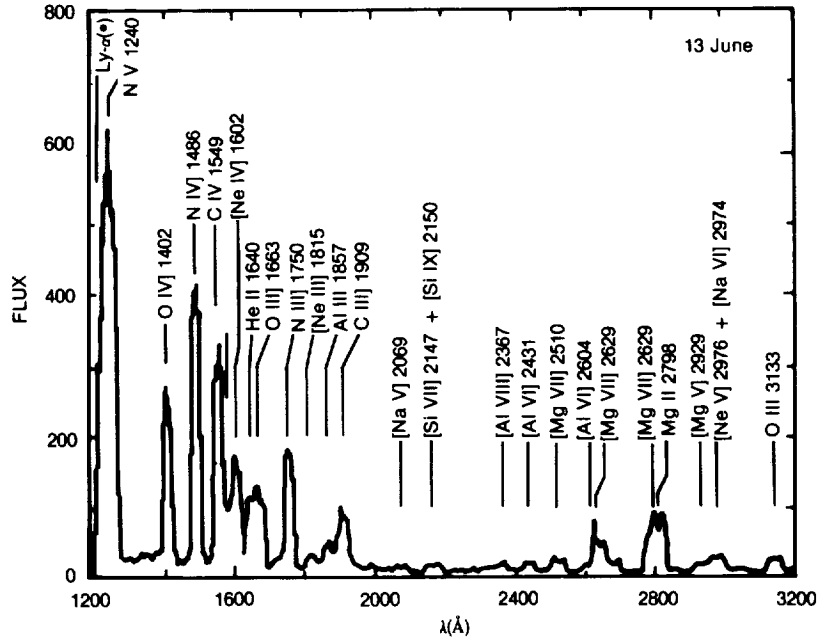

Figure 6-48. Low dispersion UV spectrum of Nova CrA on June 13, 1981. Units of flux are 10^{-14} erg cm^{-2} s^{-1} Å^{-1}. (from Williams et al., 1985)

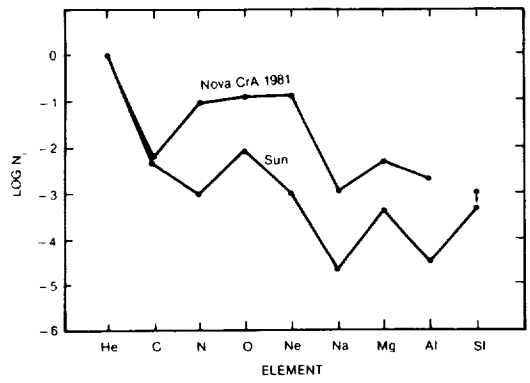

Figure 6-49. The logarithm of the abundances, by number, of the elements that it was possible to analyze for both Nova CrA 1981 and the Sun. (from Williams et al., 1985)

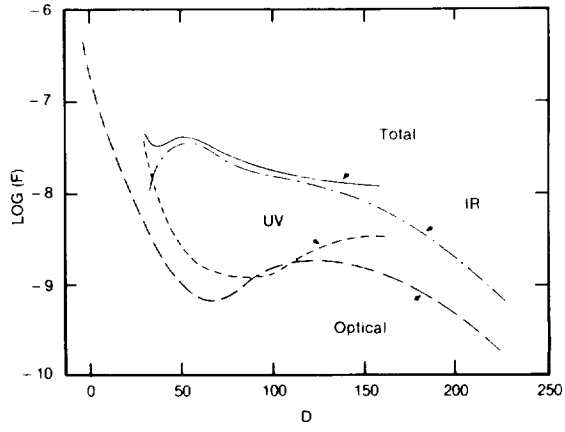

Figure 6-50. Nova Aql 1982: Smoothed curves showing the time-variation of total fluxes (corrected for IS extinction) in the UV (912 Å-3200 Å), optical (3200-10000 Å) and IR (>10000 Å). (adapted from Snijders et al., 1984)

The first IUE observation (d=29) showed the presence of dramatic P Cyg features with velocities of up to 10^4 km s^{-1}. If this edge velocity is interpreted as a terminal velocity, it is very high; only supernovae show such values, while the highest velocity observed in the Orion system of novae is –3800 km s^{-1} (Payne Gaposchkin, 1957).

N Aql 1982 was characterized by a remarkably composite structure in the UV lines which show:

1) Quite "narrow" emissions of semiforbidden and permitted lines (FWHM 2000 km s^{-1}).
2) Broad absorptions up to -4000 km s^{-1} in the common resonance lines like NV and CIV.
3) An unusually high-velocity component with edge velocity at -10,000 km s^{-1} (system b); this high-velocity gas has been detected *only in the UV* and was evident on February 24 and March 2 (days 29 and 36 after OB).

It is notable that systems *a* and *b* are observed in the resonance lines of CIV and SiIV, while only system *a* is observed in the resonance doublet of Al III and only system *b* is observed in an excited line of NIV, which has high excitation. This might suggest that system *b* is formed closer to the pseudophotosphere, and the slower system *a* consists of material ejected earlier and swept up by system *b*.

The electron density of the medium velocity gas has been determined using the ratio SiIII 1892/CIII 1908 yielding $N_e \sim 1 \times 10^{10}$ el. cm^{-3}. Another set of emission line ratios provided a separate determination of T_e and N_e that resulted in these ranges: $9600 \leq T_e \leq 11{,}000$, and $1.6 \times 10^8 \leq N_e \leq 5 \times 10^8$ with a best estimate for the diagnostic, in which $T_e = 10^4$ K and $N_e = 2.5\ 10^8$ cm^{-3}.

Using the above parameters, abundances of several elements have been calculated by Snijders et al. (1987b) for the medium velocity gas

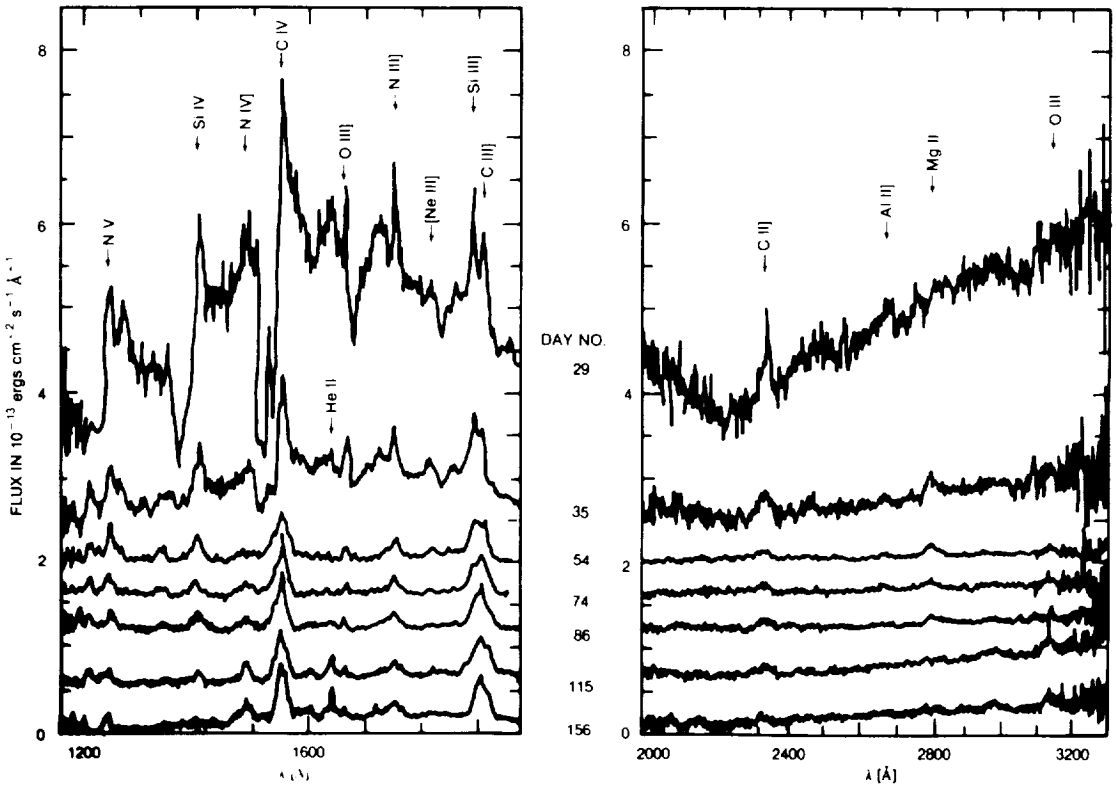

Figure 6-51. Nova Aql 1982: Fluxes observed with IUE (uncorrected for extinction). The fluxes shown are shifted upwards by constant amounts for each day number, by 3.2 on d=29; by 2.4 on d=35; by 2.0 on d=54; by 1.6 on d=86; by 0.6 on d=115 and by 0.0 on d=156.
(from Snijders et al., 1987 b)

on d=156. The high overabundances of sulphur, nitrogen, and neon are remarkable: (N/H=0.21, Ne/H=0.73, S/H=0.064).

These overabundances resemble those found in the shell ejected by Nova Cr A 1981.

The mass of the medium velocity gas was estimated as 7 x 10 $^{-6}$ $M_{\odot}$ indicating that the total mass ejected was about 10^{-2} less than in other novae.

Due to the great intensity of the neon lines in its spectrum, N Aql 1982 has been labelled as a "neon nova." However, as pointed out by Friedjung (1988), the gas-phase abundance of neon was larger than that for other abundant elements only because neon is a noble gas and does not condense into grains.

U Sco. The outburst of this recurrent nova was first recorded on June 24, 1979. This OB was much faster than either the OB of N Cyg 1978 or N Cr A 1981; it was an extremely rapid, burst-like event. The IUE observations started on June 24 and continued until 11. The spectrum (Williams et al., 1981; Sparks et al., 1980) was initially a mixture of both high-ionization and low-ionization lines. NV 1240 was strong, HeII, CIV, SiIV, N IV] 1486 were present, with PCyg profiles in CIV and Si IV lines. Unlike in other recurrent novae in outburst, no forbidden coronal lines have been observed. (Figure 6.52). After June 30, the absorptions disappeared and the general level of ionization increased.

The emission and absorption features were all very broad, characteristic of expansion velocities up to -7500 Km s^{-1}.

It is noteworthy that there was no change in the color temperature over the period covered by the observations of Williams et al. The observed ratio F_{vis}/F1300 remained nearly constant around the value of 0.5.

According to Barlow et al. (1981), over a large part of the dereddened optical and UV ranges, the continuum of July 6 could be fitted by a power-law F (λ) ~ $\lambda^{-2.4}$. However, this index should be

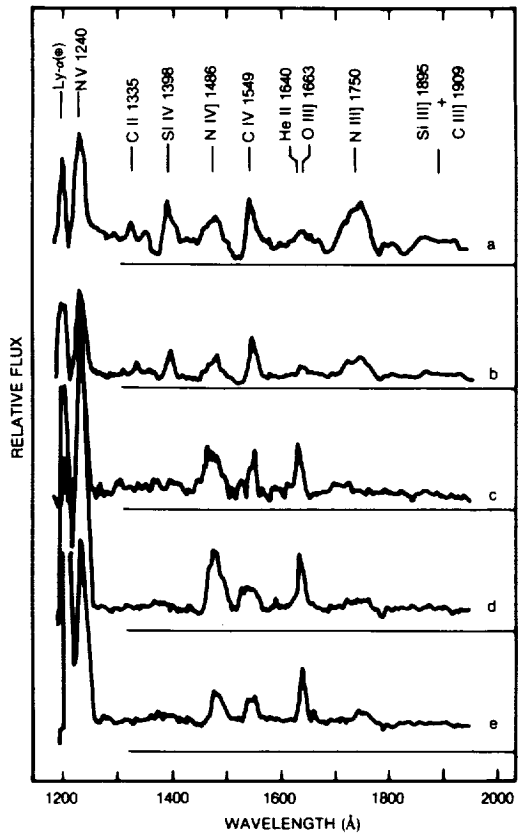

Figure 6-52. UV spectra of U Sco in the period following outburst. The dates for the IUE scans, together with the visual magnitude as determined from the Fine Error Sensor, are as follows: a) June 28, V=11.4; b) June 30, V=11.9; c) July 2, V=13.1; d) July 4, V=13.8; e) July 11, V=14.3.
(from Williams et al., 1981)

taken with caution because of the uncertainties in the reddening correction.

A detailed analysis of the emission lines shows that the ejecta are very rich in N, although the combined CNO abundance seems essentially solar, because carbon is very underabundant with respect to nitrogen. A depletion of H is indicated by the optical spectra which suggest that He/H is about 2 (in number density).

The amount of ejected mass was only 10^{-7} $M_{\odot}$, about 10^{3} smaller than that usually ejected in a classical nova outburst.

It is noteworthy that both U Sco and N Aql 1982 have shown an unusual spectral evolution during outbursts: no color changes (no flux redis-

tribution toward the IR and UV), similar spectral indexes (λ^{-2} in N Aql 82, $\lambda^{-2.4}$ in U Sco), ejection of a less massive envelope than the other novae ($\sim 10^{-6} \div 10^{-7}$ $M_\odot$ instead of $\sim 10^{-4} \div 10^{-5}$ $M_\odot$).

The fifth recorded OB of U Sco occurred in 1987, only 8 years after the previous one. Such a short recurrence time cannot be easily explained in terms of the present TNR theories for the OB of recurrent novae.

N Sgr 82. The OB was discovered on October 4, 1982, and the visual maximum was reached on October 15. The IUE observations of this fast nova started on October 18, when the object was in the early decline. The continuum was that of an early F-type object with T around 9000°K (Mazeh et al., 1985a). It was similar to that of N Cyg 1978 in the corresponding stage (Figure 6.53). The UV continuum of October 18 was very weak and started increasing at the end of October as a consequence of the commonly observed flux redistribution toward UV (and IR) after the visual maximum. The line spectrum was initially characterized by emissions and absorptions of low ionization like FeII, OI, and other neutrals. The MgII doublet showed a P Cyg profile with v edge = -1700 Km/s.

In the following stages, the evolution was quite similar to that of N Cyg 1978, and the nebular stage was reached about 210 days after outburst.

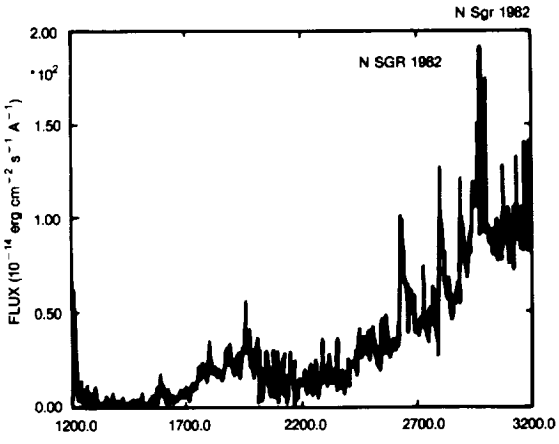

Figure 6-53. Observed UV energy distribution of N Sgr 1982 on Oct. 14, 1982 (about four days after maximum). The spectrum is very similar to that of N Cyg 1978 shortly after maximum.
(from Cassatella and Gonzales Riestra, 1988)

N Ser 1983. This is a very fast nova with $t_3 \sim 5$. The first IUE observations were made 11 days after maximum. A peculiarity of its UV spectral behavior is the wide ionization range with the presence of ions ranging from FeI to NV. CIII] 1908 is also present. (Drechsel et al., 1984) (Figure 6.54).

The emissions are strong and broad and the P Cyg profiles in the CIV and MgII doublets indicate extremely high outflow velocities of -9000 km s^{-1} and -1000 km s^{-1} respectively. These velocities are comparable with those reported by Snijders et al. (1987b) for N Aql 1982.

N Mus 1983. The outburst of this moderately fast nova was reported on January 18, 1983. IUE observations started on February 19, 1983, (Krautter et al. 1984, Krautter, 1986) and continued for several months, covering the Orion to nebular phases. The first spectra showed a wide excitation range and the presence of several semiforbidden lines also (Krautter et al., 1984). The overall evolution was quite similar to that of N Cyg 1978, and ionization increased while the spectral evolution was approaching the nebular phase (Figure 6.55). From August 1985 to June 1986, the [OIII] line fluxes decreased substantially, while high ionization species like [Fe VII] showed an increase of the line intensities.

In the early spectra, the structure of the MgII lines is complex with components at -320 and +540 Km/s. The HeII, SiIII] and C III] emissions shows also a composite structure and have FWZI of about 1500 Km s^{-1} (Figure 6.56).

The total luminosity near maximum (January 21) was estimated at about 1.5 L_{Edd} (for a $1 M_\odot$ white dwarf), assuming that the UV flux distribution decreased in the UV as it did for N Sgr 1982 early in the decline. For March 4, 1983, a SWP IUE spectrum and m_v permit a rough estimate of 0.5 L_{Edd}, with the assumption that the $F \propto \lambda^{-2}$ distribution still holds for the optical and IR range.

An abundance analysis has led to the determination of considerable nitrogen enrichment with respect to carbon and oxygen [N (N) = 80 times the solar value]. From the strength of CNO lines, an overabundance of all these elements seems indicated. It is noteworthy that more than one year after OB (on April 20, 1984), soft x-ray emission was detected by EXOSAT (Ogelman, et al., 1984).

At that epoch also FeX 6374 was detected in the optical. The values of temperature (3.5 10^5 K) and L (10^{37} erg s^{-1}) derived from this emission suggest its origin from the surface of a very hot white dwarf.

Nova Vul 1984 1 (PW Vul)

High resolution spectra of PW Vul (Visual magnitude at maximum 6.4) have been obtained two months after maximum. The spectra are crowded with absorption and emission lines from Si II, N II and Fe II. The absorption lines have at least three separate components at different expansion velocities: at about 0 km/s, -750 km/s and -1550 kms. Figure 6.57 shows the profiles of multiplet 191 of Fe II and multiplet 1 of Si II in the region 1780-1820. A, and the region 1710-1770

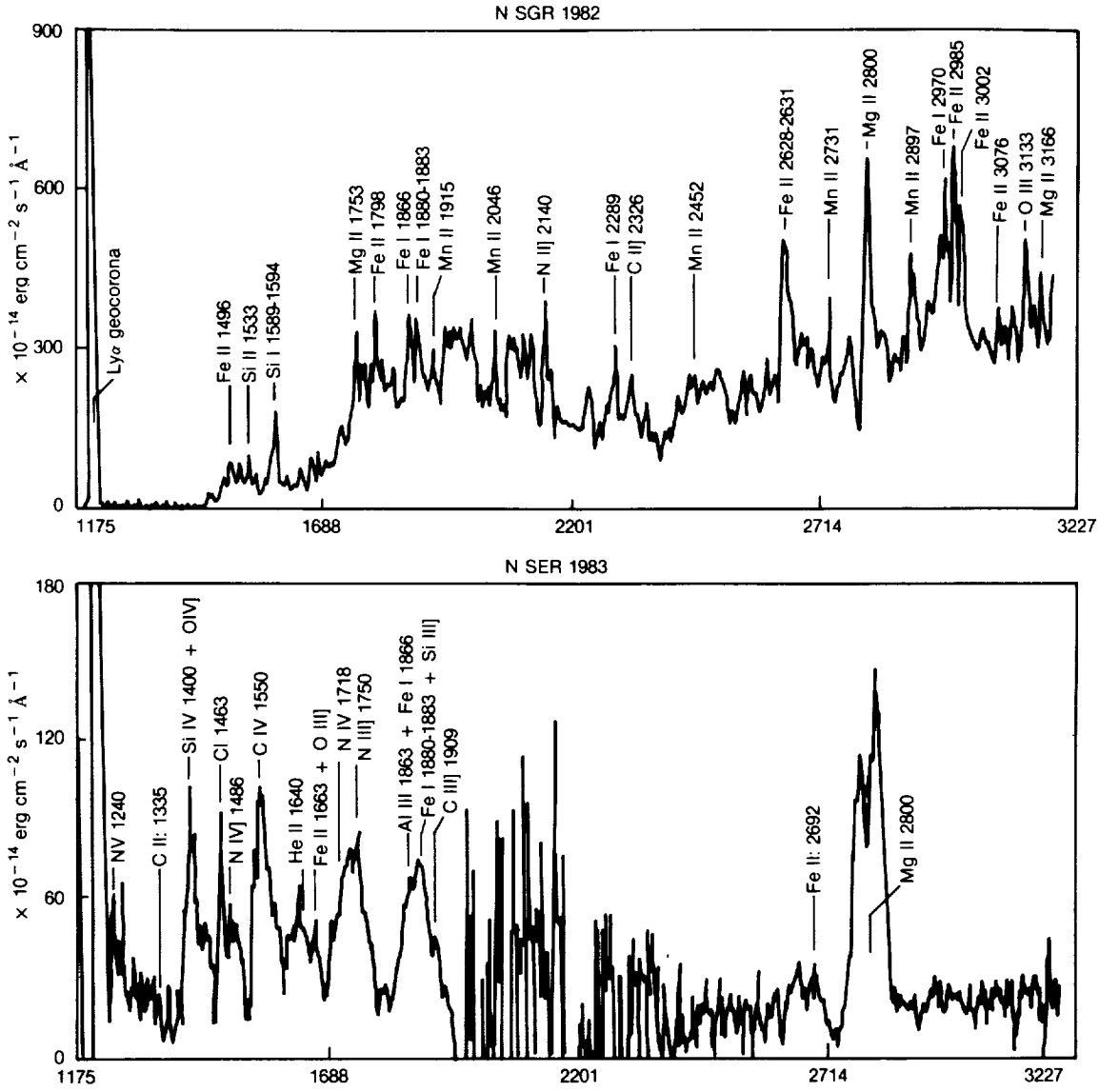

Figure 6-54. Dereddened IUE spectra of the classical novae N Sgr 1982 and N Ser 1983. (from Drechsel et al., 1984)

where several lines of Fe II and Ni II are present. The three absorption components are clearly detectable in the lines of multiplet 191 of Fe II and in the ground multiplets of Si II and Ni II.
6-75

RS Oph 1985 An outburst of this recurrent nova was announced on January 26, 1985, and IUE osbservations started on February 8 and continued for about two months (Cassatella et al. 1985). The UV spectral evolution after OB has collowed the trend of increasing ionization level with time. In a graph emission intensity versus time, the emission intensity from highly ionized species peaks at a much later stage in the decline than emissions from low-ionization species. A decrease of N_e with time was deduced by using the N_e sensitive ratio SiIII] 1892 /CIII] 1908.

The UV FeII emission lines of RS Oph have been studied by Cassatella and Gonzalez-Riestra (1988).

Figure 6.58 shows how the fluxes of the FeII emission lines from multiplet UV 1 (around 2600 A) vary with time during the 1985 outburst of RS Oph, compared with other strong emission lines of different ionization level such as OI 1300 A, N IV] 1487 A, NV 1240 A, and [FeXI] 2648.7 A. The figure shows clearly that the FeII lines peak in intensity very soon after the outburst, like the low-ionization line OI 1300 A (and MgII 2800 A, not shown in the figure). Emission lines from higher ionization species, on the contrary, reach a maximum at later stages: NIV], for example, is maximum around day 35; NV, around day 43; while the [FeXI] line is maximum in a plateau between days 42 and 62. The time of maximum is then correlated with ionization potential of the line considered.

Apart from the UV 1 multiplet, other FeII lines are present, although fainter, in the postmaximum spectra of RS Oph: the ones which could be identified with more confidence are those from multiplet UV 191 around 1786 A and those from UV 62 and 63.

In the later decline stages, forbidden emissions from [FeXI] 1467 and 2649 and from [FeXII] at 1350, 2406, and 2568 (Figure 6.59) were detected. The time evolution of the profile of the

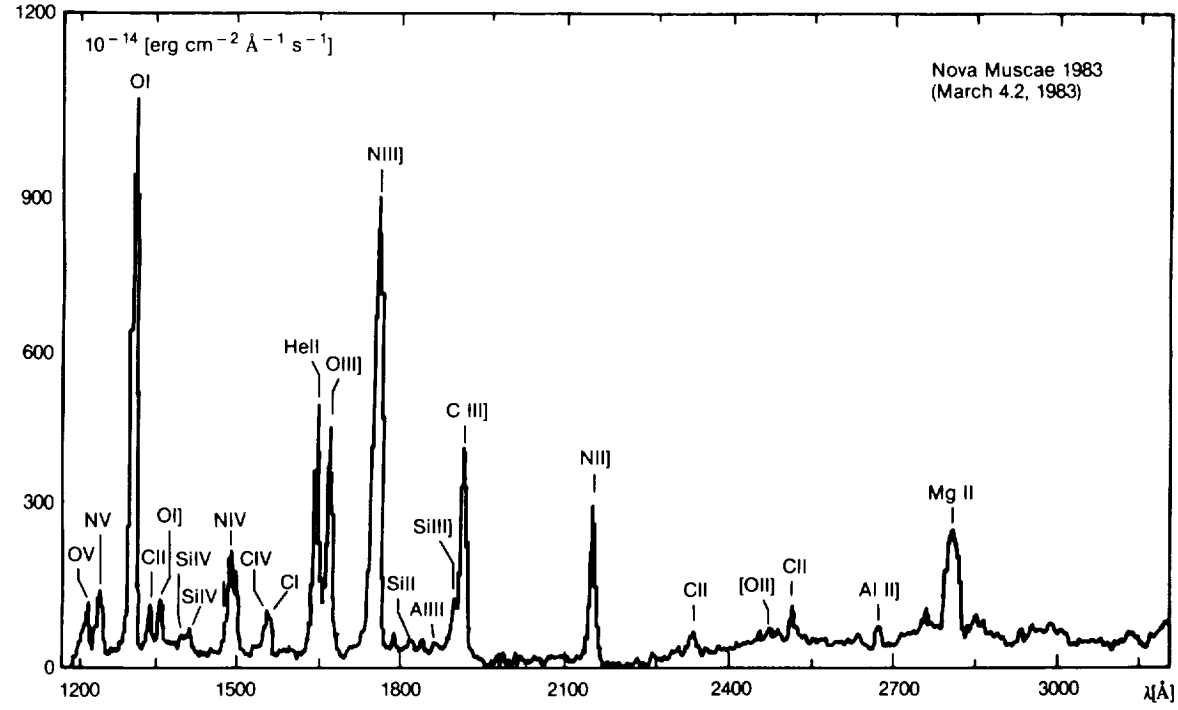

Figure 6-55. The UV spectrum of N Mus 1983. (from Krautter et al., 1984)

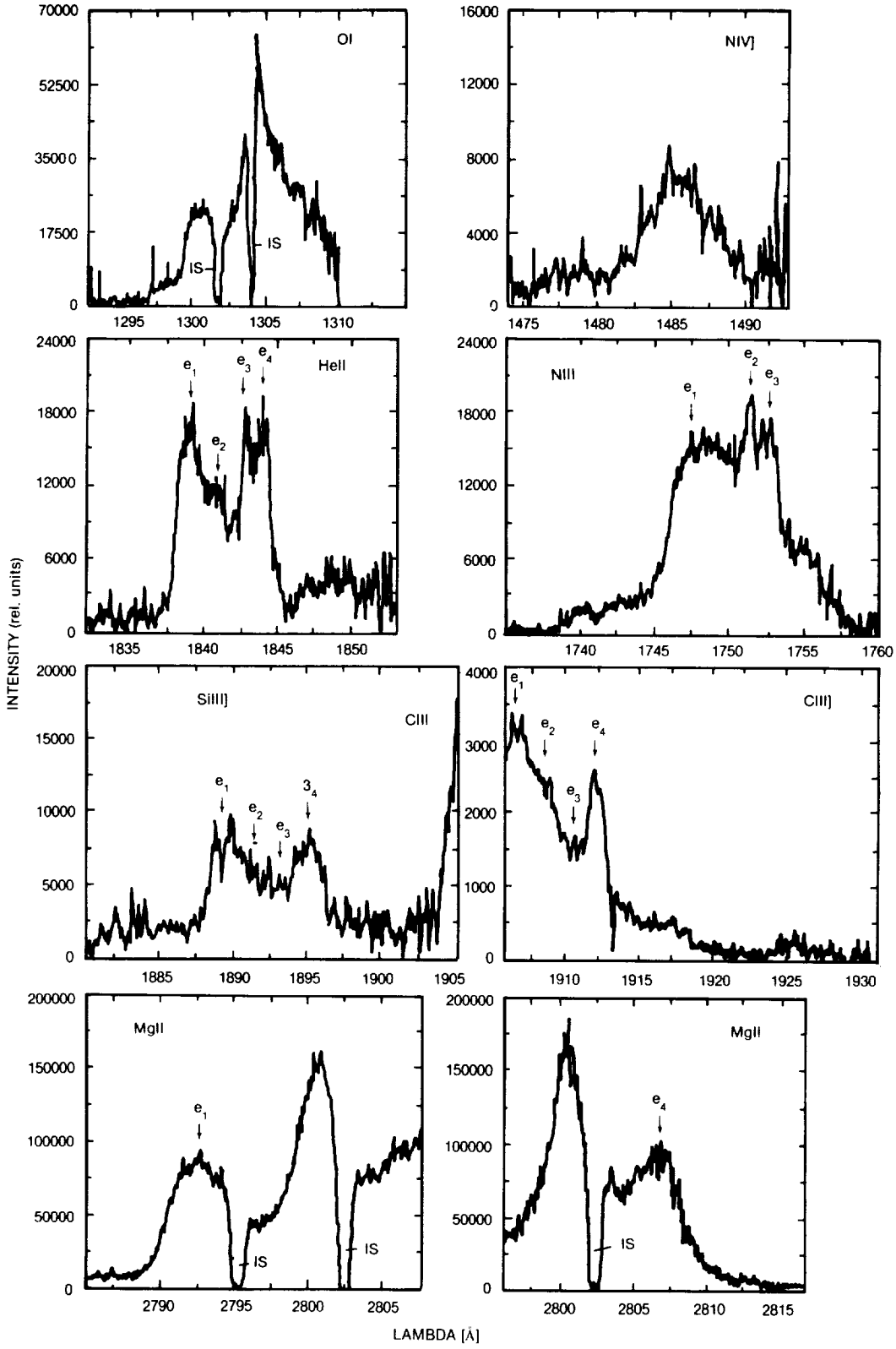

Figure 6-56. High-resolution profiles of the most prominent emission lines of N Mus 1983. (from Krautter et al., 1984)

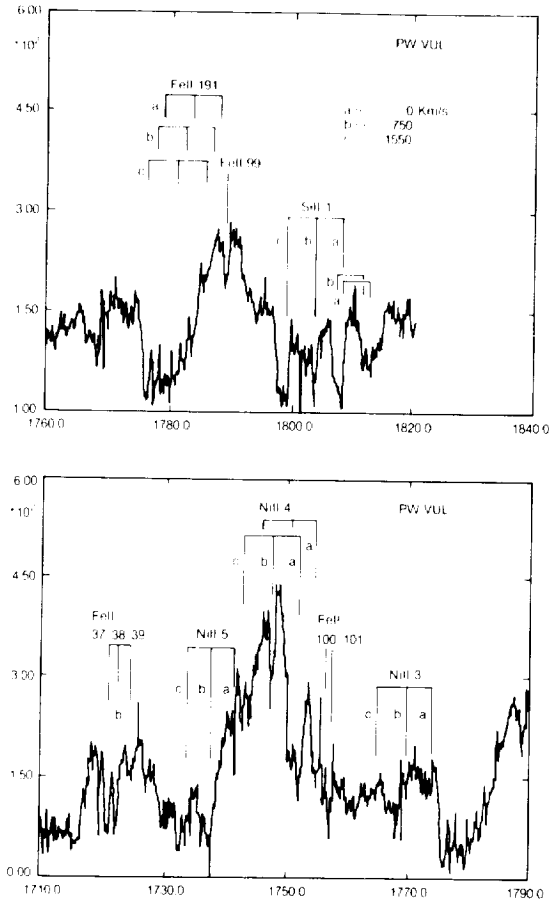

Figure 6-57. High-resolution spectra of N Vul 1984 a in two wavelength regions. The spectra are crowded with absorption and emission lines from Si II, N II and Fe II. The absorption lines have at least three separate components at different expansion velocities: at about 0 km/s,-750 km/s and -1550 km/s. Particularly strong is the emission-absorption structure from Fe II UV multiplet 191 and N II UV multiplets 4 and 5.

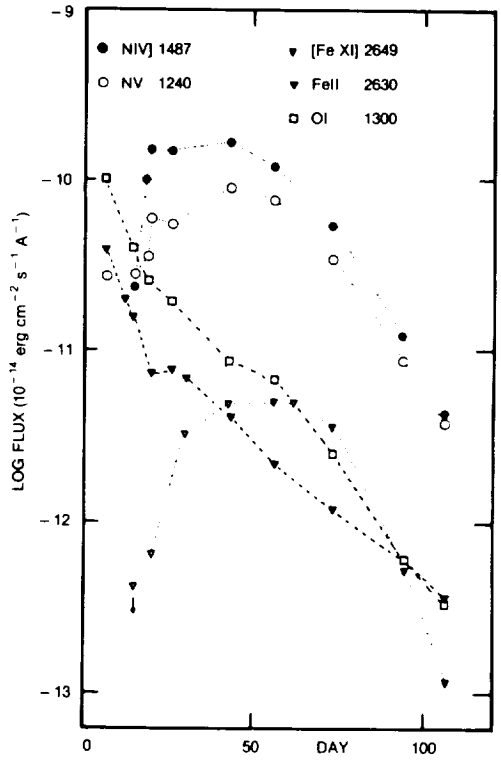

Figure 6-58. Time variability of the emission lines in RS Oph during its outburst of 1985. Abscissae represent the time after maximum, assumed on Jan. 28, 1985. The figure shows that the lines of lower ionization level peak very soon after maximum while [Fe XI] 2648.7 is maximum in a plateau between day 42 and 62.
(from Cassatella and Gonzales Riestra, 1988)

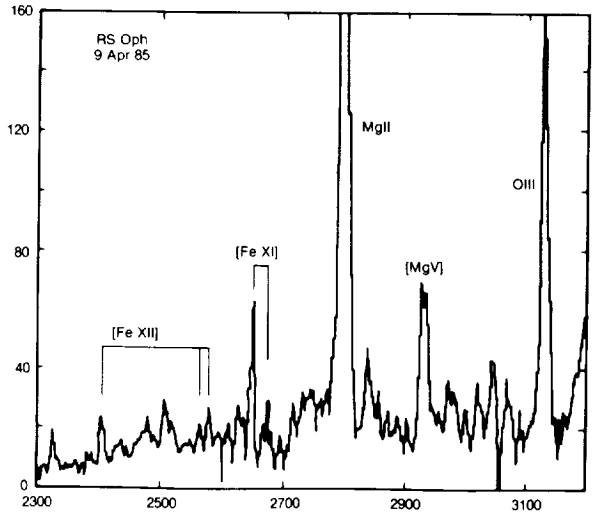

Figure 6-59. The spectrum of RS Oph in the interval 2300-3200 A. High excitation lines are clearly present.

[FeXI] 2648.7 A line is shown in (Figure 6.60). Such data can provide important clues to the understanding of the dynamics and geometry of the ejection. The complex profile of [FeXI] is probably indicative of a non-spherically symmetric and, perhaps, discrete ejection process. It is worth recalling that RS Oph is the first astrophysical source in which so strong high-ionization lines were detected in the ultraviolet, apart from the solar corona.

Snijders (1987a) made an estimate of the mass of the ejected shell and, using the method developed by Pottash (1959), obtained M(eject)~ 5 x 10^{-7} $M_{\odot}$.

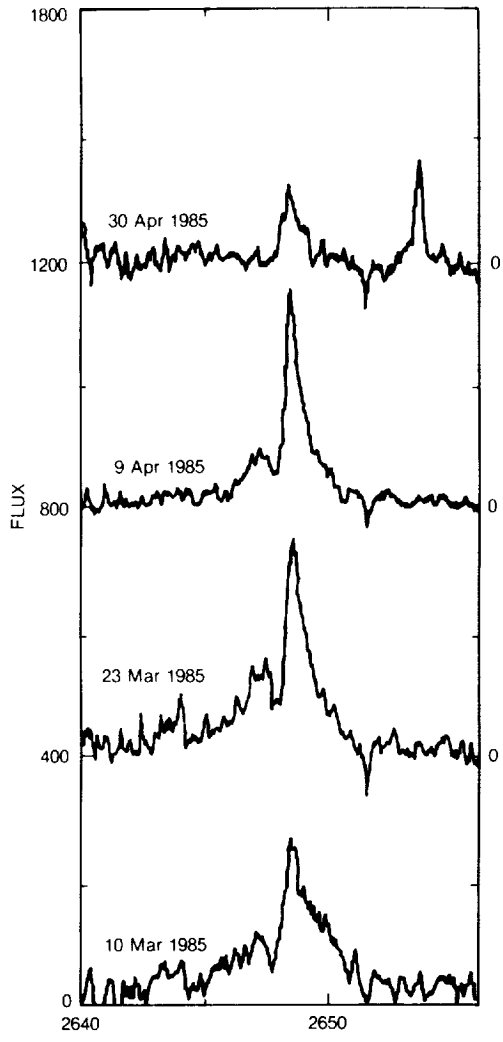

Figure 6-60. High-resolution data of the recurrent nova RS Oph (outburst of 1985) showing the time evolution of the profile of [Fe XI] 2649 A.

This quite low value is in agreement with previous estimates and theoretical expectations (Starrfield et al., 1985) from a recurrent nova outburst. Snijders also made an estimate of the luminosity after OB and found a peak value of about 4 L_{Edd} and a plateau value $L = L_{Edd}$ for a massive white dwarf.

A considerable enrichment of nitrogen seems to be present in the ejecta, as was found in other novae. The ratio N(He) / N(N) is in the range 3-40.

The cause for the recurrent outbursts of RS Oph (every 9 to 35 years since the first event was discovered in 1898) may be different from the thermonuclear runaway invoked for classical Novae (Livio, Truran, and Webbink, 1986). Also, it is possible that important differences exist, for example, in the total mass ejected and in the ejection velocity, compared to classical novae. In any case, *RS Oph* offers a unique opportunity to study one important phenomenon: the interaction of ejected matter with the stellar wind from the cool giant companion and with the surrounding circumsystem material, not yet dissipated at the time of the new outburst.

The appearance of strong emission lines from very high-ionization species observed shortly after the outburst both in the optical (Joy and Swings 1945; Rosino, Taffara, and Pinto, 1960) and in the ultraviolet (Cassatella et al. 1985), as well as the detection of a strong x-ray flux (Mason et al. 1987) is a demostration of the effectiveness of such an interaction.

Intense soft x-ray emission (1 - 6 keV) has been detected with EXOSAT in March 22, 1985. The characteristic temperature (Mason et al. 1987) is of the order of a few million degrees, and the total flux, after correction for the interstellar medium (ISM) absorption is of the order of 10^{-9} erg cm^{-2} s^{-1}.

It is noteworthy that this strong emission is seen a long time after OB and that there is no short-time variation associated with it.

Moreover, a weak, but significant, residual x-ray emission was still detected in October 1985.

This much weaker emission is consistent with temperatures of the order of 3 - 5 x 10^5 K as found for Nova Mus 1983 (Ogelman et al., 1984).

V. I. CONCLUDING REMARKS

6-79

As it has emerged from the description of individual objects, each nova in OB has shown some peculiar characteristics that have made it different from the other novae; however, in spite of these individualities, the study of the UV data, both in the continuum and in the emission lines, has been of fundamental importance for the determination of some basic common properties in the behavior of novae in OB. The studies of the UV observations have led to two important results:

1)-Accurate determinations of chemical composition of the ejecta

No one object has ejected material of solar-like composition. Large enrichments of CNO have been found in practically all ejecta, while, in a substantial fraction, a large over-abundance of Ne has been found. Several considerations (see, for example, Truran, 1985), have led to the conclusion that the enrichments in the ejecta are not a direct consequence of nuclear reactions in the nova envelope, but rather reflect the composition of the envelope at the onset of the TNR. The most likely mechanism responsible for this enrichment is outward mixing of core matter from the interior to the surface of the white dwarf, a consequence of the shear-induced turbulence produced by the accreted material when it strikes the dwarf surface layers. Thus, CNO over-abundances can be explained in terms of TNR in a shell already enriched of these elements in a CO white dwarf. The enrichment of Ne (as detected from the anomalously high intensity of the λ 1602 Å line four novae) has been an important and unexpected result, indicating that the ejected material was processed to Ne during the previous evolution in a very massive O-Ne-Mg white dwarf (Law and Ritter, 1983). Iben and Tutukov (1984), from theoretical considerations, estimated a ratio of approximately 35 for systems containing a CO white dwarf to systems with an (O-Ne-Mg) white dwarf. The reason for the observed higher percentage of (O-Ne-Mg) white dwarfs in novae is not clear and could be explained on the basis of selection effects, since nova OBs are expected to be more frequent in the more massive (O-Ne-Mg) white dwarfs. The implications of the presence of this kind of white dwarf on our understanding of the nova phenomenon and the evolutionary state of the system are still to be investigated.

2)-Reliable estimates of the bolometric luminosity and of its variations with time.

IUE observations of the continuum of novae in outburst have confirmed the general trend of the redistribution of the flux toward the UV (and the IR) as the outburst progresses, and shown that the bolometric luminosity in the early postmaximum phases remains nearly constant or declines more slowly than the visual one.

The total luminosity is generally closed to the Eddington limit for a $1M_\odot$ star($\sim 1.55.10^{38}$ erg s^{-1}), but the exact value depends critically on the distance that has been assumed.

The possibility that L exceeds L_{Edd} would have as a consequence the formation of a supercritical wind, accelerated by the high radiation pressure corresponding to that super-Eddington Luminosity.

Before the launch of IUE, it was not clear whether the ejection of mass from the "nova" was instantaneous (i.e., occurring in a short time interval as compared with the typical time scale of the "nova" phenomenon) or continuous. Friedjung (1977a) suggested that even using only ground-based observations, there was a good evidence for continued ejection decreasing with time, although most mass was probably ejected near visual maximum. The smallness of the decline in L_{bol} after visual maximum, as found using UV (and IR) observations, has been interpreted as a suggestion that nuclear burning continues on the white dwarf surface after the initial explosion,

thus producing a continuous ejection of mass (after the sudden ejection of the first shell). The presence of very high-velocity components (up to 10^4 km s^{-1}) in the UV spectrum of Nova Aql 1982 and in other novae in OB has been interpreted by Friedjung as an evidence of the presence of super-critical winds accelerated by radiation with super-Eddington luminosity.

6-80

There are, however, several problems related with the continuous ejection model that are still unclear, as, for instance, the interpretation of all the absorption systems. Collisions between envelopes at different velocities are expected, leading to x-ray emission observable in the late outburst stages. The x-ray emission detected in N Muscae (Ogelman at al., 1984) could be due to this mechanism.

VI. THE X-RAY EMISSION OF NOVAE AND RECURRENT NOVAE
(Written by Selvelli)

Accretion, which is the main source of the UV radiation emitted by novae in quiescence, is also responsible for the x-ray radiation emitted by these objects. In the standard picture (a geometrically thin, optically thick accretion disk) a rough estimate of the energy dissipation indicates that about one half (that is $\frac{1}{2} G \frac{M \dot{M}}{R}$) of the accretion luminosity is released in the disk as optical and (mainly) UV radiation, while the other half is released as soft/hard x-ray radiation in the boundary layer, the region at the interface between the innermost disk part and the surface of the white dwarf.

Generally, the keplerian or nearly keplerian velocity of the material in the inner disk is much greater than the velocity at the surface of the white dwarf but, as it approaches the white dwarf, it must become slower, and the excess of mechanical energy will be dissipated. Simple calculations (see, for example, Kylafis and Lamb (1982), Ferland et al (1982b) show that if the boundary layer is assumed to be optically thick, for parameters typical of a CV ($\dot{M} \sim 10^{18}$ gr s^{-1}, $M_1 \sim 1 M_\odot$, $R_1 \sim 10^{-2} R_\odot$), it will have temperatures of the order of 2-5 $\times$ 10^5 °K and, therefore, will emit most of its radiation in the EUV-soft-x-ray range). The boundary layer can be defined as the region between the point where the angular velocity deviates from the keplerian one and the surface of the white dwarf. (See Chapter 4. IV. F.) The presence of a hard x-ray component (E~a few keV) with a much lower luminosity than that expected for the EUV-soft-x-ray component, and the lack of detection of the soft component (this absence, however, can find a natural explanation in terms of interstellar absorption) indicates that the real picture is more complex and that a more detailed modelling of the boundary layer is required. See, for example, Ferland et al. (1982a,b), Patterson and Raymond (1985a,b), and Jensen 1984. It must also be pointed out that the presence of the boundary layer as described above, depends critically on the absence (or weakness) of the magnetic field in the white dwarf.

If a strong magnetic field ($\geq 10^7$ gauss) is present, the accreting material will flow along the lines of the magnetic field and the accretion disk will be disrupted at a radius of the order of the Alfven radius. In this case, the accretion material will form accretion columns at the magnetic poles of the white dwarf. In this chapter, only the x-ray behavior of classical and recurrent novae, in which the magnetic field intensity is less than 10^6 gauss and therefore not so high as to affect seriously the disk structure, will be described, leaving out the magnetic CVs (polars or AM Her stars, magnetic field ~ 10^8 gauss).

VI.A. X-RAY OBSERVATIONS OF POST-NOVAE

The HEAO-1 X-ray survey of cataclysmic variable stars (Cordova at al, 1981a) revealed that quiescent novae were, at best, low luminosity sources with fluxes, in the 0.18 - 2.8 keV range, below the HEAO -1 A2 detector thereshold (of the order of 2 -3x 10^{-11} erg cm^{-2} s^{-1}). Thanks to the higher sensitivity of the instruments onboard HEAO-B (EINSTEIN), a positive detection of about ten sources and the assignment of upper limits for a few other ones has been possible.

Several old novae are indeed X-ray sources but at a quite lower level (L ~ 10^{31} -10^{32} erg s^{-1}) with

respect to the UV and optical fluxes. Table 6.15 is a compilation of data from the observations made mainly by Becker and Marshall (1981), Cordova et al (1981a,b) and Cordova and Mason (1984). A description of the EINSTEIN imaging proportional counter (IPC) detector used to make the observations is reported in Giacconi et al (1979). The data of table 6.15 refer to the energy interval 0.16 - 4.5 keV. The conversion from counts s^{-1} to intensity is a critical point, since it depends on the adoption of a spectral distribution. Generally, since most data are indicative of a quite hard thermal component, a nominal 10-KeV thermal bremsstrahlung spectrum, and $N_{H} \sim 10^{20}$ cm^{-2} have been assumed. With these assumptions, one IPC count s^{-1} from a source with such spectrum corresponds to a flux at the Earth of 3.6 x 10^{-11} erg cm^{-2} s^{-1} in the 0.15 - 4.5 keV range (Patterson and Raymond, 1985). This conversion factor is not very sensitive to kT and N_{H}, however. In most studies a conversion factor of 2.7 was assumed, but in the last processing of the IPC date the conversion factor 3.6 was suggested (Patterson and Raymond 1985), and, in the compilation of Table 6.15, this last value has been used. It is evident from Table 6.15 that the mean 0.1 - 4.0 keV luminosity of old novae is of the order of 6 x 10^{31} erg s^{-1}. We recall that their UV luminosity is instead much higher, of the order of 10^{34} -10^{35} erg s^{-1}. Old novae are generally "hard" x-ray emitters with hardness ratio H/S (counts above 0.55 keV to counts below 0.55 keV) larger than one (from 2.2 $\pm$ 0.9 for RR Pic to 37.6 for GK Per). The "hardness" of GK Per has been confirmed by Cordova and Mason (1984) who found a distribution with kT > 8keV. The recurrent nova T CrB is the weakest source detected. A very soft component (kT ~ 50 e V), such as that observed in U Gem and SS Cyg during optical outburst, is not present in quiescent novae. It is also remarkable that a weak "hard" X-ray emission is a common characteristic of all classes of cataclysmic variables. This fact is an indication that the same mechanism is responsible for the X-ray emission in all these systems.

TABLE 6.15

X-Ray Fluxes and Luminosities of the Post-Novae Detected with EINSTEIN

Object	Data of Observation	IPC counts/s	FLUX (0.16–4.5 KeV) in 10^{-13} erg s^{-1} cm^{-2}	Lx (0.16–4.5 KeV) in 10^{32} erg s^{-1}
	56/1979	0.310	111.60	3.06
GK Per	239/1979	0.174	64.08	1.73
RR Pic	298/1979	0.031	11.20	0.31
CP Pup	328/1979	0.060	21.60	1.27
T CrB	57/1979	0.0083	2.99	0.60
V 841 Oph	265/1979	0.019	6.84	0.61
V 1017 Sgr	98/1980	0.022	7.92	-
V 603 Aql	265/1979	0.279	100.00	1.70
		0.71	220.00	4.50
V 1059 Sgr	295/1979	0.014	5.04	1.13
HR Del	311/1979	0.0084	7.00	0.20

The brightest sources of Table 6.15 are GK Per and V 603 Aql, which have also provided enough photons for time variability studies. Becker and Marshall (1981) reported a short-lived flare in V 603 Aql during which the x-ray intensity doubled. GK Per was found to be variable (during optical quiescence) by Cordova and Mason (1984) in data taken during three consecutive days. They detected variations by a factor of 2 on a time scale of hours and, in addition, significant variations on time scales of about 100 s.

No evidence was found for extended X-ray emission corresponding to the 60-arcsecond size of the optical remnant. GK Per was detected as a transient x-ray source by the Ariel V SSI (2-18 KeV) at a time (June 19 to July 31, 1978) of an optical brightening by about 1 magnitude (King et al., 1979). After the launch of EXOSAT, Watson et al. (1984) reported observations of GK Per during an optical brightening on August 9, 1983. During these activity phases, GK Per is the brightest x-ray source among CVs, with a quite hard spectrum and a 2 - 20 KeV luminosity of about 10^{34} erg s^{-1} (Figure 6.61).

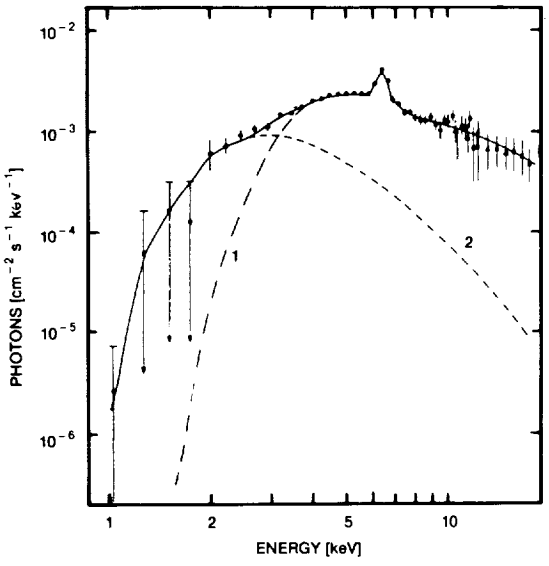

Figure 6-61. The spectrum of GK Per for the range 1 to 20 keV.
(from Watson et al., 1984)

Interestingly, this hard X-ray emission shows a strong coherent modulation with a period of 351 s. The pulse wave form is nearly sinusoidal (Figure 6.62).

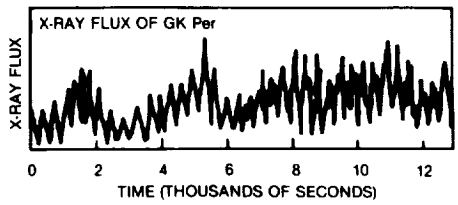

Figure 6-62. The X-ray flux curve of GK Per observed by EXOSAT (2-10 keV) during an optical brightening. The curve is a modulated sinusoidal with a pulsation period of 351 s.
(from Watson et al., 1985)

It is still unclear how bright GK Per becomes bolometrically during these activity phases, because the X-ray spectrum is complex with evidence for two hard components above 2 KeV and a soft component below 0.1 keV. Thus a substantial part of the X-ray luminosity lies outside the spectral range accessible to EXOSAT.

V 603 Aql was reobserved in 1981 (by Drechsel et al., 1983a, b) with the IPC and MPC instruments on board the EINSTEIN observatory. Periodic phase-related flux-variations were detected. The maximum X-ray luminosity in the 0.15 -20 keV range was of about 3 x 10^{33} erg s^{-1} with indication of a hard spectrum.

Although the sample of old novae observed with EINSTEIN was small and liable to selection effects, it has been possible to look for correlations between L_x and other parameters. Becker (1981) suggested a possible correlation of the X-ray luminosity with the inclination of the system, in the sense that in highly inclined systems (e. g. , DQ Her, T Aur) there was a substantial lack of X-ray emission, while the low-inclination system V603 Aql was one of the most luminous. RR Pic, which probably has a high-inclination angle, as derived from the presence of photometric eclipse-like effects (Vogt, 1975), is, however, an X-ray emitter and shows a hot UV continuum. Becker, alternatively, suggested that the speed class of the nova outburst was correlated with L_x in the sense that the four most luminous old novae were all "fast" novae with $L_x \sim 10^{32}$ erg s^{-1}, while those old novae with the most severe upper limits were all "slow" novae with $L < 5 \times 10^{31}$ erg s^{-1}.

At variance, Cordova and Mason (1984) noted that the two old novae which pulse optically (DQ Her and V 533 Her) both lack X-ray emission ($F_x < 1x10^{-13}$ erg cm^{-2} s^{-1} in the 0.16 - 4.5 keV range), and the orbital inclination of V 533 Her is not high, since no evidence of eclipses has been found (Patterson, 1979a).

It is notable that fast old novae, with $L_x \sim 10^{32}$ erg s^{-1}, had a high probability of being accidentally detected by EINSTEIN. However, the EINSTEIN observatory has not been successful in locating previously unidentified cataclysmic variables (Becker, 1981), thus leading to a discrepancy between the assumed space density of classical novae systems (10^{-4} pc^{-3}), (Bath and Shaviv, 1978), and the accidental detection rate of CVs by the IPC. The scarceness of X-ray emitting old novae could be attributed either to a much lower actual space density, of the order of 10^{-7} pc^{-3}, or to a large decrease in L_x occurring many years after the nova outburst.

VI.B. X-RAY OBSERVATIONS OF NOVAE IN OUTBURST

Nova Mus 1983 has been the first classical nova to be detected in the X-ray range during outburst phases (Ogelman et al., 1984). A few previous attempts with earlier X-ray satellites gave negative results, e.g., Nova Cyg 1975 (Hoffmann et al., 1976) using Ariel (2 - 18 keV, threshold limit ~ 3.5 10^{-11} erg cm^{-2} s^{-1}). The lack of detection was probably due to the fact that X-ray observations were made soon after outburst, when the high-density envelope absorbed the soft X-ray emission. The initial discovery of soft X-rays from Nova Mus 1983 was made using the EXOSAT satellite, on April 20, 1984, about 460 days after optical maximum. Other observations were made on July 15, 1984, and December 22, 1984 (Krautter et al., 1985). The spectrum was quite soft and was observed with the LE telescope in the 0.040 - 2 keV range. No flux was detected with the ME detector (1 -50 keV).

The X-ray flux was roughly constant from April to December 1984, while the optical magnitude decreased significantly. The measured low-energy count rates resulted in fluxes on the detector of blackbody-type input spectra in the 0.01 - 0.40 keV temperatures range, or thermal bremstrahlung spectra in the 0.30 - 3 keV temperatures range. Column densities $N_H \sim 3 \times 10^{21}$ [cm^{-2}] were assumed.

A further observation (July 17, 1985) showed a decline by a factor larger then two in the X-ray flux (Ogelman et al., 1987).

The data reported above were interpreted as compatible either with a shocked shell of circumstellar gas emitting 10^7 °K thermal bremsstrahlung at luminosity of about 10^{35} erg s^{-1}, or with a hot white dwarf remnant emitting 3.5 x 10^5 °K blackbody radiation at about 10^{37} erg s^{-1}.

Considerations on the cooling time for a circumstellar plasma at 10^7 K lead to values of the order of 30 - 60 years, a time scale which contrasts with the drop in the X-ray flux in the 1985 observation.

One additional indication in favor of the origin of the X-ray emission from the central star (which became very hot after outburst) and not from the shell is the fact that Nova Vul 1984 became observable with EXOSAT only a few months after the outburst. (Ogelman et al 1984). However, optical spectra of Nova Mus showed the strong coronal line of FeXIV 5303, which requires temperatures of the order of 2 x 10^6 °K.

The discovery of soft X-rays from Nova Mus 1983 stimulated EXOSAT observations of other novae during outburst phases. (Ogelman et al., 1987).

Nova Vul 1984-1 and Nova Vul 1984-2 were observed in various epochs, from the onset of the outburst until the first year after the outburst.

The data indicated intensity values and rise time values that are consistent with those expected from a constant bolometric luminosity model of a hot white dwarf remnant.

With the assumption that Nova Mus 1983 and Nova Vul 1984-1 and -2 had similar X-ray light curves, Ogelman et al. (1987) suggested that the X-ray emission from novae increases from zero at outburst to a plateau in a time scale of about 400 days; it remains constant for approximately 400 days and then decays with approximately the same time scale. The X-ray life time of the remnant is thus of the order of 2 - 3 years.

The EXOSAT observations of RS Oph in 1985 have provided the first X-ray recording of a recurrent nova in OB. RS Oph was one of the brightest sources recorded by EXOSAT LE telescope.

Mason et al. (1987) reported intense soft X-ray emission with a characteristic temperature of a few million degrees approximately 2 months (March 22, 1985) after the January 1985 optical outburst. The intensity steeply decreased between 60 and 90 days after the OB (April and May 1985). A lower limit for the total flux between, 1 -6 keV in March 22, 1985, was estimated at about 1.5×10^{-10} erg cm^{-2} s^{-1}. Bode and Kahn (1985) have interpreted this X-ray emission in terms of the interaction of the ejecta with the envelope produced by the wind of the red giant. A weak residual X-ray emission was detected with the LE telescope about 250 days after OB, in October 1985. This flux is indicative of a temperature of ~ 300.000 °K and is consistent with the presence of a hot white dwarf of $L \sim 10^{37}$ erg s^{-1}, $R \sim 10^{9}$ cm at a distance of ~1.6 Kpc ($N_H \sim 3 \times 10^{21}$ cm^{-2}).

It is remarkable that these values for L and T are in agreement with those proposed by Ogelman et al. (1987) for the soft X-ray emission from Nova Mus 1983.

VII. FINAL DECLINE AND NOVA ENVELOPES.

(written by Duerbeck and Hack)

VII.A. THE FINAL DECLINE OF NOVAE

From the theorist's side, who wants to check predictions of current nova models, the final decline of novae is interesting because it presumably encompasses several decisive moments in the development of a nova outburst:

1) The shell should be depleted, either by a strong wind or by dynamical friction in the shell by the secondary star, to such an extent that nuclear burning is halted in the shell. The remaining material should then settle down on the surface of the white dwarf.

2) The accretion disk should be reestablished, possibly only for a short time (hibernation model, see Chapter 7).

From the observer's side, in the past, spectroscopic investigations were, in most cases, restricted to the emission lines, leaving the continuum underexposed. The use of linear receivers has improved the situation recently.

The situation is somewhat better for photometric observations. Light curves that cover the late decline for some bright objects are available. The interpretation of such light curves is complicated by the fact that the flux of the nova is composed of several components: the light of the central object (a continuous spectrum, in first approximation a blackbody spectrum), the nebula (emission line spectrum plus free-free and bound-free continua), and, in some cases, wavelength-dependent obscuration represents modulation of the continuum by circumstellar dust.

Most available light curves have the disadvantage that they are broadband (e.g., visual, photographic, Johnson filters) and thus include both the continuum and strong nebular lines. More useful data are obtained in spectral regions isolated by medium-or narrow-band filters (e.g., Stromgren *y*). Absolute spectrophotometry from objective prism spectra or with digital receivers calibrated by spectrophotometric standards is, of course, ideal, because it gives both information on emission line strengths and the continuum energy distribution.

The decline of a nova becomes more difficult to interpret if excessive dust formation occurs in the shell. A good example is FH Ser, which remained at a constant bolometric luminosity

until about 200 days after maximum; in the beginning, the visual decline was caused by a shift of the maximum of radiation to the ultraviolet. In later stages, dust formation shifted the peak of radiation to the middle infrared (3 - 6 μm). In such a case, spectrophotometry in the optical does not at all give an indication of the total energy output of the nova and its variation.

This example shows that the sum of the contributions of all radiation sources in the visual band is not very helpful in describing the development of the outburst in its late stages. Even if all contributing sources in the optical region can be clearly disentangled, the problem is still there that the overall energy distribution is only incompletely known. Observations in the infrared and ultraviolet, as well as in the x-ray region, have in recent years improved the situation quite a lot; how scarce they might be for some objects or at some phases of the outburst. Indeed, the late decline is covered least by such multifrequency observations, and more or less regular observations of a future (bright) nova might remedy the situation somewhat.

As mass loss is decreasing with time, the photospheric radius decreases and, since the energy source has not yet turned off completely, the photospheric temperature rises. The associated hardening of the radiation causes the nova to become a UV, an EUV, and ultimately a soft x-ray source (detectable with EXOSAT or equivalent X-ray facilities). Infrared emission of x-ray heated grains should also be detectable during the soft X-ray phase.

In the past, a description of the (broadband) decline of light curves in the optical region was introduced by Vorontsov-Velyaminov (1940, 1948, 1953). He approximated a nova light curve by

$$m(t) = m_0 + b_1 \log (t - t_0), \qquad (6.1)$$

where t is measured in days, and, if a discontinuity occurs in a later stage, by

$$m(t) = m_1 + b_2 \log (t - t_0) \quad (\text{for } b_2 > b_1). \qquad (6.2)$$

For the average nova, b_1 has the value 2.5, and thus the luminosity in the visual region can be described as L = A/t. Discontinuities occur mostly at $\Delta m = 3.8$ (counted from maximum), and at $\Delta m = 6.3$. They indicate the onset and end of the transition stage.

A large collection of m / log t curves has been compiled by Vorontsov Velyaminov (1948, 1953) (see Figure 6.63) and by Gershberg (1964).

Most of the better observed objects, where continuum and line intensities are available, are discussed below.

V1500 Cyg. The data used are those of Lockwood and Millis (1976), based on Strömgren *y* photometry. Another illustration of the usefulness of well - defined spectral regions is the plot of continuum and line fluxes (continuum at 0.479 μm and 2 μm, as well as Hβ and [O III] fluxes). While the continuum fluxes and Hβ decline at a more or less equal rate, the [O III] flux decreases more slowly. Also, the visual flux decreases more slowly in late phases, when it vanishes as does also the IR flux, which originates from optically thin free-free emission, but comes from the remnant (Figure 6.64, Ferland et al., 1986). In the first phase, the slope in the relation m(t) = a log t is 4.5. Here, as usual, the zero-point of the time is the moment of maximum light.

Similar data are available for V1668 Cyg. Kaler (1986) used Strömgren and Hß wide filters to study the decline in late phases. The continuum slope is first 3.5, then 6.5, possibly even steeper in the very late phases. The Hß flux (which also includes some contribution of [O III]) declines much more slowly.

The light curve of V446 Her, also studied with a narrow-band filter in a relatively line free spectral region by Gyldenkerne, Meydahl, and West (1969), gives a slope of 4.11. Pioneering spectrophotometry by Meinel (1963) is also available for this object. The light curve of V533 Her, from spectra calibrated by broad band photometry, and derived continuum fluxes by Friedjung and Smith (1966) yields a slope of 3.57.

Spectrophotometry of "historical" novae by means of objective prism plates was carried out by Payne-Gaposchkin and collaborators: DQ Her (Whipple and Payne-Gaposchkin, 1936, 1937, Payne-Gaposchkin and Whipple, 1939); RR Pic (Payne-Gaposchkin, and Menzel, 1938), and GK Per, V603 Aql, and others (Payne-Gaposchkin and Gaposchkin, 1942).

The spectrophotometry of HR Del by Drechsel et al. (1977) is also based on objective prism spectra. The continuum magnitude yields, after an unusually long plateau with a practically negligible slope, an extremely rapid and nonlinear decline of about 8.3, which is faster than that of a fast nova, because it occurs at a much later time as counted from maximum. (see Figure 6.65).

The physical reason for the time scale of the return to the prenova state is not yet understood. A $M_\odot$ is required to trigger a runaway. Nuclear burning proceeds at a luminosity of approximately $3 \times 10^4 L_\odot$, thus the nuclear burning time scale is approximately 300 years. MacDonald, Fujimoto, and Truran (1985) think that the time scale of classical nova systems is of the order 10 - 30 years. The spectrophotometric analyses (especially the study of FH Ser over a wide wavelength band) indicates that turnoff for this fairly slow nova occurs 200 days after outburst.

Turnoff requires fuel exhaustion either by nuclear burning (which appears not to be the case, in view of the quoted time scales), some sort of quenching of the nuclear reactions, or some mechanism of mass loss. This can be the "thick wind" of outbursting novae (Bath, 1978; Ruggles and Bath, 1979), or the loss of the shell through the outer Lagrangian points of the binary system as a result of dynamical friction during the common envelope phase (MacDonald, Fujimoto and Truran, 1985; MacDonald, 1986).

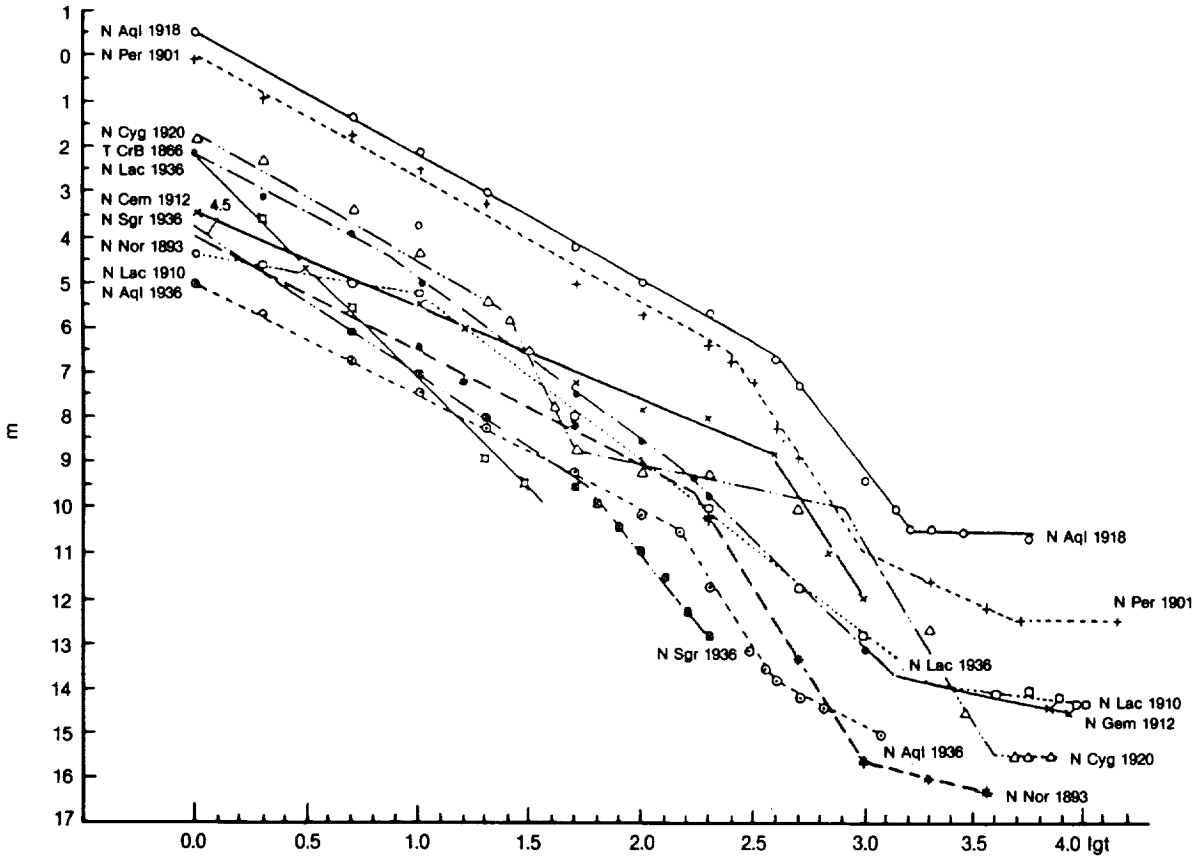

Figure 6-63. An m-log t diagram of visual nova light curves (from Vorontsov-Velyaminov, 1953)

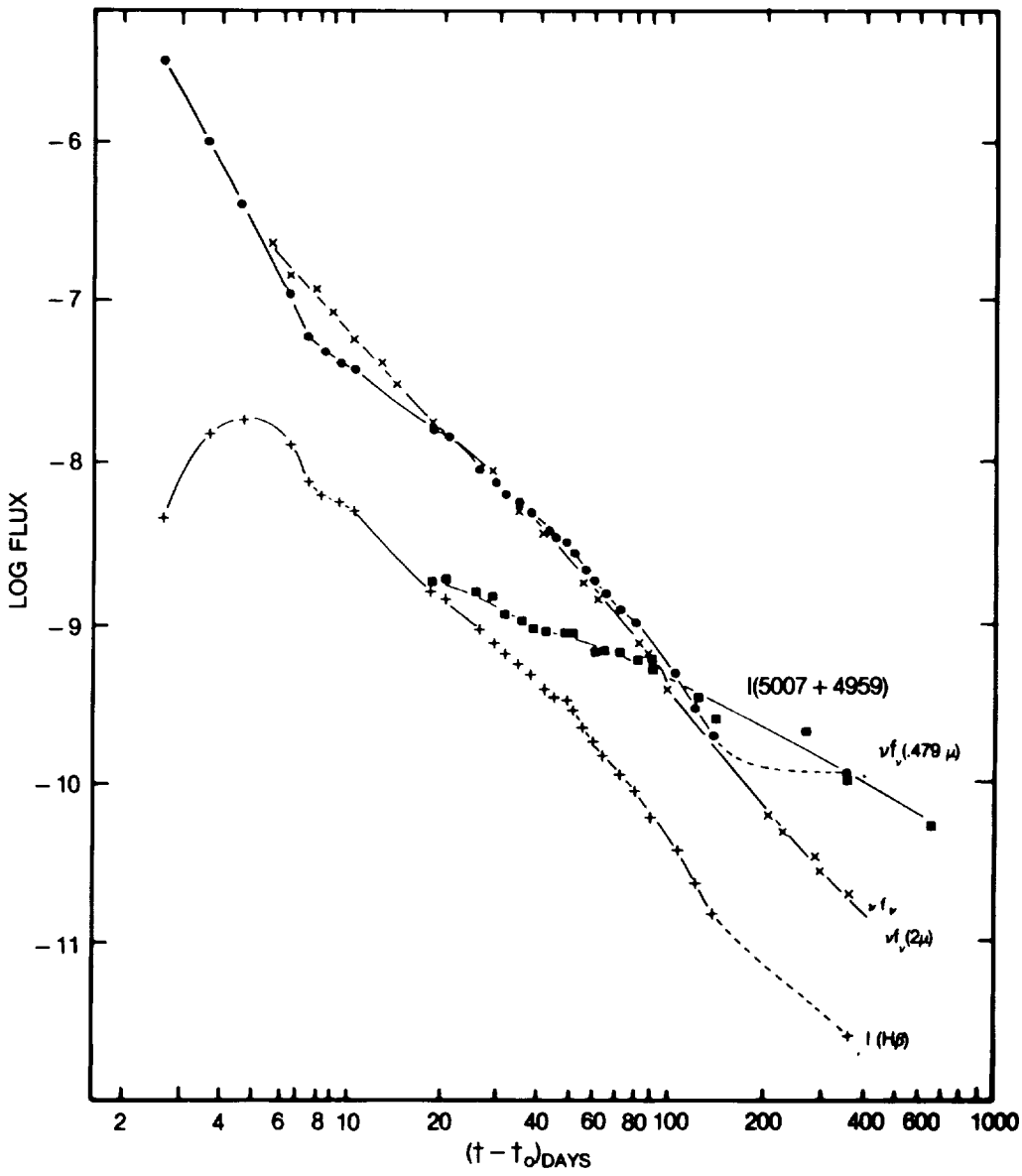

Figure 6-64. The development of line and continuum strengths in Nova V 1500 Cyg during its decline. The plotted quantities have not been corrected for interstellar reddening and are either the integrated strength of the emission line in erg s^{-1} cm^{-2} or νf, a continuum measure with similar units. The continua at 2 μm and 0.479 μm are shown by x and • respectively. These nearly coincide during the interval over which the optical and infrared continua are optically thin free-free emission (t=10....150 days) and sharply diverge when the underlying remnant becomes visible, about one year after outburst. The Hβ line follows the continuum strength closely, while [O III] 5007 and 4957 line declines much more slowly.
(from Ferland et al., 1986)

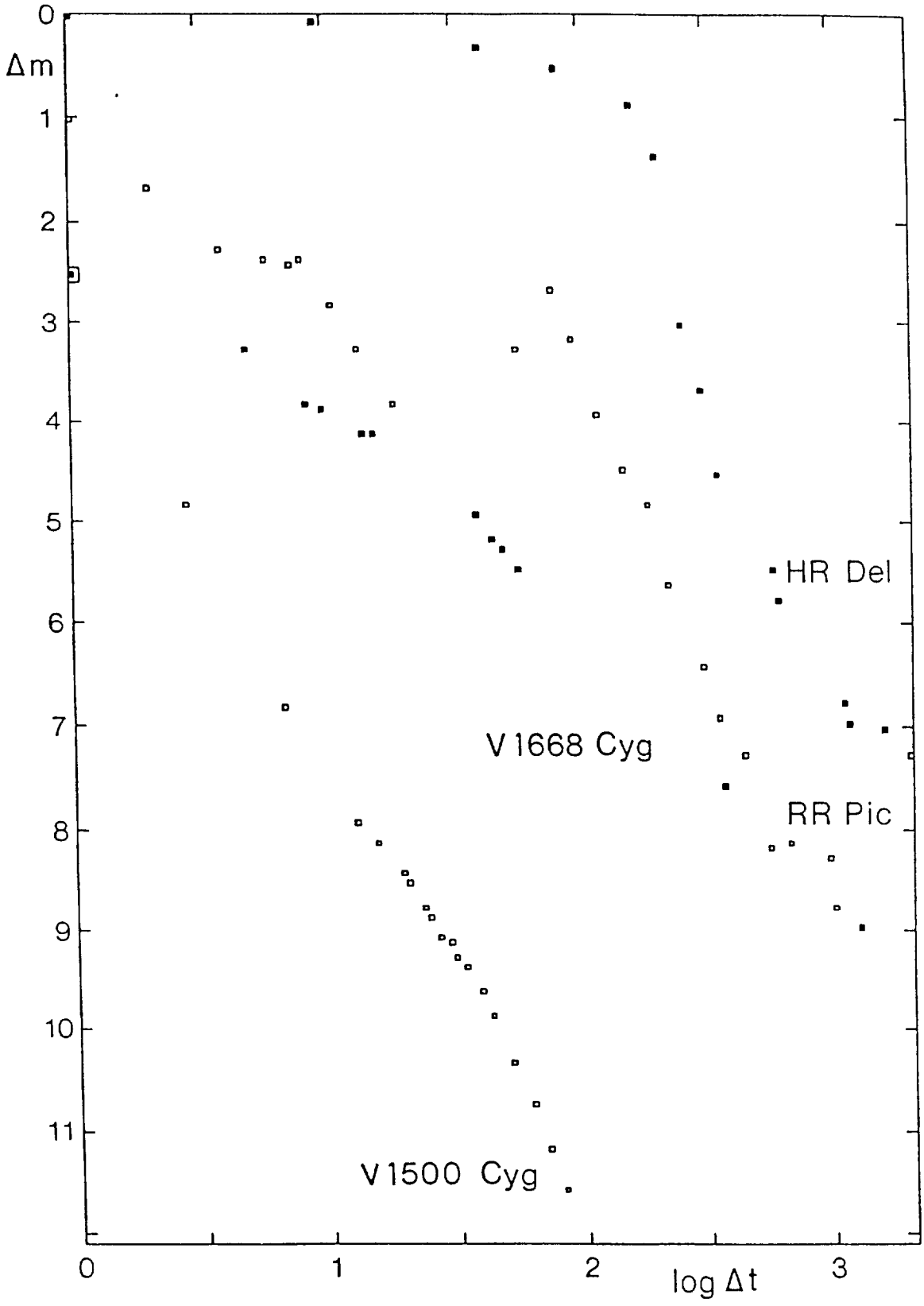

Figure 6-65. Δm(continuum)-log Δt diagram for several novae (for references, see text).

VII.B. THE POSTNOVA PHASE WITH SURROUNDING NEBULOSITY

When the nova has declined to its preoutburst state, the only remaining sign of the outburst is the surrounding expanding nebulosity. This seems to be a comparatively short-lived phenomenon, since no "past nova" or "nova-like object" without recorded outburst could be identified as a nova because of an observable shell. A few counter examples, e.g., E2000+223 (Takalo and Nousek, 1985) and 623+71 (Krautter et al. 1987), are extremely dubious. This can be explained by the fact that nova shell masses are fairly small and are easily lost several decades after outburst when their surface brightness becomes very small. This has to do with the fact that the "central stars" are not very powerful in exciting the surrounding nebulosities, and most energy is drawn from the interaction with the interstellar material. Thus, in the course of time, nova shells are decelerated, interaction becomes less powerful, and the shells are less excited and fade in optical light.

Combined spectroscopic and direct observations can give information on their distance, on the mass lost in the outburst, and on their chemical composition and physical structure.

One of the best methods for deriving the distance of a nova is to measure the angular size of the nebula formed around it as the result of the explosion. By knowing the expansion velocity and the time elapsed since the explosion, we can compute the real dimension of the nebula and derive its distance. The distance determined by this method can be used for calibrating the relationship between absolute magnitude at maximum and rate of decline.

McLaughlin (1960) and Cohen and Rosenthal (1983) have studied twelve old novae in order to measure the surrounding nebula. Cohen (1985) added eight new spatially resolved nova shells. The data relevant for the determination of the size of the envelope, and therefore for the the distance, are given in Table 6.16 (adapted from Cohen and Rosenthal, 1983, and Cohen, 1985, while Table 6.17 (from Cohen and Rosenthal, 1983) gives the observed and expected radii of the shells. The majority of these shells have nonspherical shape. The expansion velocities from McLaughlin, from Cohen and Rosenthal, and from Cohen (1985) are in rather good agreement, with the exception of V603 Aql and CP Lac. For these objects, the radial velocities are supposedly those of the accretion disk. The shells are too faint to be discovered by those authors.

Cohen (1985) has observed all classical novae that exploded before 1976, which were at maximum brighter than V = 6.6 mag, and are observable from Mt. Palomar. Of the 18 objects, 9 showed no detectable shell. Since the shells emit especially in the light of Hα + [N II], interference filters centered at Hα, having a full width at half maximum (FWHM) of 16 and 30 Å were used.

Like supernova shells, the expanding nova shells interact with the surrounding interstellar material. The kinetic energy of a nova shell shortly after outburst is, however, already much smaller; it lies between $2\ 10^{45}$ and $1\ 10^{44}$ erg (e.g., Chevalier, 1977). The snowplow model, put forward by Oort (1946, 1951), has been applied to old supernova remnants and nova remnants with satisfactory results (see Chapter 7).

Recently, by comparing outburst photographs and CCD frames of nova shells taken at different times, Duerbeck (1987a) found noticeable decelerations with time, as postulated by the snowplow model.

The temporal variation of the shell radius r (in arc seconds) is approximated by

$$r(t) = c_0 + c_1\, t + 0.5\, c_2\, t^2 \qquad (6.3)$$

where c_0, the size of the shell at the time of outburst, is assumed to be zero. c_1 is the initial expansion rate, measured in arc sec yr^{-1}. c_2 is the deceleration parameter (in arc sec yr^{-2}), which can be converted into the braking b (in km s^{-1} yr^{-1}):

$$b = \frac{c_2}{c_1} V_{exp}. \qquad (6.4)$$

TABLE 6-16a NOVA CHARACTERISTICS

Nova	Exp.rate "/y	Expansional (1) km/s	velocity (2)	Distance pcs	m_{max}	m_{min}	absorption (1)	(2)	M_{vis} Max (1)	(2)	Min
V 603 Aql	.956	1700	255	376	-1.1	10.8	.2	.2	-9.2	-9.15	+2.7
T Aur	.117	460	655	830	+4.2	15.4	.7	1.5	-6.2	-7.9	+5.0
V476 Cyg	.093	700	790:	1590	+2.0	16.1	.6	.6	-9.6	-9.85	+4.5
DQ Her	.27	290	315	230	+1.4	15.1	.2	.2	-5.6	-6.2	+8.1
CP Lac	.25	1600	295:	1340	+2.1	15.3	.8	.8	-9.3	-9.35	+3.9
GK Per	.54	1200	1200	470	+0.2	13.5	.3	.3	-8.5	-8.55	+4.8
RR Pic	.18	410	475	480	+1.2	13.3	.2	.2	-7.4	-7.3	+4.7
CP Pup	.21	700	710	700	+0.4	17.5	.3	.3	-9.1	-9.55	+8:
HR Del			520		+4.8			.2		-5.05	
V533 Her			580		+3.5			.2		-7.45	
BT Mon*			800								
FH Ser			560		+4.4			2.8		-7.55	

*) BT Mon was discovered only in its late decline stage.
(1) Data by McLaughlin (1960).
(2) Data by Cohen and Rosenthal (1983).

TABLE 6-16b. NOVA LUMINOSITIES AND LIGHT CURVES (from Cohen, 1985)

Object	V_{erp} (km s^{-1})	Source of V_{erp}	A_1 (mag)	m_v(max)[a] (mag)	t_2 (days)	Light Curve Source	M_v(max) (mag)	M_v(15) (mag)
Novae of Paper II (Cohen, 1985)								
v1229 Aql 1970	575	1	1.2 ± 0.5	6.5	18	7	-6.6	-4.8
v500 Aql 1943	1380	2	3.0 ± 1.5	6.5:	20:	8	-10.35	-8.85
*v1500 Cyg 1975.....	1180	1	1.2	1.85	2.4	9	-9.95	-5.1
*v446 Her 1960	1235	3	0.8	2.75	5	7	-8.7	-5.55
*v533 Her 1963	1050	4	0.6	3.5	26	10	-7.7	-6.6
DK Lac 1950	1075	5	1.4	5.0	19	5	-9.35	-7.35
XX Tau 1927	650:	1	$1.3^{+0.2}_{-0.7}$	6.0	24	11	-8.05	-6.75
RW UMi 1956	950:	1	0.1	≤6.0	200:	12	≤-7.85	...
*LV Vul 1968	860	6	1.2	4.5	21	6	-6.75	-5.25
Novae Discussed in Paper I (Cohen and Rosenthal,1983)								
*603 Aql 1918	....	....	....	..	4	....	-9.15	-5.35
T Aur 1891	....	....	1.2 ± 0.5	..	80	....	-7.4	-7.0
v476 Cyg 1920	....	....	....	..	7	....	-9.95	-6.85
HR Del 1967	....	....	....	4.6	> 150	....	-5.25	-5.25
*DQ Her 1934	....	....	....	..	67	....	-6.2	-5.2
*CP Lac 1936.....	....	....	....	..	5	....	-9.35	-5.95
BT Mon 1939	....	....	....					
*GK Per 1901	....	....	....	..	6	....	-8.55	-5.75
*RR Pic 1925	....	....	....	..	80	....	-7.3	-6.0
*CP Pup 1942	....	....	....	..	5	....	-9.55	-5.55
T Sco 1860	....	....	0.6	7.0	9	13	-8.9	-6.5
FH Ser 1970	....	....	....	..	42	....	-7.55	-6.55

NOTE--Sources of data in cols (3) and (7) are as follows: (1) V_{erp} from double spectrograph observations at current epoch; (2) Sanford 1943; (3)V_{erp} from Cohen's measurements of spectra from plate vault of Mount Wilson and Las Campanas Observatories; (4) Baschek 1964; (5) Larsson-Leander 1953, 1954; (6) Hutchings 1970; (7) AAVSO (Mattei 1984); (8) Gaposchkin 1943; (9) Young et al. 1976; (10) Chincarini 1964; (11) Cannon 1928; (12) (Kukarkin 1963, Ahnert 1963; (13) Sawyer 1938.

The half-lifetime is determined by

$$t_{1/2} = \frac{V_{exp}}{2b} = \frac{1}{2}\frac{c_1}{c_2} \qquad (6.5)$$

The observational results of four shells are listed in Table 6-18.

The deceleration is larger for higher expansion velocities, the mean half-time, after which the expansion velocity has dropped to half its initial value, is 75 years. The expansion of a pronounced feature of the shell of GK Per, the "bar," is illustrated in Figure 6-66. The results are in accordance with expectations from the snowplow model put forward by Oort (1946, 1951).

This braking must be taken into account in the determination of nebular expansion parallaxes. Errors can be as large as 20 to 30%, which is about as large as the uncertainty of choosing the "true" expansion velocity of the shell, derived from the Doppler displacement of absorption lines at maximum. Usually, it is assumed that the "true" velocity is that of the principal spectrum, which is lower than that of the diffuse-enhanced and of the

TABLE 6-16c. SHELLS NOT DETECTED (from Cohen, 1985)

Object	Seeing (FWHM) (arcsec)	Central Pixel (DN)	m_v(max)[a] (mag)	r (mag)	Hα (mag)
IV Cep 1971	1.3	13,200	7.5	16.08	16.14
Q Cyg 1876	1.0	30,700	3.0	14.93	14.94
v450 Cyg 1942	1.0	5,600[b]	7.8	16.48	16.58
DI Lac 1910	1.0	58,675[c]	4.6	14.58	14.90
HR Lyr 1919	1.0	18,300	6.5	15.95	15.99
v841 Oph 1848	2.5	11,700	5.0:	....	....
v368 Sct 1970	1.0	9,070	7.0	....	12.71
v373 Sct 1975	1.0	3,600[b]	6.0	18.07	16.98
WY Sge 1783	1.0	4,120	6:	18.10	17.89

[a] From Payne-Gaposchkin 1957, 1977.
[b] Faint star(s) closer than 4" to postnova star.
[c] Cental pixel saturated. Its value was extrapolated using the point-source image profile.

TABLE 6-17. SIZES OF NOVA SHELLS

NAME	RADIUS (arcsec) Observed (1981)	Expected	NOTES
V603 Aql ..	not detected	60	
T Aur	9.5	10.5	1
V476 Cyg ..	5.7	5.7	
DQ Her	10.5	12.7	1
CP Lac	not detected	11.3	
GK Per	41.5	43.2	1
CP Pup	7	8.2	2
RR Pic	11.5	9.7	1,3
HR Del	1.8	....	1,4
FH Ser	2.0		
V533 Her ..	1.6		
BT Mon	3.8		

NOTES—(1) Shell non-spherical. (2) Radius from Williams 1982. (3) Radius from Williams and Gallagher 1979. (4) Radius from Kohoutek 1981.

(From Cohen and Rosenthal, 1983)

TABLE 6-18. EXPANSION AND DECELERATION OF NOVA SHELLS

nova	V_{exp} (km s^{-1})	c_1 ("yr^{-1})	b (km s^{-1} yr^{-1})	$t_{1/2}$ (yr)	d (pc)
V603 Aql	1700	1.09	13.2	65	330
GK Per	1200	0.65	10.3	58	390
V476 Cyg	725	0.10	3.1	117	1500
DQ Her	335	0.26	2.4	67	265

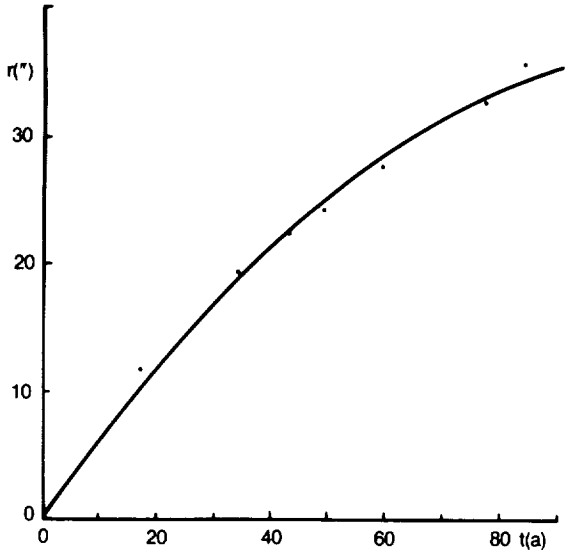

Figure 6-66. Deceleration of the bar in the shell of GK Per, using data of Duerbeck (1987a).

Orion spectra. At visual maximum, when the principal spectrum is dominating, the mass loss rate also reaches a maximum, and the main portion of the shell is formed.

An estimate of the masses of the shells is made by Cohen and Rosenthal (1983) by using several assumptions. The absolute flux of Hβ, corrected for interstellar absorption, gives the electron density. The electron temperature is assumed to be 10^4 K. It is also assumed that the shell thickness *a* is 10% of the shell radius, and that the filling factor *b* of this shell is 10%. With these assumptions, the masses of the shells are computed and the values are found to range between 1.9 x 10^{-5} $M_\odot$ for V1500 Cyg and 1.3 x 10^{-4} $M_\odot$ for V476 Cyg. These data are given in Table 6-19, together with other values for the same and different objects, determined by different methods. The uncertainty in mass determinations is clearly seen. Masses of the shells of classical novae cluster between 1 - 10 x 10^{-5} $M_\odot$.

TABLE 6-19. DETERMINATIONS OF NOVA SHELL MASSES (in 10^{-5} $M_\odot$)

Type	Object	Mass	Reference	Method
F	V603 Aql	10	Gordeladse (1937)	wind model
		14	Pottasch (1959d)	Hα flux
F	V1301 Aql	1	Snijders et al. (1984)	UV spectrum
F	T Crb	10	Gordeladse (1937)	wind model
F	V478 Cyg	0.2	Gordeladse (1937)	wind model
		13	Cohen, Rosenthal (1983)	Hβ flux
F	V1500 Cyg	4.5	Neff et al. (1978)	opt. spectrophotometry
		24	Hjellming et al. (1979)	Radio
		14	Seaquist et al. (1980)	Radio
		6.1	Duerbeck (1980)	wind model
		1.9	Cohen, Rosenthal (1983)	Hβ flux
F	V1668 Cyg	1.7	Duerbeck (1980)	wind model
		0.9	Peimbert and Sarmiento (1984)	UV spectrum
S	HR Del	25	Malakpur (1973a)	Hβ flux
		9	Anderson, Gallagher (1977)	Hβ flux
		1000	Antipova (1977)	optical spectroscopy
		≤145	Robbins, Sanyal (1978)	
		8.6	Hjellming et al. (1979)	Radio
		11	Duerbeck (1980)	wind model
		2.2	Cohen, Rosenthal (1983)	Hβ flux
		0.2	Solf (1983)	
	DN Gem	0.4	Gordeladse (1937)	wind model

S	DQ Her	9	Gordeladse (1937)	wind model
		0.7	Pottasch (1959)	Hα flux
		4.6	Mustel, Boyarchuk (1970)	optical line flux
		4.8	Ferland et al. (1984)	UV, optical spectrum
F	V533 Her	2.0	Cohen, Rosenthal (1983)	Hβ flux
F	CP Lac	3.6	Pottasch (1959)	Hα flux
F	RS Oph	0.5	Sayer (1937)	
		0.02	Folkart et al. (1964)	
		0.05	Pottasch (1967)	
			Snijders et al. (1987)	
F	GK Per	0.3	Gordeladse (1937)	wind model
		3.8	Pottasch (1959)	Hα flux
S	RR Pic	14	Gordeladse (1937)	wind model
		10	Pottasch (1959)	Hα flux
S	T Pyx	8	Seitter (1987)	Hα flux
S	FH Ser	4.3	Seaquist, Palimaka (1977)	Radio (spherical)
		3.1	Seaquist, Palimaka (1977)	Radio (polar)
		4.5	Hjellming et al. (1979)	Radio
		6.1	Duerbeck (1980)	wind model
		2.0	Cohen, Rosenthal (1983)	Hβ flux
F	LV Vul	7.8	Duerbeck (1980)	wind model
F	NQ Vul	13	Duerbeck (1980)	wind model

VII.B.1. MORPHOLOGY OF NOVA SHELLS

A general overview of nova shell morphology is given by Mustel and Boyarchuk (1970). They found, from a study of a handful of objects, that most shells have an oval shape, exhibit "polar blobs" at the end of the major axis, and an "equatorial belt", which coincides with the plane of the minor axis.

DQ Her: The system is seen perpendicular to the major axis; the shell is oval. "Polar condensations" are situated at the very ends of the large axis, and an equatorial belt is visible.

V603 Aql: The system is seen nearly parallel to the major axis; the shell appears nearly circular. An approaching polar condensation is seen in spectra and on direct images of 1933 and 1940. A system of several (two to three) rings seems to exist in the equatorial region. A thorough study of spatially resolved spectra in the nebular phase by Weaver (1974) confirmed largely the findings of Mustel and Boyarchuk (1970). Weaver's model is shown in Figure 6.67.

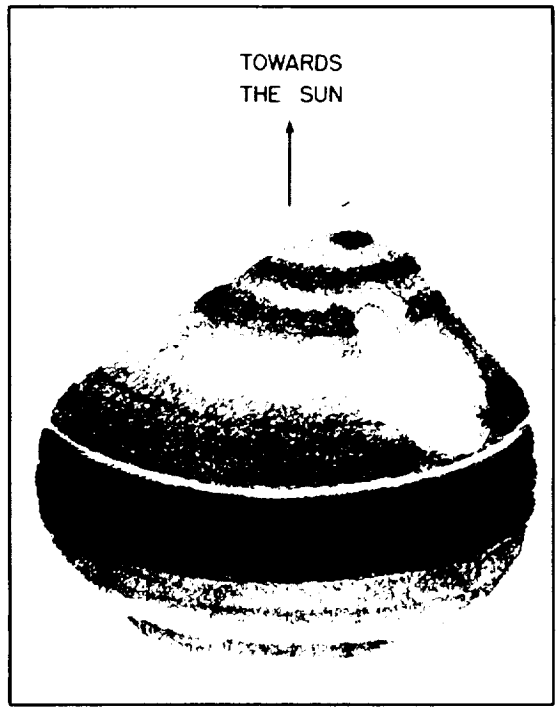

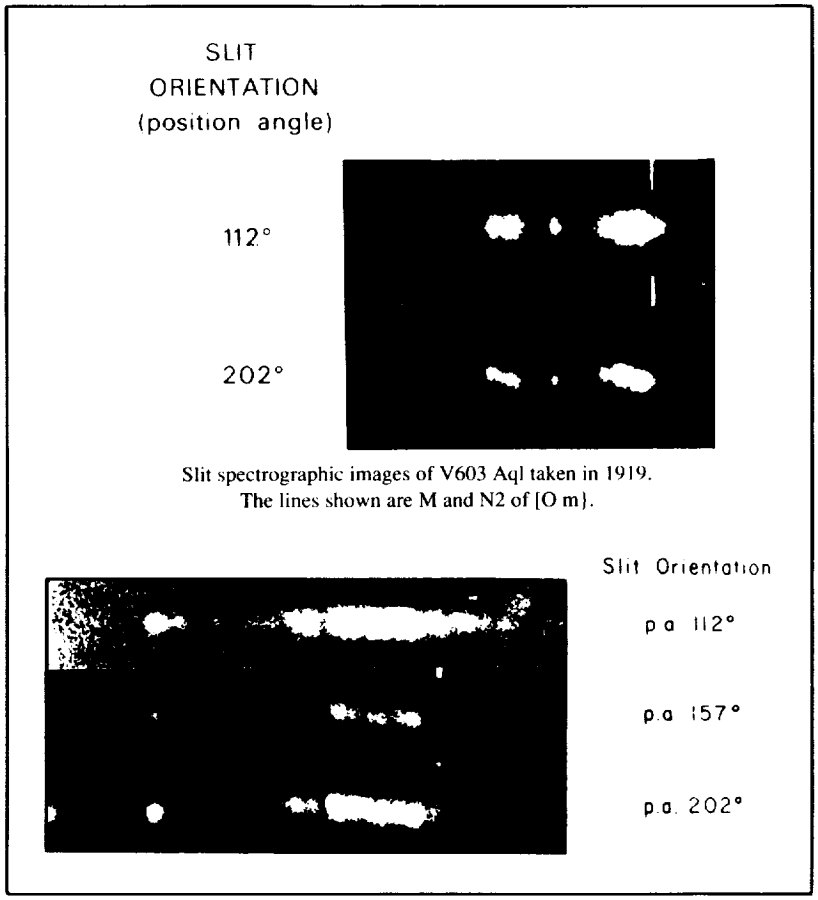

Figure 6-67. a) Drawing of a three-dimensional model of the shell of V 603 Aql, derived from b) space-resolved spectrograms taken at Lick Observatory in 1919. (from Weaver, 1974)

T Aur (See Figure 6.68): The system may have the same orientation as DQ Her, because eclipses of the central object also occur. The shell appears oval. Polar condensations and the equatorial belt seem to be missing, possibly due to the old age of the remnant. Generally, the authors argue that the equatorial belt is in the equatorial plane of the binary and polar blobs perpendicular to that plane (see also Chapter 7).

RR Pic (See Figure 6.69): The shell appears nearly circular, but this may be due to an inclination effect: it is oval when looked at in the plane of the binary. The absence of eclipses and the presence of periodic features in the light curve are in agreement with this assumption. A double-ring blob system is obvious, which can be explained by precessional motion of the erupting object in the course of the extended outburst. Deep CCD frames indicate the presence of high-velocity clouds surrounding the brighter parts of the shell, which could be material from the diffuse-enhanced mass outflow (Duerbeck, 1987b). However, a spectroscopic investigation of this faint halo is necessary to prove whether it is outflowing nova material or shocked interstellar material.

CP Pup (See Figure 8.30): The shell appears circular, but may be inclined by an angle of 30°

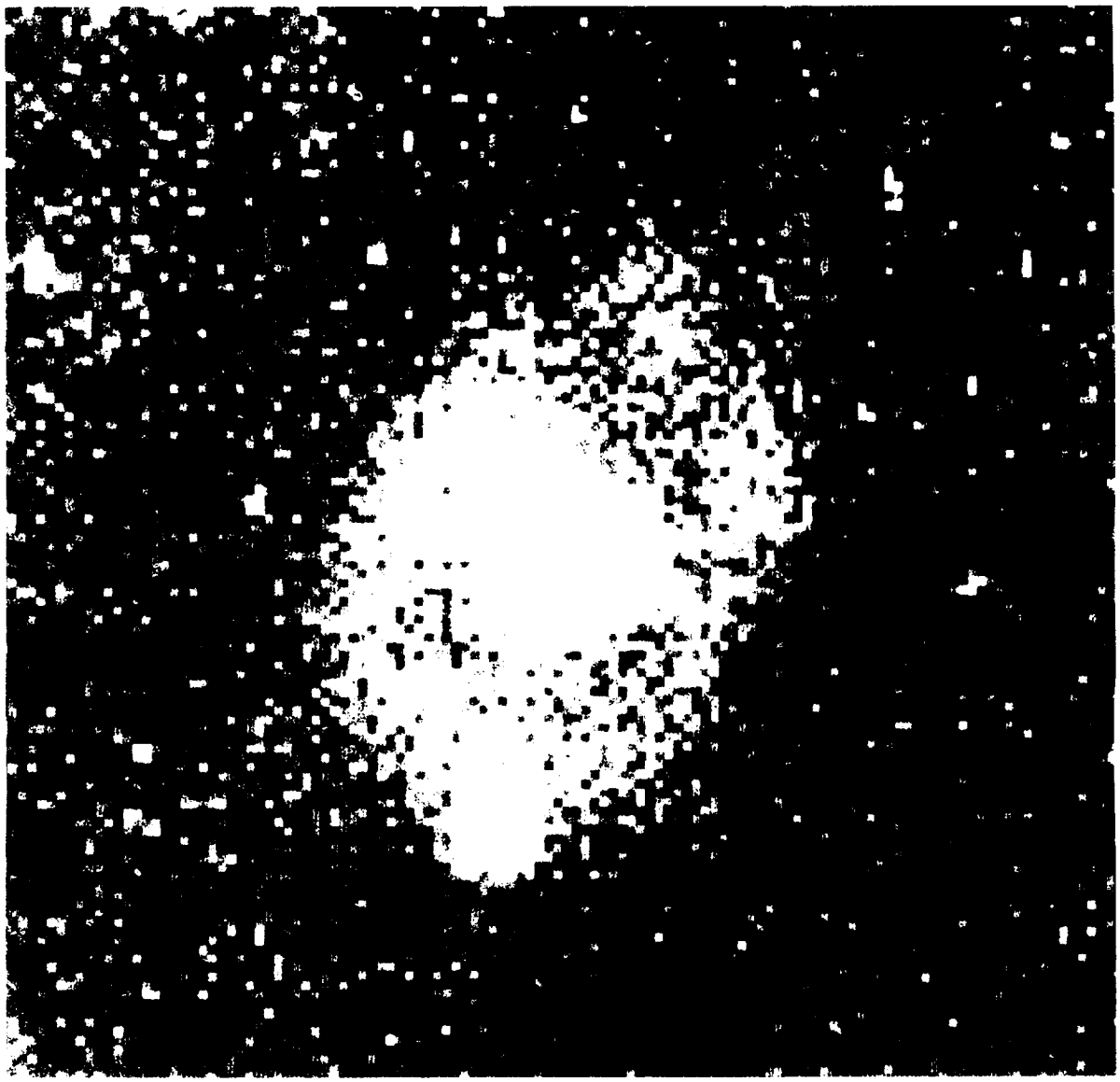

Figure 6-68. CCD frame of the shell of T Aur, taken through an Hα filter with the Calar Alto 2.2 m telescope.

with respect to the celestial plane, as revealed by radial velocity determinations. The circular belt is fragmented into at least 11 condensations, which apparently were already present a few months after outburst, as noted in high-dispersion spectral studies of CP Pup in the nebular stage.

Seitter (1971), Hutchings (1972), and Malakpur (1973a) have modelled nova shells from the nebular spectra of HR Del, FH Ser, and LV Vul, respectively. They also yield a ring/shell-type structure, which was confirmed for the objects Hr Del and FH Ser by direct imaging in later phases.

Hutchings (1972) discussed this nonspherical distribution of the matter in the nebula as a consequence of the binary nature of the nova system. He observes that the time scale of the mass loss during the outburst is longer than the orbital period (days or months as compared with hours). The interaction will occur in a ring around the equatorial region of the expanding nova photosphere. The interaction with the companion by purely gravitational forces will have the effect to reduce the original spherical symmetry to two polar cones and to give rise to a) a faster-moving ejecta that move out initially in all directions from the outer parts of the equatorial band and later either disappear or are more concentrated to the

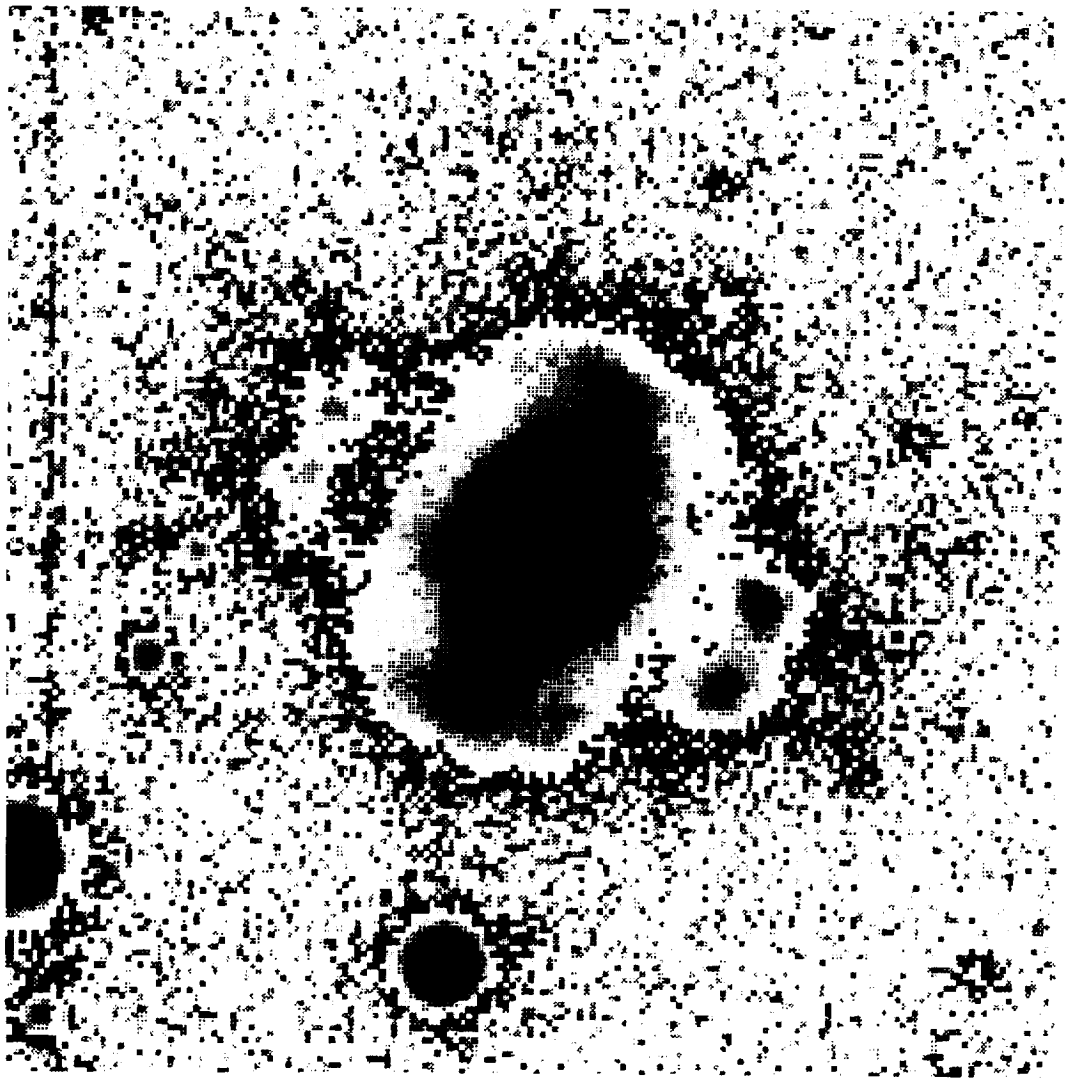

Figure 6-69. The shell surrounding RR Pic, taken through an H α filter, with a CCD camera at the ESO 2.2 m telescope. For this composite, the central section of the highly amplified picture was set to zero, and a low magnification image of the central nebula was inserted.

equatorial plane, and b) some slower-moving equatorial remnants (Figure 4 from the paper by Hutchings). The comparison of the observed emission line profiles with those computed for different geometry and inclination to the line of sight of the nova envelope will be discussed in Chapter 7.

In recent years, direct imaging and spatially resolved spectroscopy of nova shells has progressed quite much, due to the advance in detector technology. The following Table 6-20 summarizes such work.

It should be noted that the morphological description given in the table is extremely scarce. More detailed discussions of the shape of V603 Aql is given by Weaver (1974); that of GK Per is described in Duerbeck and Seitter (1987); those of RR Pic, CP Pup, and T Pyx by Duerbeck and Seitter (1979) and Duerbeck (1987b). A detailed discussion of several envelopes will be found in Chapters 8 and 9.

nuclear reactions occurring during the explosion, and hence to check the theories of the outburst. According to the theory proposed by Starrfield et al. (1977; see also Chapter 7), a fraction of the accretion disk material reaches the surface of the degenerate star (assumed to be a carbon-oxygen white dwarf) building up a layer of H-rich material on the surface. Eventually, compression of the accreting gas causes heating up to temperatures at which nuclear burning sets in. According to their calculations, if the CNO nuclei are enhanced in the envelope (as a consequence of the previous history of the material), a thermonuclear runaway occurs, producing a fast nova. Otherwise, a slow nova outburst occurs. A knowledge of the element abundance in novae is fundamental to understand the nature of the outburst and to check the theories.

A discussion of various methods for deriving the chemical composition of novae is given by Williams (1977). He shows that many causes of uncertainty affect the abundances derived from

TABLE 6.20 NEBULAR SHAPES, TEMPERATURES, AND ABUNDANCES

nova	T (K)	abundances	morphology
T Aur (1892)	low	CNO high	elliptical
DQ Her (1934)	500	[CNO/H]=100	elliptical,pol.blobs
GK Per (1901)	$\geq$20000	N enh.	single blobs; complicated structure
RR Pic (1925)	16500	He,N,Ne? enh.	ring + blobs
CP Pup (1942)	800	[N/H]=1000	many blobs
T Pyx (recurr)	$\geq$20000	solar?	several shells

VII.B.2. SPECTRA AND ABUNDANCES IN NOVA SHELLS

Besides the possibility to derive their distances and to measure their masses, nova shells are important because their spectra offer more precise methods to measure their chemical composition and therefore to verify if this is affected by the absorption spectrum around maximum light. Such a rapidly changing spectrum is very far from the usual conditions in a stable atmosphere; the abundance of CNO depends upon an assumed temperature distribution in the pseudophotosphere, which is highly uncertain. Emission line spectra in early decline give also uncertain results, because emission and ab-

sorption components are blended together, making uncertain the measure of the emission line intensity, and because of the uncertainties of the parameters of the emitting gas. One can hope that more reliable abundance determinations can be obtained by the study of the spectra of old extended shells that behave in a similar way to young planetary nebulae. At the time when the shells become spatially resolved, the density is so low that self-absorption and collisional de-excitation should be negligible. The distance between the shell and the stellar object plus accretion disk make impossible any confusion with these regions having very different physical conditions.

Table 6-21 (Tylenda, 1979) compares the average abundances of novae with those of planetary nebulae and the solar values.

Anyway, the physical and chemical properties of nova shells are difficult to determine and subject to controversy. We will quote the results of several investigations of the shells of DQ Her, RR Pic, and CP Pup. A more detailed discussion is given in Chapter 8.

Several models of the shell of DQ Her have been presented in the last decade, and every time, the previous results (or predictions) have been partially discarded. Williams et al. (1978) carried out spectroscopy in the visible region, and obtained the following results:

The electron temperature, T_e, of the shell must be low because of the narrow Balmer continuum emission at 3644. Most of the hydrogen emission and the C II, N II, and O II recombination lines originate in the cold, ionized gas. The line strengths of CNO are much greater, as compared with the Balmer lines, than in ordinary H II regions or planetary nebulae, indicating a high abundance. Lines of [N II] indicate a hot ($T_e > 5000$ K) component of gas.

Spectra at the ends of the major axis differ from those at the ends of the minor axis. While the line strengths of H, [O II] and [N II] are similar, C II, N II and O II are weaker or absent along the minor axis. Williams et al. estimate that the CNO abundances might be 100 times solar at the polar blobs and still 10 times solar in the equatorial (minor axis) region.

The source of excitation of the nebula remains a controversial topic. Williams et al. had postulated a "frozen-in ionization," but this could not explain a lower C- abundance in an earlier nebular phase, because C^{++} recombines Z^2 times faster than H^+ in a time-dependent model, thus C^{++}/H^+ should decrease with time.

A model of the nebula which is photoionized by the X-ray radiation from the central object was proposed by Ferland and Truran (1981), which showed better consistency with the observed lines in the optical regions. It predicted line strengths in the UV, which could not be verified in a subsequent study of the UV spectrum of the nebula (Ferland et al. 1984). A careful analysis of the energy distribution of the central

TABLE 6.21. CHEMICAL COMPOSITION (IN NUMBER OF ATOMS) OF NOVA DEL 1967 AND OTHER OBJECTS*

Element	Novae [1]	Planetary nebulae [2]	Sun [3]	Cosmic [4]
He/H	0.25	0.10	0.085	0.085
10^4×N/H	30	1.0	0.98	0.91
10^4×O/H	50	4.9	8.3	6.6
10^4×Ne/H	1	1.3	1.3	0.83

References: [1] Collin-Souffrin (1977); [2] Aller (1978); [3] N and O from Lambert (1978); He/O and Ne/O from Bertsch *et al.* (1972); [4] Allen (1973). *from Tylenda (1979)

object was made (which contradicted many previous models because of its deficient far UV and X-ray flux). Using the deduced continuum flux, photoionization models of the nebula are calculated and showed that the low observed electron temperature is the result of the very high metal abundances which are characteristic for nova shells. Infrared fine-structure lines are efficient coolants, and low temperatures are achieved for a wide variety of radiation fields.

The authors find that the 88-μm and 52-μm lines of [OIII] are extremely efficient coolants, provided that the gas density is below the critical density for the J = 1,2 sublevels of the $O^{+2/3p}$ ground state (N = 670 and 4900 cm^{-3}, respectively, see Osterbrock 1974). At high densities, only UV resonance lines are efficient coolants, and the gas equilibrates at T around 10^4 K. When the optical [O III] lines begin to cool the gas (at N < 10^6 cm^{-3}), the temperature falls to about 6000 K. Finally, the temperature falls to below 1000 K when the infrared fine-structure lines are no longer collisionally deactivated (N < 10^3 cm^{-3}). They postulate that these cold nova shells should be powerful radiators of IR lines. Together, the [OIII] fine-structure lines should have an observed flux of 2.7 x 10^{-12} erg cm^{-2} s^{-1}. Indeed, Dinerstein (1986) found for the 60-μm and 100-μm bands of the IRAS satellite the following fluxes:

F(lambda, 60 μm) = 4.8 x 10^{-13} erg cm^{-2} s^{-1}

F(lambda, 100 μm) = 1.8 x 10^{-13} erg cm^{-2} s^{-1}

Dinerstein states that Ferland postulates several 10^{-19} W m^{-2}, while IRAS measured 10^{-18} W m^{-2} in the 60 μm band. Emission in the 88-μm line is similar to that in the 52-μm for densities lower than about 10^3 cm^{-3}.

Spectroscopy of the blobs in the shell of RR Pic was carried out by Williams and Gallagher (1979), and by Duerbeck (1987b). They noted that the spectra are similar to those of high-excitation planetary nebulae, such as NGC 2022. The spectra show strong [Fe V], [Fe VI], and [Fe VII] lines, which were also prominent in the first years after outburst (Spencer Jones, 1931). An ionization model with T_* = 2.5 x 10^5 K and L_* = 2.2 x 10^{34} erq s^{-1} was applied. The electron temperature was determined to be 16,500 K. A comparison with the observed line strengths leads to an enhancement of the elements He, N, and Ne. Helium is at least twice as abundant as in the sun, oxygen seems to be normal, N is enhanced by at least a factor of 10, and Ne possibly also by a factor of 10.

The large value of N/O in RR Pic is unusual, but could possibly be accounted for if equilibrium CNO burning has occurred and converted most of the C and O into N. This is predicted for slow novae by current models. However, spectroscopy of the ring yields strong [O III] lines.

The shell around CP Pup was also studied by R.E. Williams (1982). He noted similarities with the shell of DQ Her, a similar low temperature (800 K), and a high N abundance (N/H = 0.1).

Seitter (1985) pointed out that the [O III] lines are much stronger in the polar blobs than in the equatorial ring of RR Pic. Such inhomogeneities were studied in the following years by comparing CCD frames of nova shells taken through interference filters isolating the [O III] and the [N II = Hα]

1)A bipolar structure is seen in the shell of RR Pic; the blobs radiate more in [O III].

2)A bipolar structure is seen in DQ Her; the polar regions radiate in the [O III] filter region, while no [O III] has been found spectroscopically.

3)A bipolar structure is visible in the recurrent nova T Pyx (Duerbeck 1987b).

4)A bipolar structure is visible in the shell of GK Per. This shell has often been classified as irregular, but the chemical inhomogeneities show a regular pattern. IUE spectroscopy of different parts of the shell gave good arguments for the reality of chemical inhomogeneities (Bode, Duerbeck, and Seitter, 1988).

Thus, chemical (or excitation) inhomogeneities are well established in nova shells.

Spectra of RR Pic taken with the Cassegrain spectrograph and a CCD receiver at the ESO 2.2 m telescope are shown in Figure 6-70.

In addition to several classical novae, Cohen (1985) discusses the spectrum and the image of the nebula around CK Vul 1670, which was recovered by Shara and Moffat 1982).

Associated with the central object, which is below the limit of the Palomar charts (Shara and Moffat, 1982), are two faint nebulosities at 5" or 6" from the nova candidate, displaying spectra similar to those of the nova ejecta, plus other fainter nebulosities. Two images obtained in the light of Hα and in the nearby continuum show that the nebulae are visible only in the first one; i.e. (Figures 6.71 a,b) the continuum is absent or too faint (Shara et al., 1985).

The nebulosities in the light of Hα and S II, after subtraction of the continuum are shown in Figures 6.72 and 6.73 together with their isointensity maps. The spectra of the nebulosities indicated in Figure 6.72 with 1,2,3, and 5, are shown in Figures 6.74 a-d. Figure 6.75 shows an expanded part of the spectrum of nebulosity 1 in the region of Hα. The strength of [N II] 6584 is impressive. It is the strongest line, followed by a blend of Hα and [N II] 6548. Also the intensities of [S II] 6716, and 6730 are remarkable. According to Cohen (1985), these spectral peculiarities are rather more characteristic of a supernova remnant than a nova. However, the low expansion velocity and the small size of the shell (less than 10") indicate that CK Vul is a slow nova. Cohen suggests that the similarity with the supernova spectrum can be due to the fact that CK Vul, being much older than all the other novae for which the nebular spectrum is known, has swept up more than its own ejected mass (estimated to be about 10^{-4} solar masses, see Cohen and Rosenthal, 1983) in the interstellar material. Hence, the emission may be from shock-heated gas at the interface between the expanding shell and the interstellar medium, rather than from the standard mechanisms prevailing in low-density nova shells.

According to Shara et al. (1985), the spectra of the equatorial and polar ejecta are similar to those of the slow recurrent nova T Pyx, but with lower excitation.

Shara et al. (1985) discuss the possibility that CK Vul is a different kind of object than an old nova. In fact, its very low luminosity is comparable to those of the faintest dwarf novae (M_R = 10.4+/-0.8) and certainly much lower than that typical of old novae (M_V = +4.5, Warner, 1976; Patterson, 1984). This luminosity can be explained by a normal red dwarf M3-M5 with no contribution from the white dwarf or from the accretion disk. This may indicate that mass transfer has probably stopped in the system. This luminosity could also be explained by an accretion disk with mass-accretion rate as low as 10^{-12} solar masses /year. Shara et al. examine the possibility that CK Vul is a young planetary nebula, or a Herbig-Haro object. But in the first case, the central star would be fainter by two orders of magnitude than any other known nucleus of planetary nebula, and the nebula mass is two orders of magnitude lower than that typical of planetary nebulae. In the second case, although the expansion velocity is similar to that of jets around HH objects, there are no young objects in the vicinity of CK Vul; moreover, its chemical composition, e.g., the nitrogen overabundance, indicates that CK Vul is an evolved object. The conclusion is that CK Vul has been a genuine classical nova, and if it is typical of classical novae in the thousand years between eruptions, their faintness makes them very difficult to find. Hence, our statistics on the space density of old novae may be grossly underestimated.

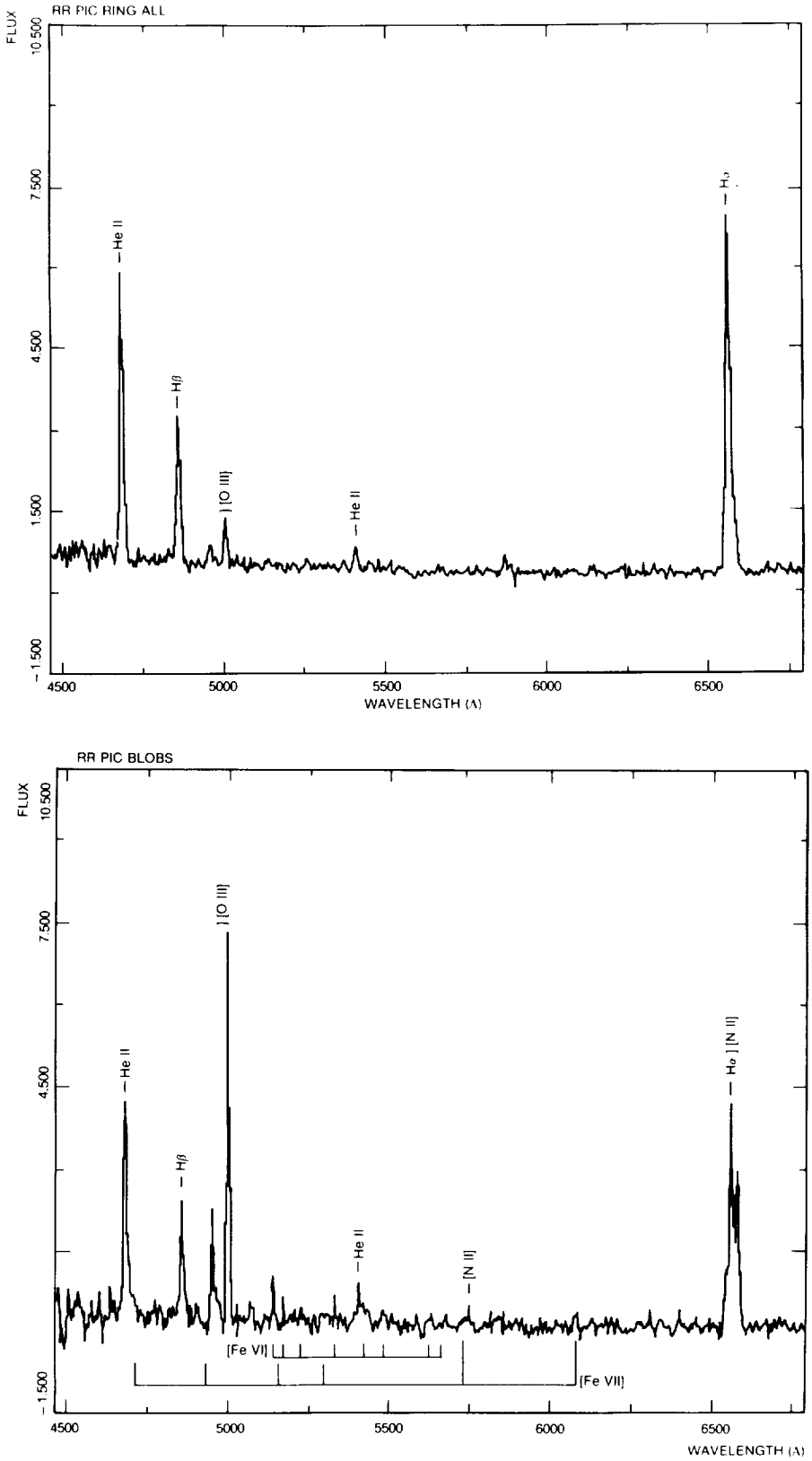

Figure 6-70. The optical spectrum of the polar blobs and the equatorial ring of the shell of RR Pic, observed with a Cassegrain spectrograph + CCD at the ESO 2.2 m telescope.

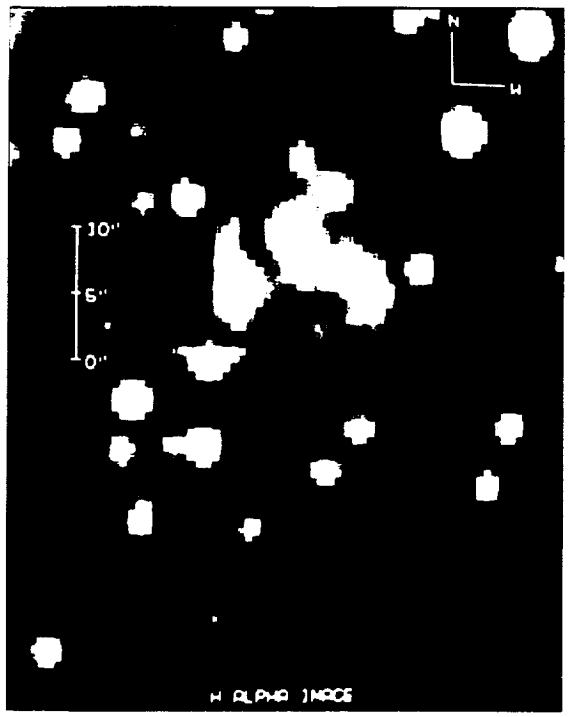

Figure 6-71. The nebulosities in the vicinity of the old nova CK Vul 1970. Image in the light of Hα. (from Shara et al., 1985)

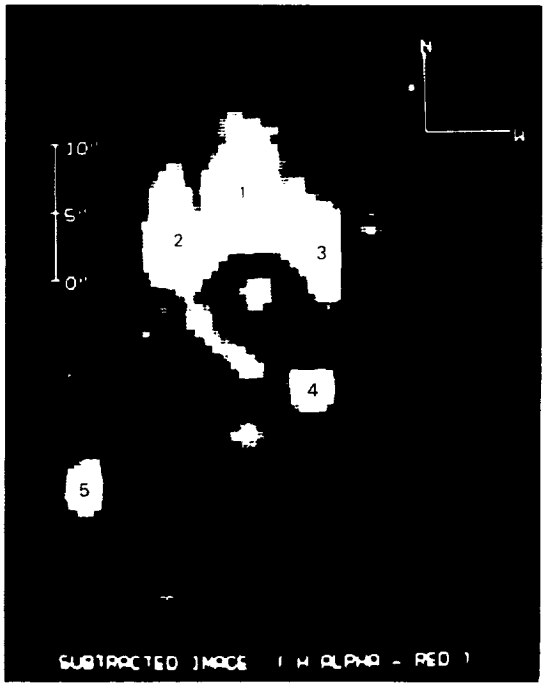

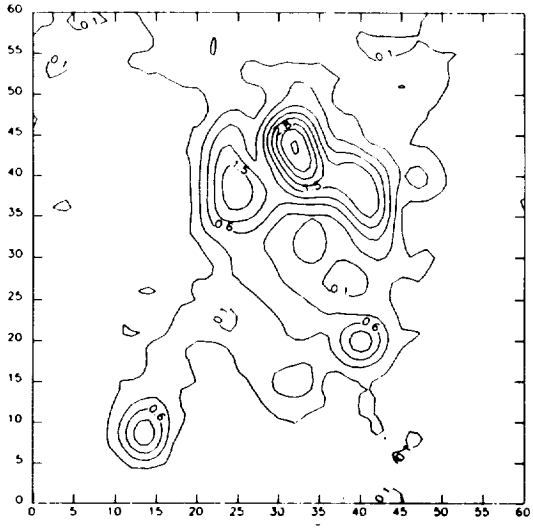

Figure 6-72. The same nebulosities shown in Figure 6-71, after substraction of the continuum, in the light of Hα, and the relative isointensity map. (from Shara et al., 1985)

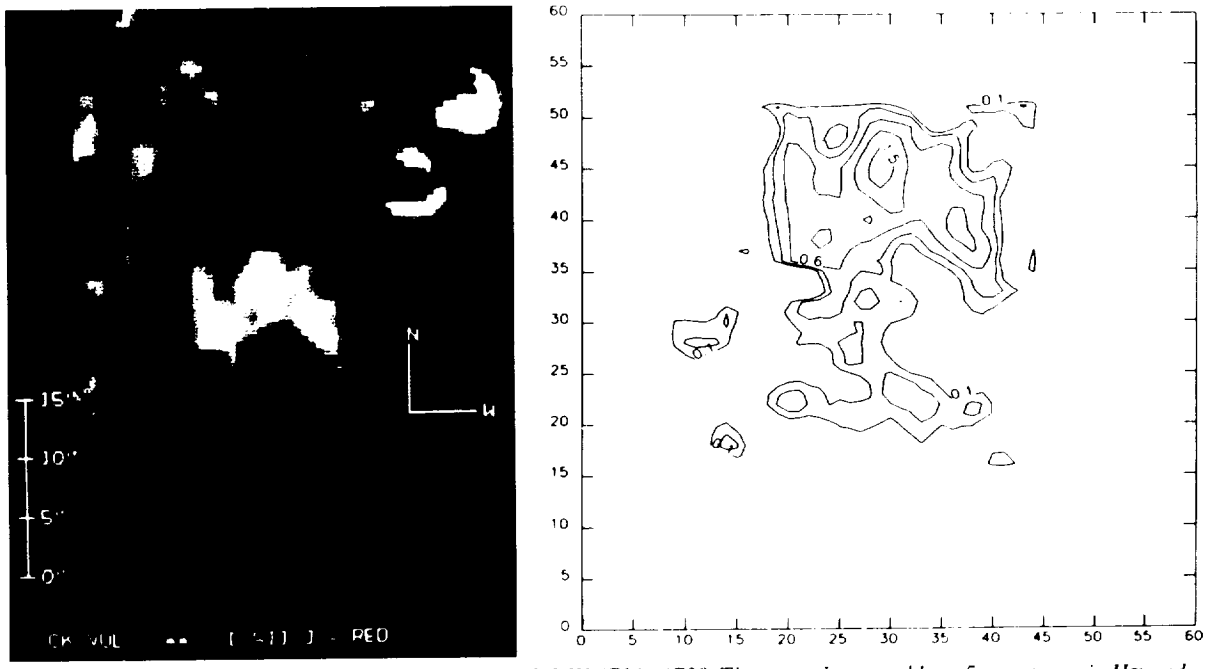

Figure 6-73. Same as Figure 6-72, but in the light of [S II] 6716+6730. The central star and knot 5 are strong in Hα and absent in the light of [S II]; knot 4 is much weaker than in Hα.
(from Shara et al., 1985)

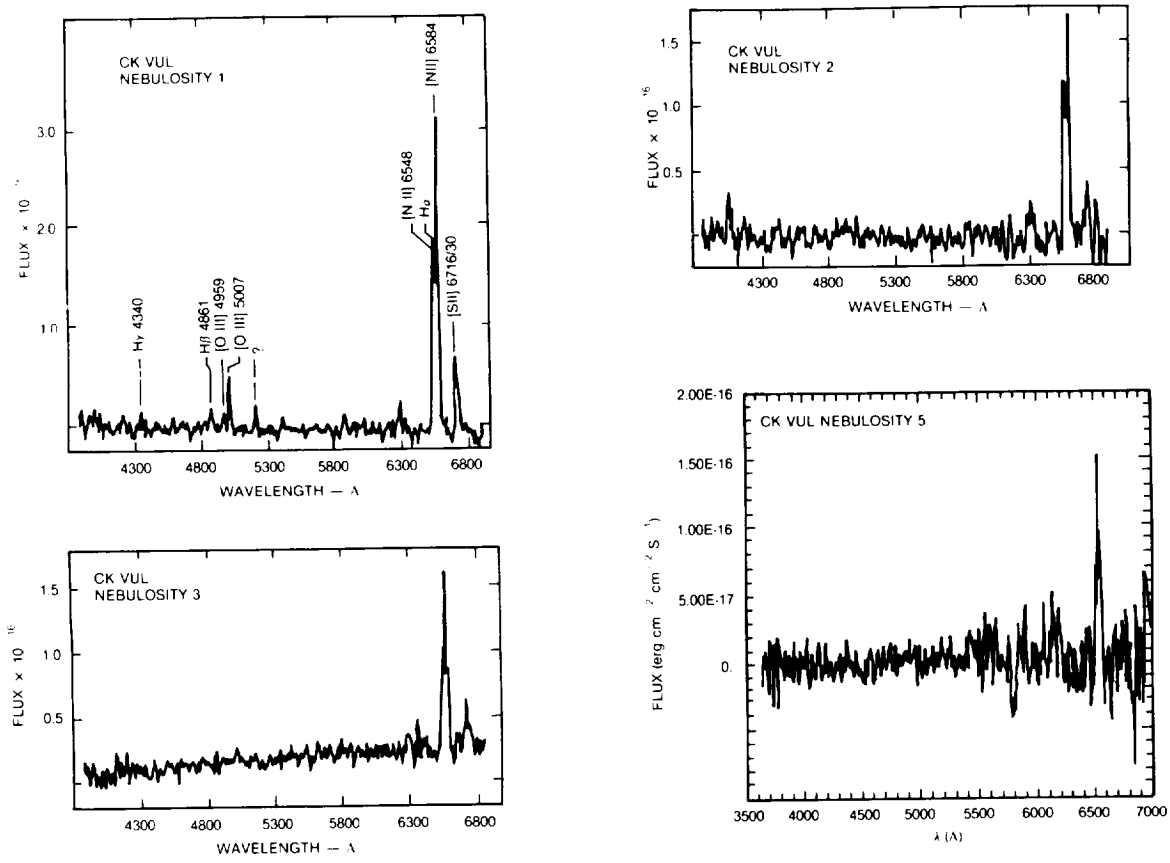

Figure 6-74. a) The spectrum of the nebulosity labeled 1 in Figure 6-72; b) the same for nebulosity labeled 2; c) the same for the nebulosity labeled 3; d) the same for the nebulosity labeled 5.
(from Shara et al., 1985)

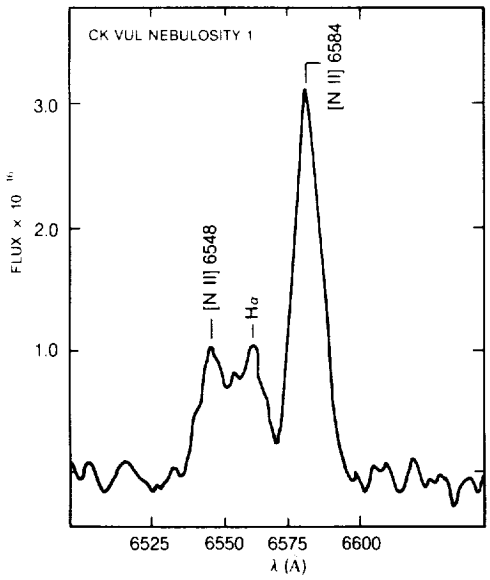

Figure 6-75. Expanded portion of the spectrum of nebulosity labeled 1 in the Hα region. from Shara et al., 1985)

VIII. RADIOASTRONOMICAL OBSERVATIONS OF NOVA ENVELOPES
(written by Hack)

Radioemission from novae has been observed in few cases: Wendker (1978 and successive updating) has collected data published before 1980. Positive detections have been obtained for the very slow nova HR Del 1967, the exceptional fast nova V 1500 Cyg 1975, the fast nova V 368 Sct 1970, and the moderately slow nova FH Ser 1970. Other novae have been searched for radioemission, (T CrB, DQ Her, V 533 Her, Nova Cep 1971), but with negative results.

A high-sensitivity radio survey of classical novae has been made with VLA by Bode et al. (1987a) at 1.5 GHz and 4.9 GHz. Of the over 26 objects observed, including very old novae like CK Vul 1670 and recent novae like V1370 Aql 1982 and V 4077 Sgr 1982, only two were detected: NQ Vul 1976 and V 4077 Sgr 1982. The radio "light curves" for HR Del, FH Ser, and V 1500 Cyg are given in Figure 6-76. The spectra are consistent with thermal radiation of expanding envelopes of ionized gas at high emission measures (where the emission measure E is given by N_e^2 x s with s dimension of the emitting body, N_e electron density, and is measured in pc cm^{-6}) as shown by Hjellming and Wade (1970). Altunin (1976) has measured a flare at 989 MHz from V 1500 Cyg. It exceeds by more than three orders of magnitude the flux expected at the same frequency and about the same date from the thermal spectrum; it can be explained by nonthermal synchrotron radiation.

An extended discussion of the radio observations for these three best studied novae is given Hjellming et al. (1979). The most important conclusion from this study is that the radio emission comes from the nova shell, as indicated by the fact that it reaches its maximum much later than the optical and also than the infrared maximum. If we identify with t(o) the beginning of the outburst, the maximum radio emission from the very fast nova V 1500 Cyg is reached at t-t(o) between 100 and 200 days, and for the moderately slow nova FH Ser, between 400 and 600 days. The observations of the very slow nova HR Del started almost at the epoch of maximum radioemission, which can be placed at a t-t(o) of about 1000 days.

In no case was the radio emission observable earlier than 50 days after outburst.

Hjellming et al (1979) show that a spherical symmetric isothermal model defined by three parameters-mass, inner velocity, and outer velocity-fits reasonably well the observed "radio light curves." Masses of 8.6 x 10^{-5}, 4.5 x 10^{-5}, and 2.4 x 10^{-4} solar masses, inner velocities of 200, 48, and 200 km/s and outer velocities of 450, 1000 and 5600 km/s have been found for HR Del, FH Ser, and V 1500 Cyg, respectively. A detailed discussion of these models will be given in Chapter 7.

We remark that slow novae like FH Ser and very fast novae like V 1500 Cyg present very similar radio "light curves" and radio spectra. Hence, the way their gas shells expand is very similar. Their dust shells, on the contrary, behave very differently as indicated by their infrared fluxes and their variation with time from outburst.

Chevalier (1977) predicted that also old novae should be observable radio emitters, but at rather low levels (<1 mJy). In the attempt to verify this prediction, Reynolds and Chevalier (1984) have observed GK Per 1901 with the VLA at wave-

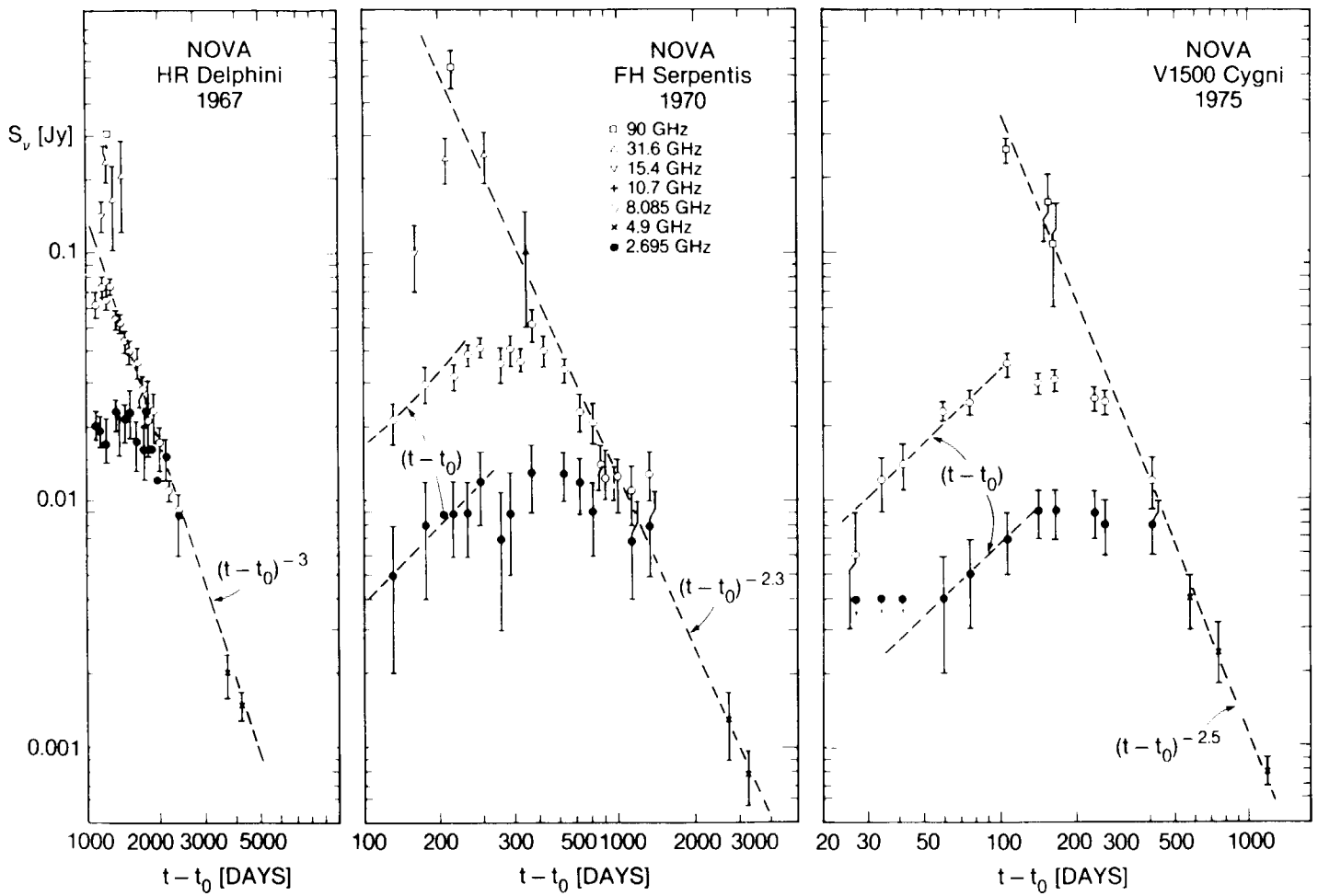

Figure 6-76. Radio "light curves" for HR Del, FH Ser, V 1500 Cyg. Also plotted are lines showing the power laws indicated for the rising and decaying radio curves.
(from Hjellming et al., 1979)

lengths of 20.5 and 6.2 cm. They detected an extended radio source within 40 are seconds of the nova position at both wavelengths (Figure 6-77). The nova was in eccentric position but within

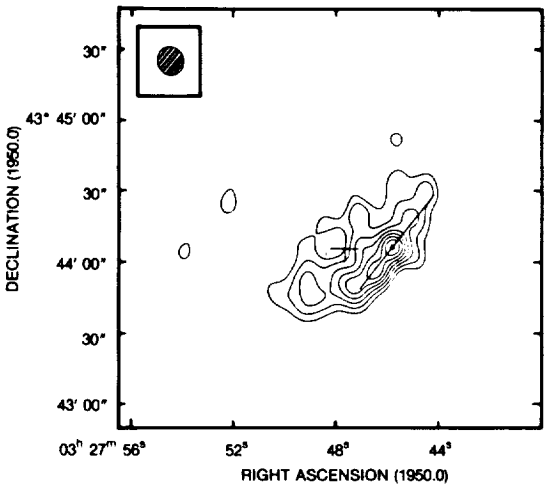

Figure 6-77. VLA map at 6 cm of the shell of GK Per. The plus sign indicated the position of the star GK Per itself.
(from Reynolds and Chevalier, 1984).

the radio source. The radio source has the shape of a partial shell and strongly resembles the optical nebulosity observable on the Palomar Observatory Sky Survey. The flux density dependence on the frequency is given by the relation $S \propto \nu^{-\alpha}$, with $\alpha = 0.67$ indicating that the emission is clearly non-thermal (differing from that observed from classical novae a few months after outburst). Although the dominant emission is synchrotron radiation, a thermal component at 6 cm cannot be ruled out. The shell ridge has several peaks qualitatively corresponding to the bright knots in the optical image.

The VLA survey by Bode et al. (1987a) of 26 classical novae has indicated no positive detection at 1.5 GHz over 18 objects observed, and two positive detections at 4.9 GHz over 8 objects observed. The value of the flux densities is the same for the two objects- the slow novae NQ Vul 1976 and V 4077 Sgr 1982- 0.6 mJy, i.e., of the same order as those observed previously by Hjellming et al. for HR Del, V 1500 Cyg, and FH Ser at similar frequencies. This fact, together with the high frequency at which the detection has been made, suggest the thermal origin of the radio emission. Since V 4077 Sgr is more distant (≈ 4100 pcs) than NQ Vul (≈ 1200 pcs), the radio luminosity of V 4077 Sgr is about one order of magnitude larger. This difference can be attributed to the fact that NQ Vul was observed when about 2000 days more than for V 4077 Sgr were elapsed from the date of the outburst. Figure 6-76 actually shows that the decline in the flux density in 2000 days for HR Del, FH Ser, and V 1500 Cyg is of one order of magnitude. However, a recent nova like N Sct 1981 placed at half the distance of V 4077 Sgr shows no measurable flux at 4.9 GHz.

As we have noted above, radio emission from classical novae has been observed not earlier than 50 days after outburst.

Observations of the recurrent nova T Cr B gave negative results. The first recurrent nova for which radio emission was detectable is RS Oph (Padin et al, 1985). The observations begin only 18 days after the recent outburst of 1985 and show a radio "light curve" different from that of classical novae. The brightness temperature is about 10^7 K, against the value of 10^4 K observed in classical novae, and therefore indicates a nonthermal origin for the radio emission. From this unique representative of recurrent novae, it seems that their radio properties are very different from those of classical novae. It is possible that the ejecta interaction with circumstellar material produces acceleration of electrons and enhancement of magnetic fields necessary to produce the synchrotron radiation. A similar mechanism was invoked by Chevalier (1982) for explaining type II supernovae. This interaction would explain also the presence of very strong coronal lines generally observed in the spectra of recurrent novae. Hence, the main difference between radio properties of classical novae and recurrent novae could be explained by the absence of circumstellar material in the first case and presence of it in the second case. This absence or presence of circumstellar material would be correlated to the fact that binary systems that explode as classical novae are composed of a white dwarf and a red dwarf, while over five recurrent novae, at least three have a late-type

companion, which is a red giant whose wind produces the circumstellar matter. A model for the radio and X-ray emission of RS Oph is proposed by Bode and Kahn (1985) and will be discussed in Chapter 7.

In concluding our discussion on radio observations of novae, we note that the data are for a very small number of objects for permitting us to generalize these results. We can just say the following:

1) the few novae observed months after outburst become thermal radiosources (expanding gas at $T \approx 10^4$). Their behavior is similar if they are either slow or fast novae, in contrast with their IR behavior.

2) the old nova GK Per shows a radio spectrum $S \propto \nu^{\alpha} \nu^{\alpha}$, which is typical of synchrotron radiation. No other novae have been found with similar properties. GK Per might be a special case since there might be interaction with strong interstellar or circumstellar material. An ancient planetary nebula surrounding GK Per was suspected recently in IRAS data (Bode et al 1987b).

3) the recurrent nova RS Oph shows a brightness temperature of 10^7 K in the radio range.

Only one recurrent nova has been detected in the radio spectral range and we cannot say if the high brightness temperature ($T \sim 10^7$ against the value of 10^4 observed for four classical novae is a common property of all recurrent novae, distinguishing them from all classical novae. However, it is possible that this difference between the observed classical novae and RS Oph is related to the fact that all classical novae, known to be members of a binary system, have for companion a cool dwarf, while RS Oph (as well as T CrB and V 1017 Sgr) have a red giant for companion. Now red giants are known to have winds, which, interacting with the ejecta, could explain the high brightness temperature and nonthermal emission (White, 1985). Hence, the negative result for T CrB may probably be related to the long interval elapsed from the last outburst.